

Geologic Characterization of the Northern Cane Creek Shale Play, Paradox Basin, Utah

Prepared for Utah School and Institutional Trust Lands Administration



(Photo: Crescent State 21-22 core of the Cane Creek, northern Paradox Basin, Grand County, Utah)

by Elliot Jagniecki, Ryan Gall, Tyler Wiseman (SITLA), and Michael Vanden Berg

June 2019



Utah Geological Survey
a division of
Utah Department of Natural Resources

Although this product represents the work of professional scientists, the Utah Department of Natural Resources, Utah Geological Survey, makes no warranty, expressed or implied, regarding its suitability for a particular use. The Utah Department of Natural Resources, Utah Geological Survey, shall not be liable under any circumstances for any direct, indirect, special, incidental, or consequential damages with respect to claims by users of this product.

CONTENTS

EXECUTIVE SUMMARY	iv
INTRODUCTION	1
ACKNOWLEDGMENT.....	10
OBJECTIVE AND GOALS	13
Objective	13
Goal	13
Tasks.....	13
PREVIOUS STUDIES.....	14
GEOLOGIC SETTING.....	14
Structure.....	14
Cane Creek Shale.....	20
Clastic Cycle 19.....	23
DRILLING AND COMPLETION METHODS.....	24
Drilling Techniques.....	24
Completion Techniques.....	25
CRESCENT STATE CORES.....	25
Cane Creek - A Zone	29
Cane Creek - B Zone	32
Cane Creek - C Zone	44
Cycle 19.....	46
GEOGRAPHIC THICKNESS.....	53
CONCEPTUAL DEPOSITIONAL MODEL	55
CONCLUSIONS AND RECOMMENDATIONS	61
REFERENCES	63

FIGURES

Figure 1. Paradox basin in the Four Corners area of Utah, Colorado, Arizona, And New Mexico	2
Figure 2. Utah part of the Paradox Basin defined by the extent of the Paradox Formation salt.....	3
Figure 3. Detailed map of the study area	4
Figure 4. Pennsylvanian nomenclature for the Paradox Basin	5
Figure 5. Southwest to northeast cross section of the Paradox Basin.....	6
Figure 6. Map of Paradox Basin showing the principal structures	8
Figure 7. Structure map of the Cane Creek unit in the Paradox Basin	9
Figure 8. Cane Creek cumulative production in the Paradox Basin	11
Figure 9. Cane Creek federal unit and neighboring units	12
Figure 10. Paleogeography of the Colorado Plateau and Paradox Basin during the Mississippian Period (340 Ma).....	15
Figure 11. Paleogeography of the Colorado Plateau and Paradox Basin during the middle Pennsylvanian (308 Ma).....	16
Figure 12. Paleogeography of the Colorado Plateau and Paradox basin during the middle pennsylvanian (308 Ma).....	17
Figure 13. Paleogeography of the Colorado Plateau and Paradox Basin during the middle Triassic (240 Ma).....	18
Figure 14. Paleogeography of the Colorado Plateau and Paradox Basin during the early	

Cretaceous (105 Ma)	19
Figure 15. Surface geology view south from Dead Horse State Park	20
Figure 16. Gamma ray and sonic travel time curves through the Cane Creek shale	21
Figure 17. Production curves for Cane Creek 12-1	22
Figure 18. Oil production curves from cycle 19 for Cane Creek 1-1, Kane Springs 16-1, and Cane Creek 36-3h	23
Figure 19. Core description of the Cane Creek from Crescent State #21-22.	26
Figure 20. Core description of cycle 19 from Crescent State #21-22.....	27
Figure 21. Core description of the cycle 19 unit from Crescent State #22-09.....	28
Figure 22. Core photograph from the Cane Creek A zone, Crescent State #21-22.....	30
Figure 23. Core photograph of cyclic facies for the Cane Creek A zone, Crescent State #21-22.....	30
Figure 24. Thin section scans of organic-rich mudstone, Crescent State #21-22 and Crescent State #22-09.....	31
Figure 25. Core photographs and thin section photomicrographs of Cane Creek facies, Crescent State #21-22.....	33
Figure 26. Total organic carbon analysis from cycle 19 and Cane Creek, Crescent State #21-22.....	36
Figure 27. Oil potential from source rock analysis of organic-rich shales from cycle 19 and Cane Creek, Crescent State #21-22.	36
Figure 28. Oil saturation index from source rock analysis of organic-rich shales from cycle 19 and Cane Creek, Crescent State #21-22.	37
Figure 29. Production index from source rock analysis of organic-rich shales from cycle 19 and Cane Creek, Crescent State #21-22	37
Figure 30. V_{ro} from cycle 19 and Cane Creek, Crescent State #21-22	39
Figure 31. Pseudo Van Krevelen plot from organic-rich shale samples from the cycle 19 and Cane Creek, Crescent State #21-22	40
Figure 32. Photograph of core from the Cane Creek B zone, Crescent State #21-22	41
Figure 33. Porosity and permeability cross plot from cycle 19 and Cane Creek core plug analysis from Crescent State #22-09 and Crescent State #21-22	42
Figure 34. Core photographs from the Cane Creek C zone, Crescent State #21-22.....	45
Figure 35. Core photographs from cycle 19, Crescent State #22-09.....	47
Figure 36. Core photographs and thin section photomicrographs from cycle 19, Crescent State #21-22 and Crescent State #22-09.....	48
Figure 37. Core photographs from cycle 19, Crescent State #21-22.....	52
Figure 38. Core photograph of cycle 19, Crescent State #22-09	54
Figure 39. Cane Creek thickness comparison from cores across the Paradox Basin	56
Figure 40. Core slab photographs representative of the Cane Creek B zone reservoir facies.....	57
Figure 41. Diagrammatic cross section of a tidal flat depositional environment	58
Figure 42. Diagrammatic box model of a sabkha depositional environment	59
Figure 43. Core slab photographs representative of the Cane Creek C zone, Crescent State #21-22.....	60
Figure 44. Maximum Tmax map of the Paradox Basin.....	62

TABLES

Table 1. Cumulative production through December 2018 from fields that produce from the Cane Creek shale.....	6
Table 2. Production for the month of December 2018 from fields producing from the Cane	

Creek shale	7
Table 3. Total undiscovered resources for the Paradox Formation total petroleum system.....	7
Table 4. Source rock analysis from Crescent State #21-22	38
Table 5. Porosity and permeability analysis from Crescent State #22-09 and Crescent State #21-22	42
Table 6. XRD results from Crescent State #21-22	43
Table 7. XRD results from Crescent State #22-09	51

APPENDICES

- A. U.S. Geological Survey assessment of undiscovered oil and gas resources in the Paradox Basin Province, Utah, Colorado, New Mexico, and Arizona, 2011
- B. Cane Creek wells in the Paradox Basin
- C. Petrographic analysis of Cane Creek 26-3
- D. Petrographic analysis of Remington 21-1H
- E. Core photographs, Crescent State 21-22 and Crescent State 22-09
- F. XRF data, Crescent State 21-22 and Crescent State 22-09

EXECUTIVE SUMMARY

The Cane Creek shale of the lower Pennsylvanian Paradox Formation is a productive, but still emerging oil and gas play in the fold and fault belt of the northern Paradox Basin, Utah. Oil production has been most successful from horizontal wells at the Big Flat field in the central play area, whereas areas to the north (Greentown and Gunnison Valley) are currently unproductive but limited historical drilling has shown significant promise. The lack of core data in the northern part of the basin has made it difficult to determine reservoir quality and facies heterogeneity. However, several cores were recently drilled along the Salt Valley anticline near Crescent Junction which provide new sedimentological data, reservoir properties, and source rock quality of the northern Cane Creek play area.

The Cane Creek is a heterolithic unit composed of meter-scale cycles of anhydrite, anhydritic-dolomitic mudstone, silty dolomite, very fine grained sandstone to siltstone, and organic-rich calcareous mudstone. Thick beds of overlying and underlying halite provide regional seals and overpressure to the reservoir, and naturally occurring fractures are important for system permeability. Siliciclastic deposits are predominantly bioturbated and contain climbing current ripples, bidirectional cross-stratification, and mud drapes along ripple foresets, all suggestive of tidal depositional processes. Anhydrite pseudomorphs after bottom growth gypsum, invasive displacive nodular anhydrite, dolomite, laminated organic-rich mudstones with Type I & II kerogen, as well as the paucity of burrows, indicate periods of restricted-evaporative sea waters in a sabkha environment. Source rock analyses indicate the northern Cane Creek is within the oil window ($V_{ro} \sim 0.80$) with up to 13 wt% TOC in several thin shale beds. Siliciclastic reservoir rocks have low permeabilities (0.009–0.202 mD) and variable porosities (6–17%) due to dolomite-anhydrite cements, and thus naturally occurring and possibly stimulated fractures are important. Nonetheless, the northern Cane Creek contains thick sandstone reservoir facies similar to those found in the successfully producing Big Flat area to the south.

Although total oil production from the Cane Creek is only about 8 MMBO, current estimates of the undiscovered resource is about 215 MMBO. The new core data provides insightful and promising potential for the presence of mature source rock and thick reservoir potential for the Cane Creek near and west of Crescent Junction. The overlying cycle 19 is also within the oil window having up to 11.5 wt% TOC and can be considered an upside secondary target for horizontal drilling in the Cane Creek play, which will help increase the undiscovered resources. With advancements in horizontal drilling, reservoir characterization, and reduction of structure related risks, the Cane Creek has the potential to become a significant resource play in the northern Paradox Basin.

INTRODUCTION

The Cane Creek shale oil and gas play is in the fold and fault belt of the Paradox Basin in southeast Utah and southwest Colorado (figure 1). This study focuses on the Cane Creek play in the northern part of the Paradox Basin, Grand County, north of the town of Moab, near Crescent Junction (figures 2 and 3). The Cane Creek is a thin heterolithic unit consisting of interbedded silty mudstones, carbonate, siliciclastic, and evaporitic rocks in the thick predominantly halite Pennsylvanian Paradox Formation (figure 4). The Paradox Basin was a restricted marine basin resulting in deposition of thousands of feet of evaporite beds. Interbedded with these evaporites are thin calcareous silty mudstones, siltstones, and sandstones interpreted to have been deposited during marine high stands (figure 5). The Paradox Formation is bounded by shallow open-marine shelf carbonates of the underlying Pinkerton Trail and overlying Honaker Trail Formations.

The Paradox Formation ranges in thickness from 500 to 5000 ft and has been an exploration target since the 1920s when oil was first produced from the formation (Chidsey and Eby, 2017). Exploration has waxed and waned spurred on by exciting discoveries followed by dry holes. Increases in oil pricing and improved horizontal drilling technology have driven the most recent activity. Throughout the play's history, the Cane Creek has produced more than 9.0 million barrels of oil (MMBO) (table 1), with only 22,000 barrels of oil (BO) produced from 29 wells in December 2018 (table 2). The U.S. Geological Survey calculated the Cane Creek has a mean undiscovered resource of 215 MMBO and 4723 billion cubic feet of gas (BCFG) (table 3 and appendix A).

The Cane Creek "shale" is not truly a shale but rather a heterolithic unit composed of interbedded anhydrite, anhydritic dolomitic mudstone, dolomite, silty dolomite, very fine grained sandstone to siltstone, and thin (inches) organic-rich mudstone beds. The thin shale beds are the primary source for hydrocarbons within the Cane Creek shale. The primary reservoirs are thick sandstone packages and to a lesser degree silty dolomite beds. The reservoir has low matrix permeability and naturally occurring fractures that are important for economic production. Other heterolithic units within the Paradox Formation are often referred to as "clastics" (e.g., Smith and others, 1978a, 1978b, 1978d; Grove and others, 1993; and Whidden and others, 2014) and each occurs within an evaporite cycle consisting of a siliciclastic package and an overlying halite package. The cycles and associated clastic units are numbered from top to bottom following Hite (1960) (figure 4).

Production from the Cane Creek is typically associated with seismically imaged structures. Faulting of the underlying Mississippian and older rocks formed blocks where the lower Paradox Formation, including the Cane Creek, was deposited and draped over the fault blocks. Some of the faults continued to move during the Pennsylvanian causing displacement of the Cane Creek and other lower Paradox cycles (Grove and others, 1993). Deposition of Permian and Early Triassic sediments shed from the Uncompahgre uplift created heavy loading on the Paradox salt. Loading on the low-density plastic salts caused it to move forming diapiric salt anticlines such as Moab-Spanish Valley, Castle Valley, and Salt Valley within Arches National Park (Doelling and others, 1988) (figures 6 and 7). Salt welds formed in the intervening synclines. The Salt Valley anticline and many other anticlines (e.g., Cane Creek anticline) in the Paradox Basin are the result of a buildup of salt that did not intrude the overlying sediments. Secondary folding in these areas within the salt developed wave-like structures with amplitudes of 15 to 100 feet and wavelengths of 300 to 3000 feet (Grove and others, 1993). The complex structural history caused numerous periods of fracturing and fracture filling within the Cane Creek and other Paradox clastics. Recent 3-dimensional (3D) seismic surveys have greatly improved the definition of these Mississippian fault blocks and salt features. However, structure alone does not guarantee successful production; sandstone

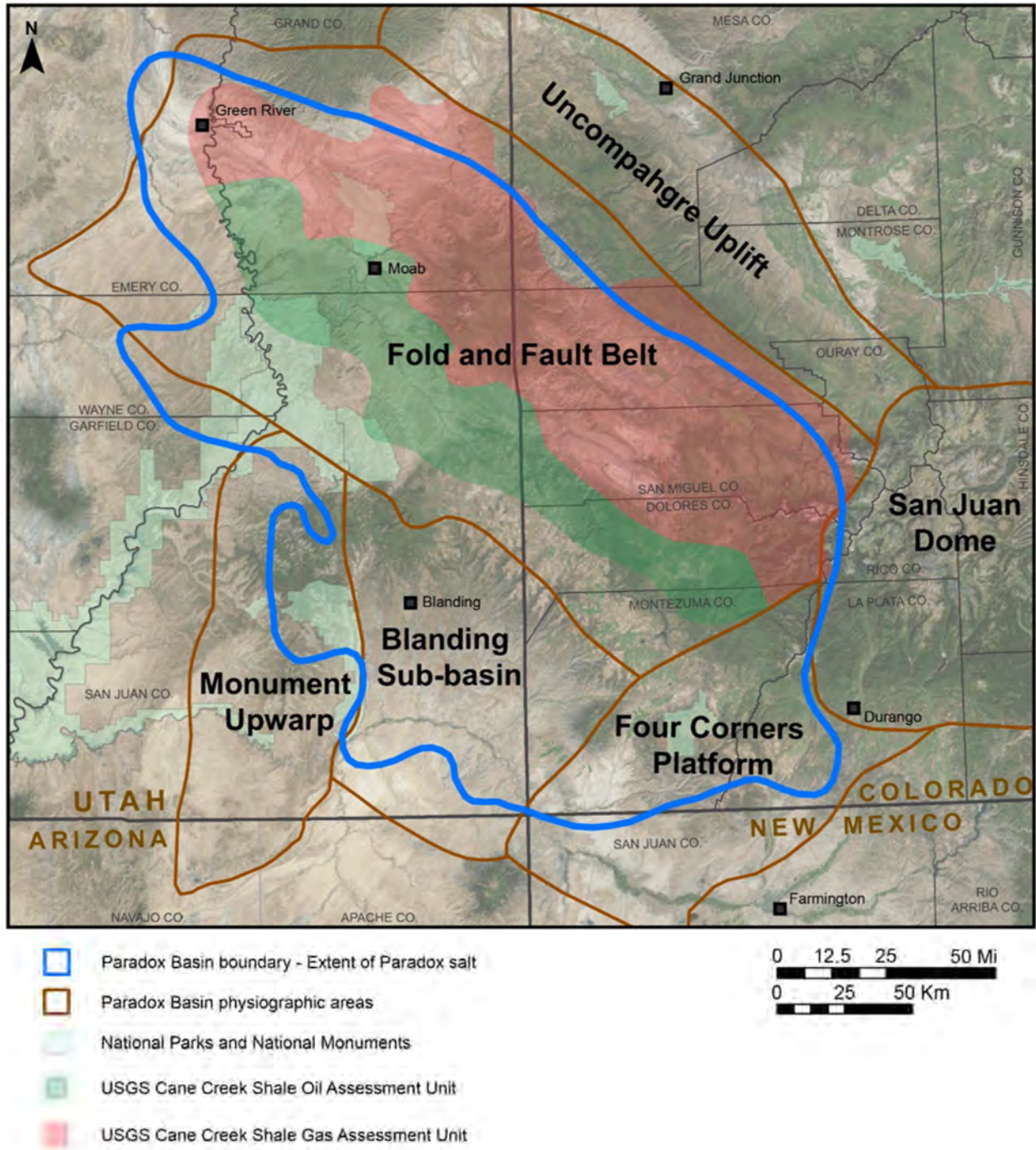


Figure 1. Paradox Basin in the Four Corners area of Utah, Colorado, Arizona, and New Mexico. The basin is defined by the extent of the Paradox Formation salt. Physiographic areas and Cane Creek assessment units from Anna and others (2014) and Whidden and others (2014). [The Cane Creek play lies within the fold and fault belt area.]

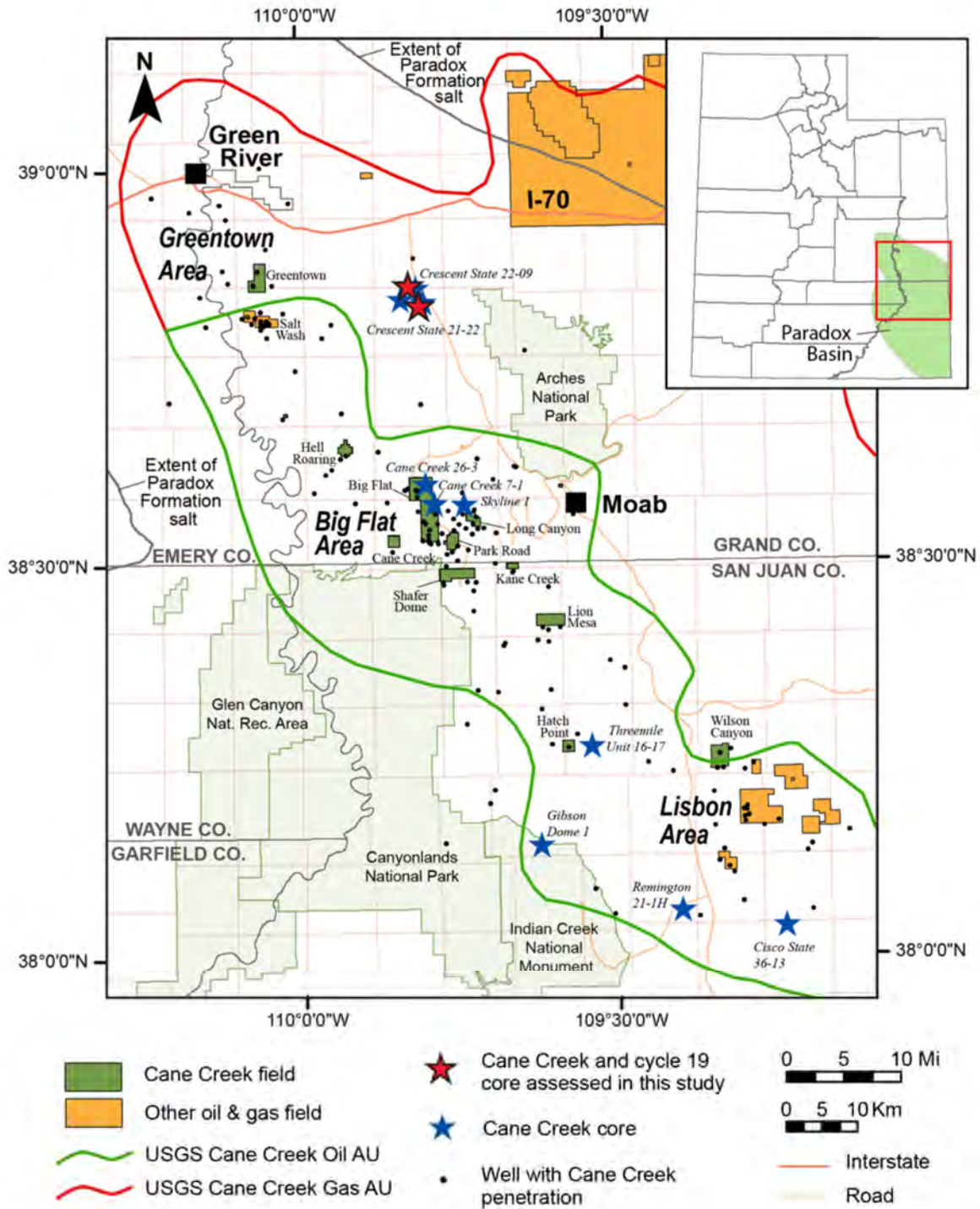


Figure 2. Utah part of the Paradox Basin defined by the extent of the Paradox Formation salt. The Cane Creek play is defined by the U.S. Geological Survey oil and gas assessment units (AU) from Anna and others (2014) and Whidden and others (2014). The play area is further divided into informal Greentown, Big Flat, and Lisbon areas.

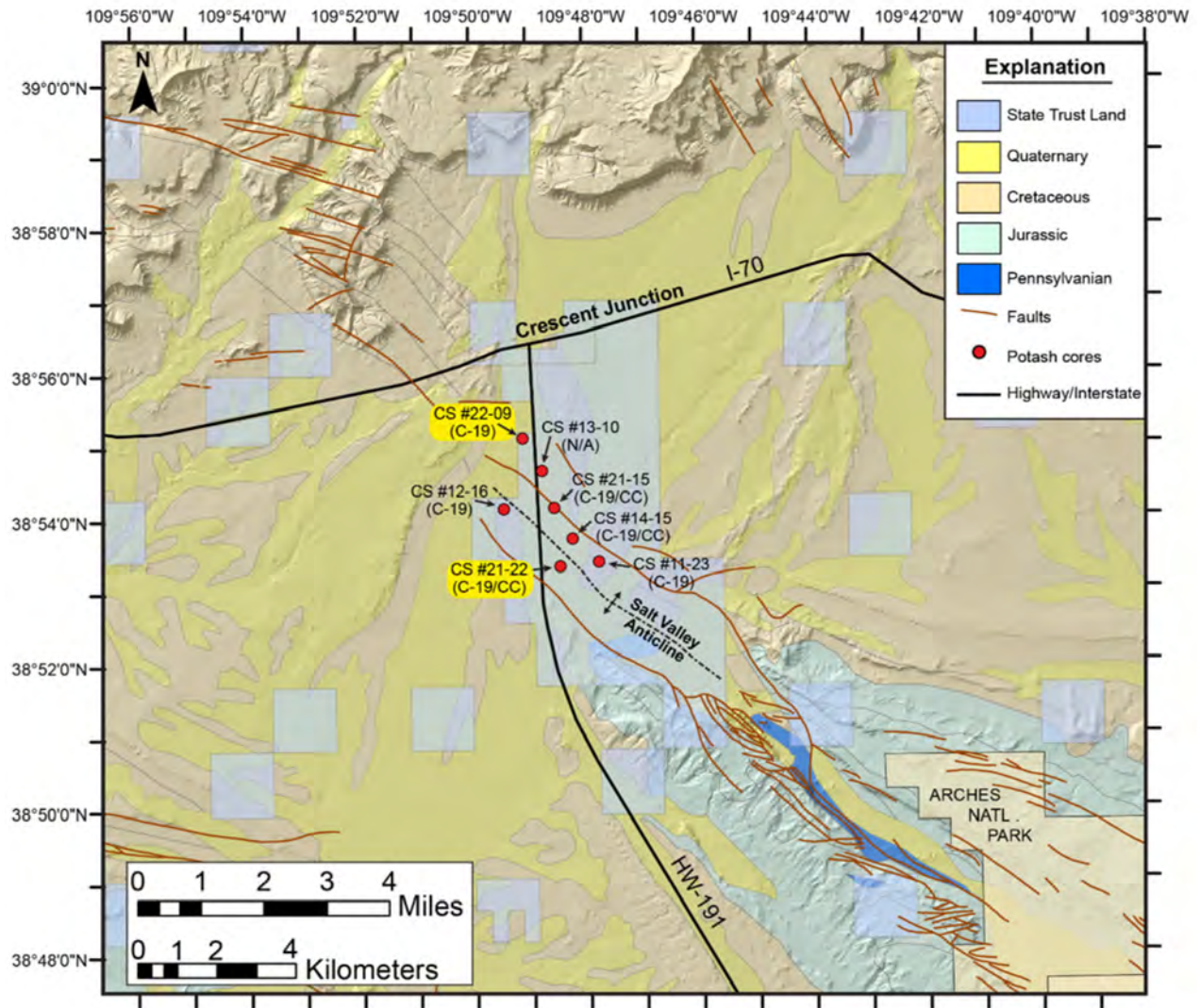


Figure 3. Detailed map of the study area highlighting locations of Pinnacle Potash International Ltd Crescent cores donated to the Utah Geological Survey. Crescent State #22-09 and Crescent State #21-22 were used in this study.

SYSTEM		SERIES	GROUP	FORMATION	MEMBER	PRODUCTION ZONE	EVAPORITE CYCLE
P E N N S Y L V A N I A N		Virgilian	H E R M O S A	Honaker Trail			1
		Missourian					2
P E N N S Y L V A N I A N		Desmoinesian	H E R M O S A	Paradox	upper	Ismay	3
							4
P E N N S Y L V A N I A N		Desmoinesian	H E R M O S A	Paradox	middle	Desert Creek	5
							6
P E N N S Y L V A N I A N		Desmoinesian	H E R M O S A	Paradox	middle	Akah	7
							8
P E N N S Y L V A N I A N		Desmoinesian	H E R M O S A	Paradox	middle	Barker Creek	9
							10
P E N N S Y L V A N I A N		Desmoinesian	H E R M O S A	Paradox	middle	Barker Creek	11
							12-13
P E N N S Y L V A N I A N		Desmoinesian	H E R M O S A	Paradox	middle	Barker Creek	14
							15
P E N N S Y L V A N I A N		Desmoinesian	H E R M O S A	Paradox	middle	Barker Creek	16
							17
P E N N S Y L V A N I A N		Desmoinesian	H E R M O S A	Paradox	middle	Barker Creek	18
							19
P E N N S Y L V A N I A N		Desmoinesian	H E R M O S A	Paradox	middle	Barker Creek	20
							21
P E N N S Y L V A N I A N		Desmoinesian	H E R M O S A	Paradox	middle	Barker Creek	22-23
							24
P E N N S Y L V A N I A N		Desmoinesian	H E R M O S A	Paradox	middle	Barker Creek	25
							26
P E N N S Y L V A N I A N		Desmoinesian	H E R M O S A	Paradox	middle	Barker Creek	27
							28
P E N N S Y L V A N I A N		Desmoinesian	H E R M O S A	Paradox	middle	Barker Creek	29
Molas		Pinkerton Trail					
Morro-wan		Atokan					
Morro-wan		Atokan					
Morro-wan		Atokan					

HOVENWEEP
GOTHIC
CHIMNEY
ROCK

CLASTIC 19
CANE
CREEK

Figure 4. Nomenclature for the Pennsylvanian Paradox Basin based on Hite (1960). The Hermosa Group consists of shallow marine carbonate and sandstone deposits of the Pinkerton Trail and Honaker Trail Formations which underlie and overlie the Paradox Formation. The Paradox is divided into oil field production zones and further divided into evaporite cycles numbered from top to bottom. The Cane Creek shale is part of cycle 21. Other organic-rich deposits with potential for oil and gas production are the clastic deposits of cycle 19, Chimney Rock Shale (cycle 5), Gothic Shale (cycle 3), and Hovenweep Shale (cycle 2).

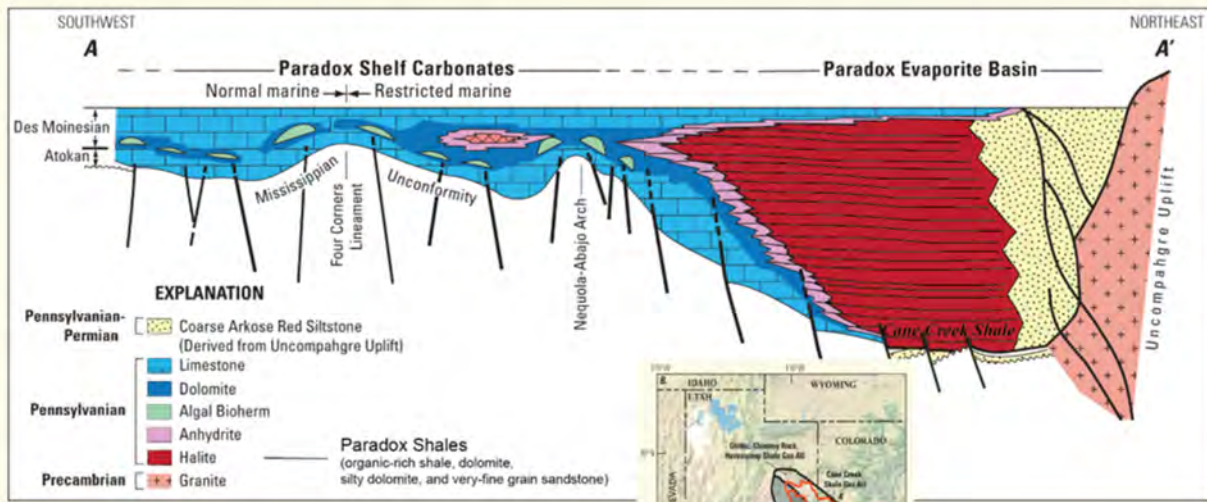


Figure 5. Southwest-to-northeast cross section of the Paradox Basin. The evaporative basin consists of a series of depositional cycles of siliciclastics-mudstones and evaporites. The Cane Creek shale is the lowermost faulted cycle in this diagram. Modified from Whidden and others (2014).

Table 1. Cumulative production through December 2018 from fields that produce from the Cane Creek shale. Data source Utah Division of Oil, Gas and Mining monthly production by field <http://oilgas.ogm.utah.gov/Publications/Publications.htm>

Field Name	Location (TR)	No. of Active Wells	Thousand Barrels of Oil (MBO)	Million Cubic Feet Gas (MMCFG)	Comments
Bartlett Flat	T25-26S, R19E	1	39	0	Original Big Flat 5 well Combined with Big Flat field
Big Flat	T26S, R19E	22	6146	4046	Cane Creek unit
Greentown	T22S,R17E	2	92	349	Two active well
Hatch Point	T29S, R21E	4	89	40	
Hell Roaring	T25S, R18E	1	678	591	Cane Creek unit One well
Cane Creek	T26S, R20-21E	3	97	51	Original exploration 1920s and 1950s
Lion Mesa	T27S, R21E	0	2	0	Abandoned
Long Canyon	T26S, R20E	1	1158	1199	One well
Park Road	T26S, R20E	2	545	256	Cane Creek unit
Shafer Canyon	T27S, R20E	0	67	64	Two wells now abandoned
Wilson Canyon	T29S, R23E	1	127	1,982	One well abandoned
Undesignated	Variable	3	30	21	Gold Bar 1 Two Fer 26-30 La Sal 29-28
Total		41	9070	8600	

Table 2. Production for the month of December 2018 from fields producing from the Cane Creek shale. Wilson Canyon and Long Canyon still produce intermittently. Data source Utah Division of Oil, Gas and Mining monthly production by field <http://oilgas.ogm.utah.gov/Publications/Publications.htm>

Field Name	Location (TR)	No. of Active Wells	Barrels of Oil (BO)	Thousand Cubic Feet Gas (MCFG)	Comments
Big Flat	T26S, R19E	22	20173	12447	Cane Creek unit
Greentown	T22S, R17E	2	314	1403	
Hatch Point	T29S, R21E	4	8	2	Threemile unit
Hell Roaring	T25S, R18E	1	480	74	Cane Creek unit
Long Canyon	T26S, R20E	1	22	0	
Park Road	T26S, R20E	2	1023	2174	Cane Creek unit
Wilson Canyon	T29S, R23E	1	0	0	
Total		33	22020	16100	

Table 3. Total undiscovered resources for the Paradox Formation total petroleum system. From Whidden and others (2012). MMBO = million barrels of oil, BCFG = billion cubic feet of gas, and MMBNGL = million barrels of natural gas liquids. See appendix A.

Total petroleum systems (TPS) and assessment units (AU)	Field type	Total undiscovered resources											
		Oil (MMBO)				Gas (BCFG)				NGL (MMBNGL)			
		F95	F50	F5	Mean	F95	F50	F5	Mean	F95	F50	F5	Mean
Paradox Formation TPS													
Cane Creek Shale Oil AU	Oil	103	198	382	215	84	175	364	193	6	14	31	15
Cane Creek Shale Gas AU	Gas					2,473	4,284	7,420	4,530	88	168	319	181
Gothic, Chimney Rock, Hovenweep Shale Oil AU	Oil	126	238	449	256	91	186	382	205	7	15	32	16
Gothic, Chimney Rock, Hovenweep Shale Gas AU	Gas					3,342	6,075	11,042	6,490	120	238	472	260

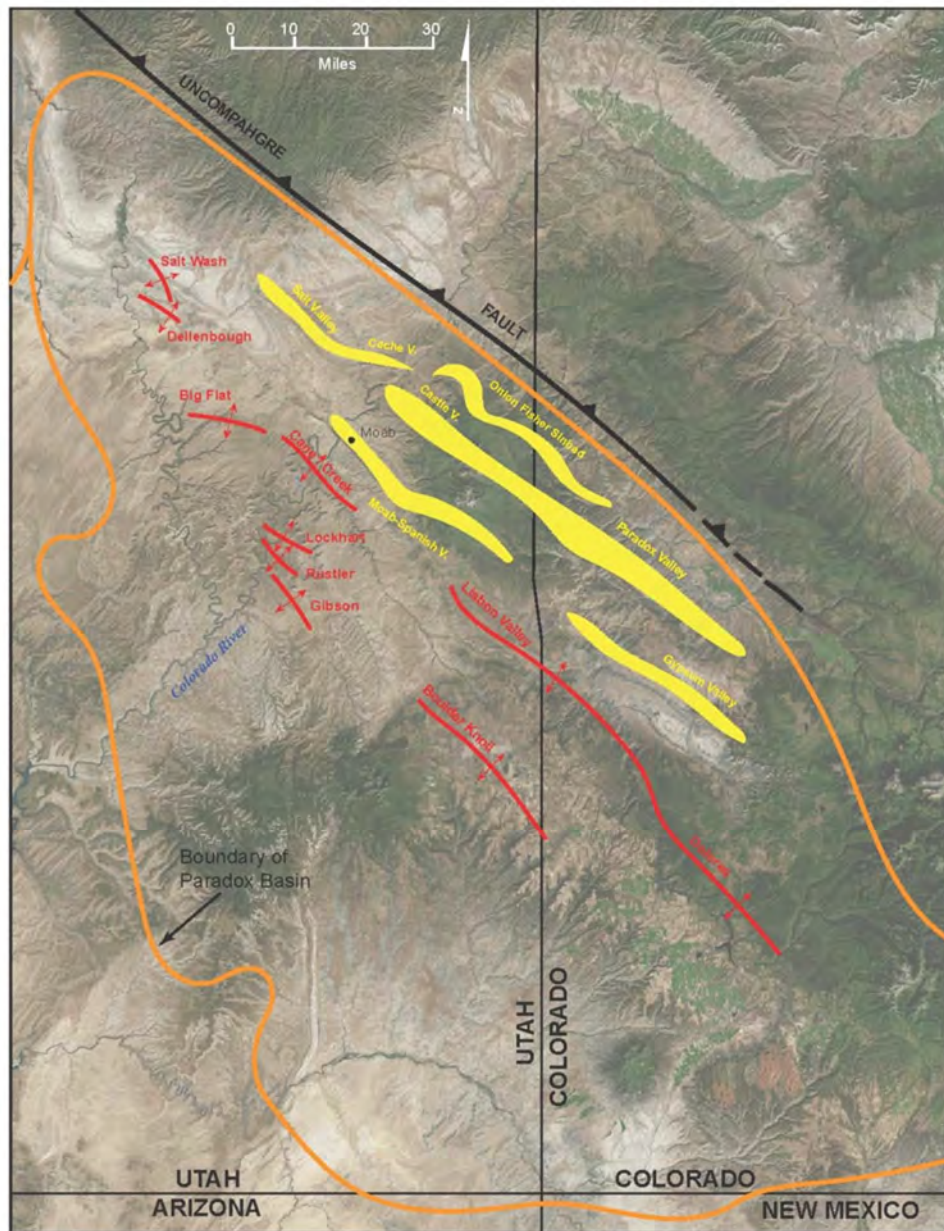


Figure 6. Map of Paradox Basin showing the principal structures. Salt valley anticlines, shown in yellow, are a result of diapiric salt movement in the Paradox Formation. Other anticlines (red) are the result of salt movement that did not penetrate the formations overlying the Paradox. Modified from Doelling and others (1988).

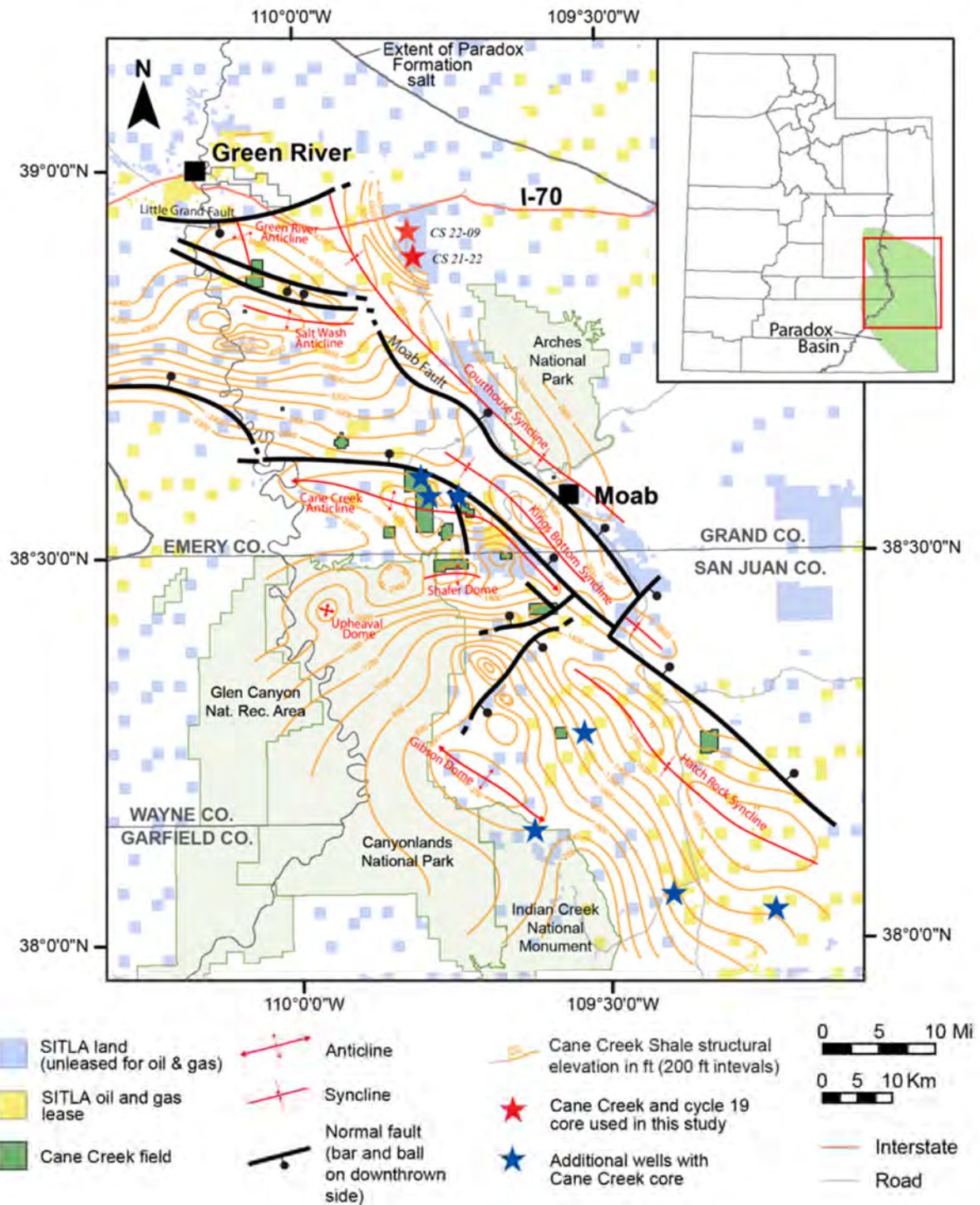


Figure 7. Structure map of the Cane Creek unit in the Paradox Basin, highlighting location of Crescent State #21-22 and Crescent State #22-09 cores used in this study. Modified from Chidsey and Eby (2017).

quality, open fractures, and the timing of oil generation all play a critical role and can result in good oil production with or without well-developed structural closure.

The success rate using horizontal drilling in the Cane Creek reservoir has been good in the Big Flat area (figures 8 and 9; and appendix B). However, the well costs are very high and many of the wells are sub- to marginally economic. The Cane Creek unit has been owned by several companies; the most active operators were Columbia Gas Development Corporation (Columbia Gas), who drilled the first horizontal wells in the unit in 1991, and Fidelity Exploration and Production Company (Fidelity E&P) who significantly increased the number of wells and production between 2007 and 2015. Fidelity E&P sold the Cane Creek unit to Wesco Operating Company (Kirkwood Resources) in 2016. Work by Fidelity E&P in the Cane Creek unit included drilling vertical pilot holes and taking core from the Cane Creek before drilling horizontal laterals. Cores were extensively evaluated using the most up to date petrophysical, geochemical, and geomechanical analyses to characterize the reservoir. Fidelity E&P acquired 3D seismic over much of the unit to map the complex structure more accurately. But even with the new reservoir characterization, the Cane Creek has not developed into a typical resource play where the drilling program is simply designed to fill in a spacing pattern. Based on the study by Morgan and Stimpson (2017), each new Cane Creek location is like a wildcat well requiring special attention to structure (potential closure or subtle folding, local dip, and faulting) and reservoir quality. Additionally, exploration outside of the Cane Creek unit has not resulted in any new high-yielding oil discoveries.

The purpose of this report is to document the hydrocarbon resource potential of the Cane Creek shale in the northern Paradox Basin where the Utah School and Institutional Trust Lands Administration (SITLA) owns significant acreage. New cores drilled along the Salt Valley anticline near Crescent Junction for the purpose of potash exploration also captured several clastic cycles including the Cane Creek and overlying cycle 19, a possible secondary horizontal target that had never been previously cored. These new cores provide the first glimpse at the geology of these intervals north of Big Flat field and were described/analyzed for reservoir characterization and quality. This evaluation provides a better understanding of the northern Cane Creek facies and proximal setting near the Uncompahgre uplift. The new core data reveals a tidal to supratidal depositional setting that encountered cyclic sea-level fluctuations that coincided with the intertonguing of siliciclastics shed from the Uncompahgre highlands. The combination of both transgressive sea levels and fluvial deposition led to relatively thick successions of porous siltstone-sandstone (reservoir) interbedded with organic-rich mudstone (source rock). Although the study area is at relatively shallow depth along the Salt Valley anticline, the data suggests similar facies and reservoir quality within SITLA and federal acreage to the west, the latter of which might be of interest for potential land acquisition.

ACKNOWLEDGMENT

In 2018, LaVonne Garrison, Assistant Director of Oil and Gas for the Utah School and Institutional Trust Lands Administration, commissioned the Utah Geological Survey to define the economic potential of the Cane Creek shale in the northern Paradox Basin on federal and SITLA land. The project was funded by SITLA and completed by the UGS under a Memorandum of Understanding between the two agencies during the 2018–2019 fiscal year. The UGS described and analyzed recently drilled cores along the Salt Valley anticline (donated to UGS from Pinnacle Potash International Ltd) and evaluated the petroleum potential of the northern Cane Creek resource play.

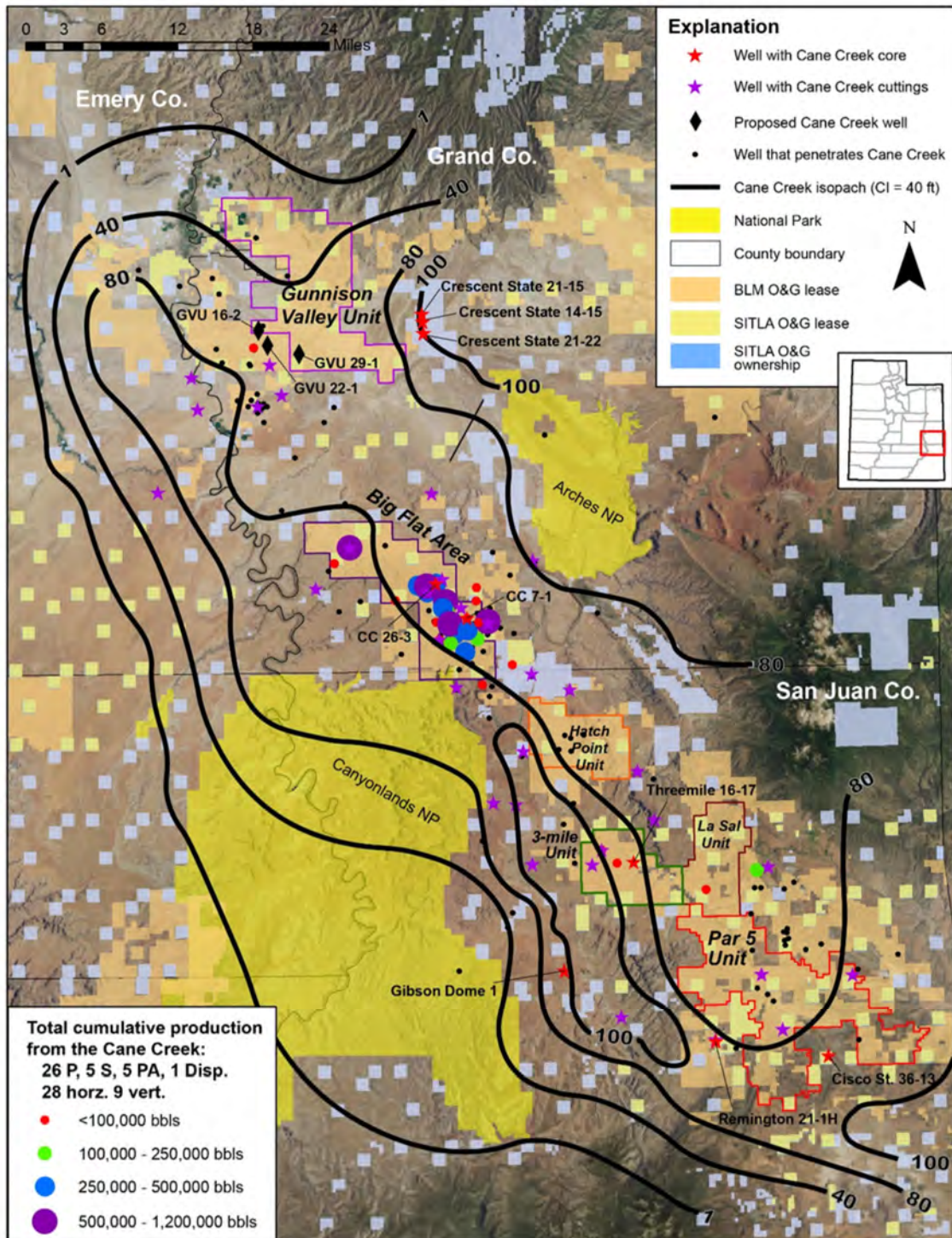


Figure 8. Cane Creek cumulative production in the Paradox Basin highlighting additional wells that have penetrated the Cane Creek. Producing fields, current oil and gas leases, and SITLA mineral ownership are highlighted.

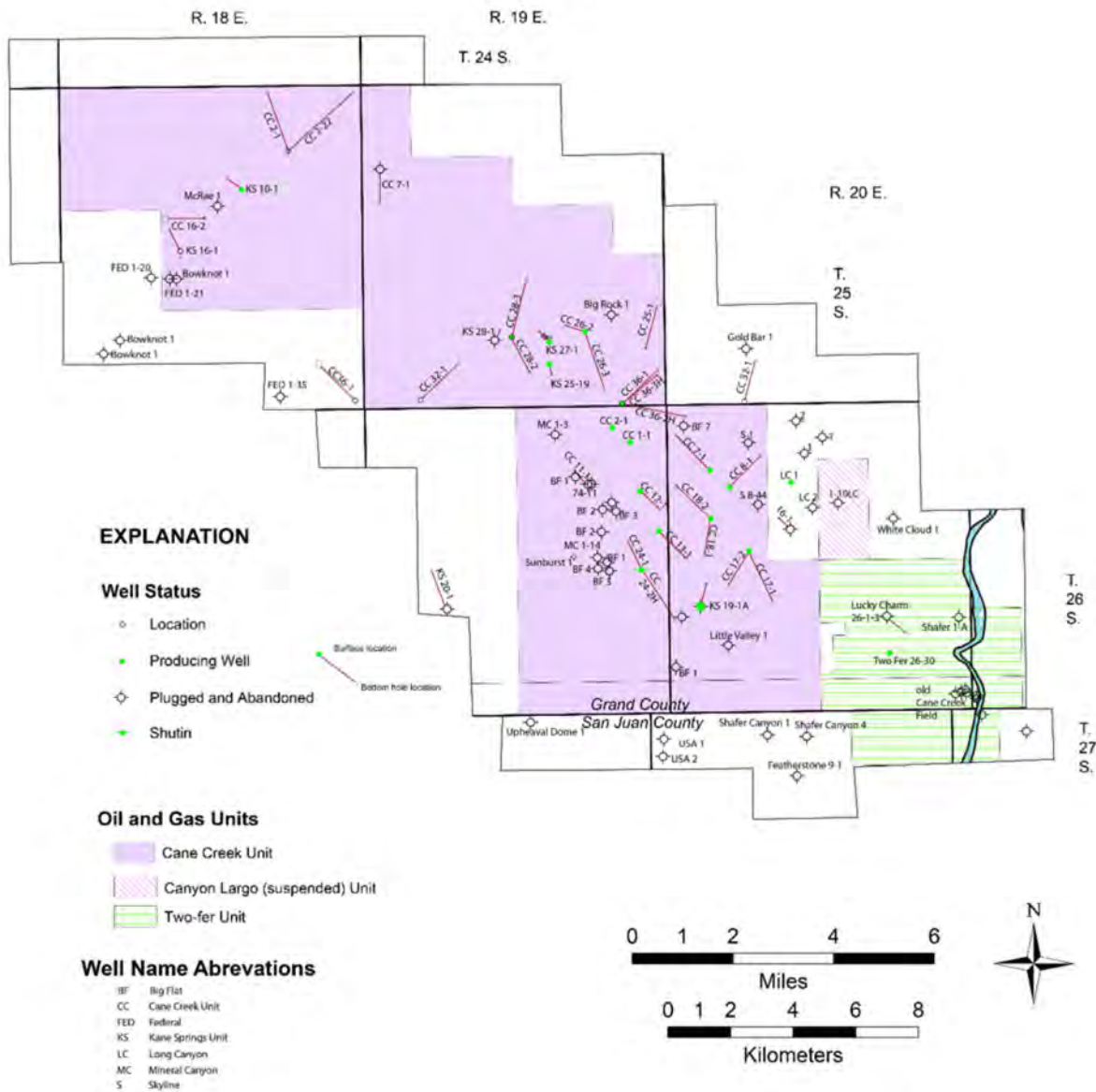


Figure 9. Cane Creek federal unit and neighboring units. Columbia Gas and Development originally formed the Kane Springs unit and drilled the first horizontal Cane Creek well, the KS 27-1. Fidelity Exploration and Production Company purchased the unit and established a new unit name, Cane Creek, covering the same acreage.

OBJECTIVE AND GOALS

The Cane Creek shale in the Paradox Basin has been a target for oil and gas exploration on and off since the 1960s and oil is produced from several fields. The play generated renewed interest in the early 1990s with the successful application of horizontal drilling. Drilling activity increased in the 2000s because of rising oil prices and continued until 2014 when prices collapsed.

Whidden and others (2012) assessed the undiscovered oil resource in the Cane Creek shale of the Paradox Basin at 103 MMBO with a 95% confidence level, 198 MMBO with a 50% confidence level, and a mean of 215 MMBO (table 3 and appendix A). Nonetheless, limited research has been conducted or published to further define the play and the reservoir characteristics, particularly in the northern part of the Paradox Basin.

Objective

The overall objective was to perform a detailed geologic characterization and evaluation of the northern Paradox Basin Cane Creek resource play taking advantage of newly recovered core material (clastic cycles 19 and 21), and to compare the results to the productive Big Flat area to the south.

Goals

The goal of our study was to generate a geologic characterization and assess reservoir quality of the Cane Creek and cycle 19 intervals in the northern Paradox with newly acquired core. Additional goals include: 1) comparing geologic attributes from the new cores to the geology in the productive Big Flat area and the mostly unproductive areas farther south (Lisbon area), and 2) discussing the drilling results in the north and why it has not been successful.

Potash exploration along the Salt Valley anticline has provided seven new cores that were drilled in 2014 and acquired by UGS in 2016. Geologic information obtained from these new cores will be useful for understanding the lateral extent of reservoir and source rock facies, as well as source-rock maturity, in the northern Paradox Formation. The data will be useful for northern Cane Creek petroleum exploration and can be compared to well test and production data from wells that are planned to be drilled in 2019 by Rose Petroleum LLC on the Gunnison Valley unit, 6 miles west of the core locations.

This research provides detailed geologic information that will hopefully help reduce drilling risk and possibly increase hydrocarbon production and recorded reserves to the north of Big Flat.

Tasks

- 1) Pull core material, evaluate quality, and pick cores to be slabbed
 - a. Four cores include Cane Creek (cycle 21), but only one (Crescent State 21-22) was considered on the basis of quality of core and completeness
 - b. Six cores include clastic cycle 19, two with possible repeat sections
- 2) Slab select core intervals and photograph core
- 3) Perform detailed geologic description of slabbed cores
- 4) Draft core descriptions and build integrated core log plates
- 5) Analyze core for source rock/reservoir quality (XRF, XRD, porosity/permeability, source rock analysis)

- 6) Create revised maps as needed (isopachs, isochore, maturity)
- 7) Generate final report with all data and analyses and summarize the petroleum potential of the Cane Creek and other clastic cycles in the northern Paradox Basin

PREVIOUS STUDIES

Geologic studies of the Paradox Basin are extensive and span the past 80 years. The basin has attracted geologists with its scenic geology, complex stratigraphy, and structural attributes as well as economic geologists interested in hydrocarbons, uranium, potash, and copper. The following is a brief overview of the available publications that are the most relevant for background information.

Recent publications on the petroleum geology of the Paradox Basin are presented in a topical Rocky Mountain Association of Geologists volume (Houston and others, 2009), which includes an extensive bibliography by Rasmussen and others (2009). Anna and others (2014) and Whidden and others (2014) present preliminary work completed for the U.S. Geological Survey resource assessment currently in final preparation.

Basin-wide studies of the stratigraphy and tectonics of the Paradox Basin include Baker and others (1933), Wengerd and Matheny (1958), Mallory (1972), Szabo and Wengerd (1975), Baars and Stevenson (1981), Goldhammer and others (1991), Montgomery (1992), Huffman and others (1996), and Blakey (2009). Studies specific to the Paradox Formation were published by Hite (1960), Peterson and Hite (1969), Hite and Buckner (1981), and Hite and others (1984).

Papers on the structure of the Paradox Basin were published by Kelley (1958), Baars (1966), Kluth and Coney (1981), Barbeau (2003), Kluth and DuChene (2009), and Trudgill (2011). Cater (1970), Hite and Cater (1972), Doelling (1988), Doelling and others (1988), and Rasmussen (2014) and all discuss the salt tectonics in the basin.

Papers specifically dealing with the petroleum system within the Paradox Basin were published by Montgomery (1992), Whidden and others (2012), Anna and others (2014), Stevenson and Wray (2014), and Whidden and others (2014). Petroleum geochemistry is discussed by Nuccio and Condon (1996), Guthrie and Bohacs (2009), and Rasmussen and Rasmussen (2009).

Smith (1978a, 1978b, 1978c, 1978d, 1978e) published papers on Bartlett Flat, Big Flat, Cane Creek, Long Canyon, and Shafer Canyon fields. Morgan and others (1991), Morgan (1992a, 1992b), and Grove and others (1993) discuss the geology of the Bartlett Flat-Big Flat (Kane Springs unit) fields, and Grove and Rawlins (1997) discuss the Cane Creek shale exploration play in the Big Flat and neighboring area.

Finally, a recent report by Morgan and Stimpson (2017) provides reservoir-specific geological and engineering analyses of the oil producing Cane Creek shale (and other potential hydrocarbon producing clastic/shale units) of the Paradox Formation in the Paradox Basin, southeast Utah.

GEOLOGIC SETTING

Structure

The Paradox Basin is a Pennsylvanian-age structural basin in the Four Corners area of southeast Utah and southwest Colorado and a smaller part of northeast Arizona and northwest

New Mexico (figure 1). Prior to development of the Paradox Basin, the Four Corners area was part of a regionally extensive, stable cratonic shelf dominated by shallow marine carbonate deposition (figure 10) (Nuccio and Condon, 1996; Blakey, 2009). Regional uplift during the Late Mississippian and Early Pennsylvanian resulted in exposure and karstification of the Mississippian carbonates (Nuccio and Condon, 1996).

At the beginning of the Pennsylvanian, the collision of the Gondwana and Laurentia plates (Barbeau, 2003; Kluth and Duchene, 2009) resulted in the rise of the Uncompahgre uplift of the Ancestral Rocky Mountains and subsidence of the Paradox Basin (Blakey, 2009) (figure 11). The area subsided along a series of northwest-trending faults forming an asymmetrical oval-shaped basin deepest along the boundary with the Uncompahgre uplift of the ancestral Rocky Mountains (figure 5). Faulting was strongly influenced by rejuvenation of pre-existing late Precambrian-age northwest-trending structures (Baars and Stevenson, 1981).

The Paradox Basin is commonly divided into the Paradox fold and fault belt, Blanding sub-basin, and Aneth platform within the Blanding sub-basin (figure 1) (Whidden and others, 2014). The Paradox Basin is separated from the Uncompahgre uplift to the east and northeast by a series of high-angle faults having thousands of feet of displacement (figure 5). The uplift had a maximum elevation of 12,000 to 15,000 feet (Stokes, 1986). The basin is bounded to the



Figure 10. Paleogeography during the Mississippian Period (340 Ma) interpreted by Blakey and Ranney (2008). The Colorado Plateau including the Paradox Basin was dominated by shallow-marine carbonate deposition with deeper open-marine deposition to the west. Modified from Blakey and Ranney (2008).



Figure 11. Paleogeography of the Colorado Plateau and Paradox Basin (outlined in blue) during the Middle Pennsylvanian (308 Ma) illustrating a highstand depositional cycle. The basin formed as a pull-apart basin along a series of northwest-trending faults forming an asymmetrical basin bounding the Uncompahgre uplift, part of the ancestral Rocky Mountains. The basin was bounded to the south by the Defiance-Zuni platform and the Emery shelf to the west. Modified from Blakey and Ranney (2008).

south and southwest by the Defiance-Zuni platform. The Emery shelf to the west separated the basin from the open-marine shelf environment (figure 11) (Herman and Sharp, 1956; Hintze and Kowallis, 2009).

The Paradox Basin was located in a subtropical, arid environment and is commonly defined by the maximum extent of the salt in the Paradox Formation of the Hermosa Group (figure 1) (Condon, 1997), although deposits of the Paradox and overlying Honaker Trail Formations extend beyond the limits of the salt. The saline deposits of the Paradox are bounded by shallow marine deposits of the underlying Pinkerton Trail and overlying Honaker Trail (figure 4).

Glacial and interglacial climatic cycles in the southern hemisphere of the Pangean continent caused cyclic fluctuations in relative sea level and salinity (Hite and Buckner, 1981; Goldhammer and others, 1991; Whidden and others, 2014). The cyclicity in the highly restricted Paradox Basin resulted in a series of upward-shoaling, disconformity-bounded deposits of marine, organic-rich, black shale through carbonate to hypersaline salt. The cycles are considered fourth-order depositional cycles (cyclothems of 0.2–0.5 m.y. [Mitchum and Van Wagoner, 1990]) (Anna and others, 2014). The 20+ cycles resulted in deposition of thousands of feet of evaporites, mainly halite, with lesser amounts of potassium and magnesium salt and

anhydrite. The salt beds are interbedded with thin clastic beds consisting of anhydrite, anhydritic-dolomitic mudstone, silty dolomite, dolomite, very fine grained sandstone and siltstone, and thin (inches) organic-rich shale (Peterson and Hite, 1969; Hite and others, 1984). The faulted terrain within the basin partly controlled deposition of the lower cyclic units and the development of salt-cored anticlines that are dominant structural features in the Paradox Basin fold and fault belt (Kelly, 1958). The stacked sequences of shale and salt that compose most of the Paradox Formation is referred to as the saline facies of the Paradox (Hite, 1960). The salt and shale sequences interfinger with clastics to the northeast that were shed off the Uncompahgre uplift and with penesaline and normal marine carbonates to the southwest (figure 5).

The heterolithic mudstone and siliciclastic packages have been lumped and termed “clastic marker beds.” The clastic packages represent condensed sedimentation deposited during relative sea-level rise and highstand (global greenhouse conditions) (figure 11) and evaporites were deposited during marine lowstands (global icehouse conditions) (figure 12) (Goldhammer and others, 1991; Whidden and others, 2014). Clastic beds range in thickness from 10 to 200 feet and are generally overlain by 200 to 400 feet of halite. The clastic beds are used as markers for regional correlation (Hite and Buckner, 1981; Goldhammer and others, 1991; Nuccio and Conden, 1996; Trudgill and Arbuckle, 2009; and Massoth, 2012). Twenty-

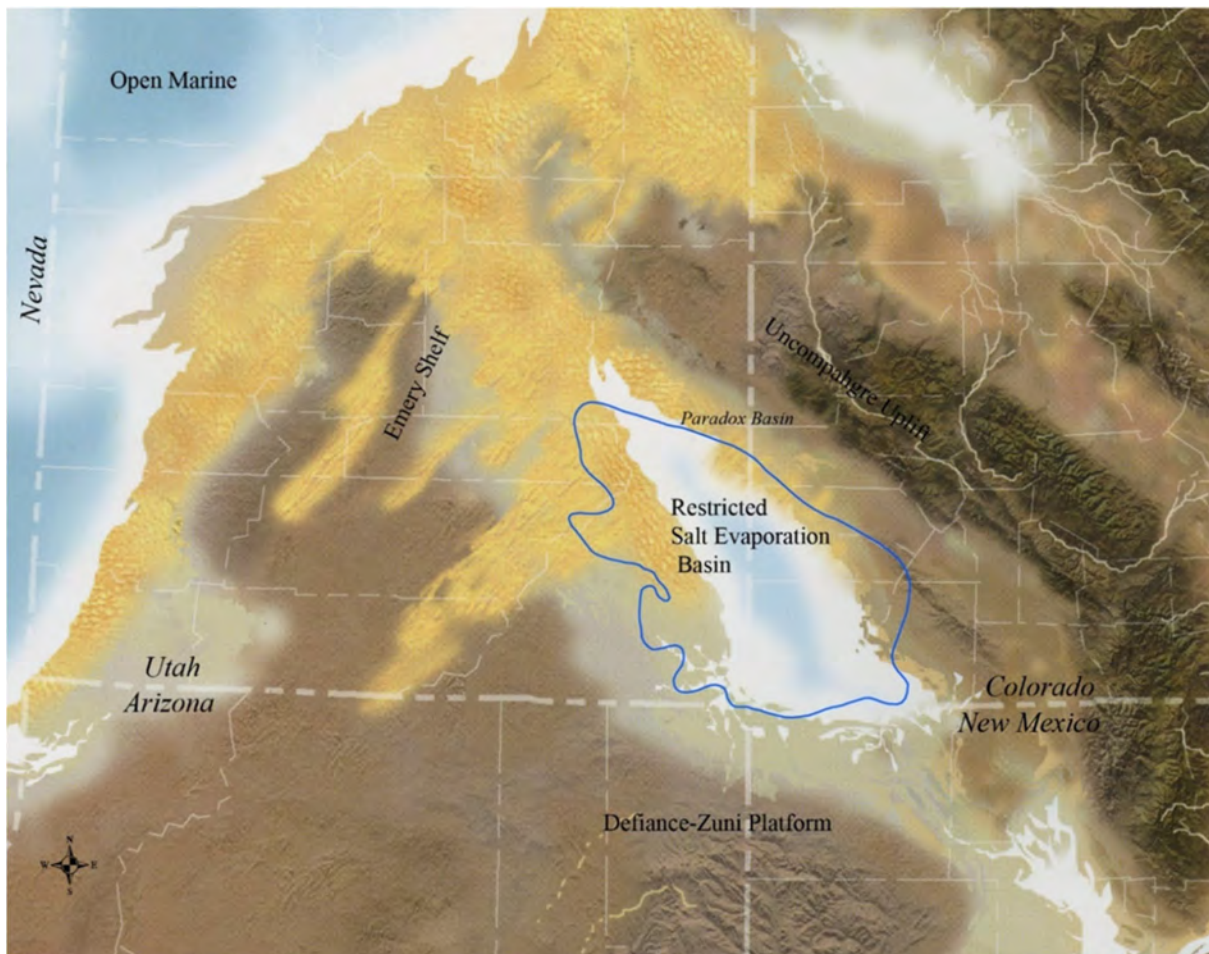


Figure 12. Paleogeography of the Colorado Plateau and Paradox Basin (outlined in blue) during the Middle Pennsylvanian (308 Ma) illustrating a lowstand depositional cycle. Dominant deposition during lowstand were the evaporites anhydrite and halite as well as coastal eolian deposits. Modified from Blakey and Ranney (2008).

nine fourth-order depositional cycles have been described in the Moab area (Hite, 1960; Hite and Buckner, 1981). Hite and Cater (1972) and Reid and Berghorn (1981) divided the Paradox Formation into informal production zones, in ascending order, Alkali Gulch, Barker Creek, Akah, Desert Creek, and Ismay (figure 4). The Cane Creek is within cycle 21 in the Alkali Gulch zone (Hite, 1960; Hite and Cater, 1972; Reid and Berghorn, 1981). Rasmussen and Rasmussen (2009) defined 80 depositional cycles in the Paradox Basin; 59 cycles are within the Hermosa Group and 21 cycles are in the overlying Elephant Canyon Formation of the Cutler Group.

Siliciclastics shed off the Uncompahgre uplift eventually filled the Paradox Basin and red-bed continental deposition dominated from the Permian through Jurassic time (figure 13). The sediment loading in the Paradox Basin caused the Paradox salt to flow laterally and vertically during the Middle Pennsylvanian (late Desmoinesian) reaching a peak in Late Pennsylvanian time (Missourian and Virgilian) resulting in numerous northwest-trending, salt-cored anticlines (figure 6) (Anna and others, 2014). Significant salt movement continued into the Early Triassic (Rasmussen and Rasmussen, 2009). The breakup of Pangaea and the resulting



Figure 13. Paleogeography of the Colorado Plateau and Paradox Basin (outlined in blue) during the Middle Triassic (240 Ma). The area was dominantly a low-lying arid environment with channel and floodplain deposits. The Paradox Basin is completely filled in and sediment loading during the Permian and Triassic initiated movement of salt and development of salt anticlines. Modified from Blakey and Ranney (2008).

Cretaceous Interior Seaway to the east caused deposition of thick marine shales and sandstones in the basin (figure 14). The Paleogene was a time of major Laramide uplift in the western interior with gentle epeirogenic uplift of the Colorado Plateau and Paradox Basin. The Paradox Basin was deeply incised during the Neogene by the present-day Colorado and Green Rivers and their tributaries. The erosion created canyons and plateaus exposing the salt anticlines and eolian deposits of the Triassic and Jurassic Glen Canyon Group throughout much of the Paradox Basin (figure 15).



Figure 14. Paleogeography of the Colorado Plateau and Paradox Basin (outlined in blue) during the Early Cretaceous (Albian, 105 Ma). With the Sevier Orogeny to the west, the Colorado Plateau subsided and the Cretaceous Interior Seaway advanced from the north into the plateau area depositing deltas, shoreline swamps, and open-marine sediment. Much of the Cretaceous deposits were removed from the Paradox Basin during uplift of the Colorado Plateau. Modified from Blakey and Ranney (2008).



Figure 15. View south from Dead Horse State Park. View area and mesas in the background are formed by eolian Triassic Wingate Sandstone and typically topped by the Jurassic Navajo Sandstone. At this location the Colorado River has incised the Lower Permian Cutler Group. Photograph by Gregg Beukelman.

Cane Creek Shale

Overall, the Cane Creek shale is mostly composed of dolomite, silty dolomite, and mixed dolomite with some limestone, often with abundant mottled anhydrite displacing dolomitic mudstones. Sandstone/siltstone beds have been identified in select cores from the Big Flat area. Thin organic-rich silty mudstone beds are the source for Cane Creek hydrocarbons. The Cane Creek is informally divided into zones A, B, and C, in descending stratigraphic order (figure 16). The A and C zones are transitional with the overlying and underlying salt beds and typically contain interbedded and nodular anhydrite with dolomite. The B zone is the primary productive unit in the Cane Creek. The average total organic carbon of the thin black shales in the B zone is 15% and some samples have up to 28% (Grumman, 1993).

The Morgan and Stimpson (2017) report provides a study by Core Laboratories (Core Labs) on the Cane Creek 26-3 well core from the Big Flat field and the following diagenetic sequence for the Cane Creek shale (appendix C): (1) early pyrite, (2) finely crystalline dolomite cement, (3) quartz overgrowth, (4) partial dissolution of less stable feldspar grains, (5) dolomitization, (6) calcite cement, (7) anhydrite cement and replacement, and (8) late stage halite fracture filling. Eby Petrography and Consulting studied thin sections from the

4301915925
Southern Natural Gas Co
Long Canyon, #1



TD 8130 FT
KB 5794 FT

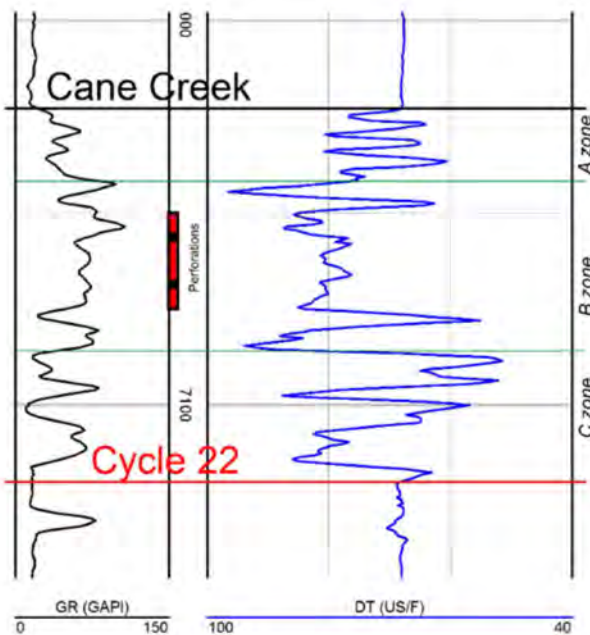


Figure 16. Gamma ray and sonic travel time (sonic) curves through the Cane Creek shale from the Long Canyon 1 well. The Cane Creek is informally divided into A, B, and C zones. The A and C zones are transitional with the overlying and underlying salt beds and contain abundant interbedded and nodular anhydrite. The B zone is the primary productive interval in the Cane Creek containing silty dolomite and very fine grained sandstone.

Remington 21-1H core (appendix D), located in the southern play area, and described some calcite in the dolomitic muds, indicating incomplete dolomitization. Anhydrite replaced some dolomite grains and dolomitic muds. Some anhydrite crystals were replaced by iron-sulfide indicating minor later stage pyrite. Some microfractures and anhydrite-filled vugs are lined with bitumen.

Siltstone to very fine grained sandstone beds within the B zone are the primary horizontal drilling targets in the Big Flat area. The sandstone has generally higher porosity than the carbonates and therefore greater storage capacity. Core plug data from the Cane Creek 26-3 well averages 10% porosity in the sandstone (24 samples) and 5% porosity in the carbonates (46 samples). The sandstone is composed of mostly very fine grained, sub-round to sub-angular, well-sorted quartz with some very fine dolomite grains interpreted as wave modified eolian deposits that accumulated on paleo highs within the basin.

Fault-associated anticlines are the primary drilling targets (Grove and others, 1993) and are believed to have the highest density of fracturing. These faults are not reflected on the surface and must be seismically imaged to be identified. Second-order folds due to salt movement have amplitudes of 15 to 100 feet and apparent wavelengths of 300 to 600 feet (Grove and Rawlins, 1997). Fracture data from orientated cores in the Cane Creek shale show a

regional northwest to southeast, near vertical, open extensional fracture system that is not significantly affected by the orientation of local folds (Grove and Rawlins, 1997).

The Cane Creek was deeply buried but is now as much as 9000 feet shallower than maximum burial due to uplift of the Colorado Plateau and subsequent erosion (Rasmussen and Rasmussen, 2009). The thick overlying and underlying salt provide an excellent seal for the hydrocarbons and fluid pressure. The fluid gradients in the Cane Creek at Big Flat range from 0.75 to 0.95 psi/ft. The oil is sweet paraffinic crude with 36° to 43° API gravity and a 40° to 45° F pour point (Grove and others, 1993). The associated gas has a heating value of 1200 to 1400 British Thermal Units (Btu) per cubic foot, with a trace of carbon dioxide (CO₂) and no hydrogen sulfide (H₂S) (Grove and others, 1993). The most productive wells to date producing from the Cane Creek shale are the vertical Long Canyon 1 well drilled in 1963 with a production over 1 million barrels of oil equivalent (MMBOE) and the horizontal Cane Creek 12 -1 well drilled in September 2012 that has produced roughly 980 MBO (0.98 MMBOE) (figure 17).

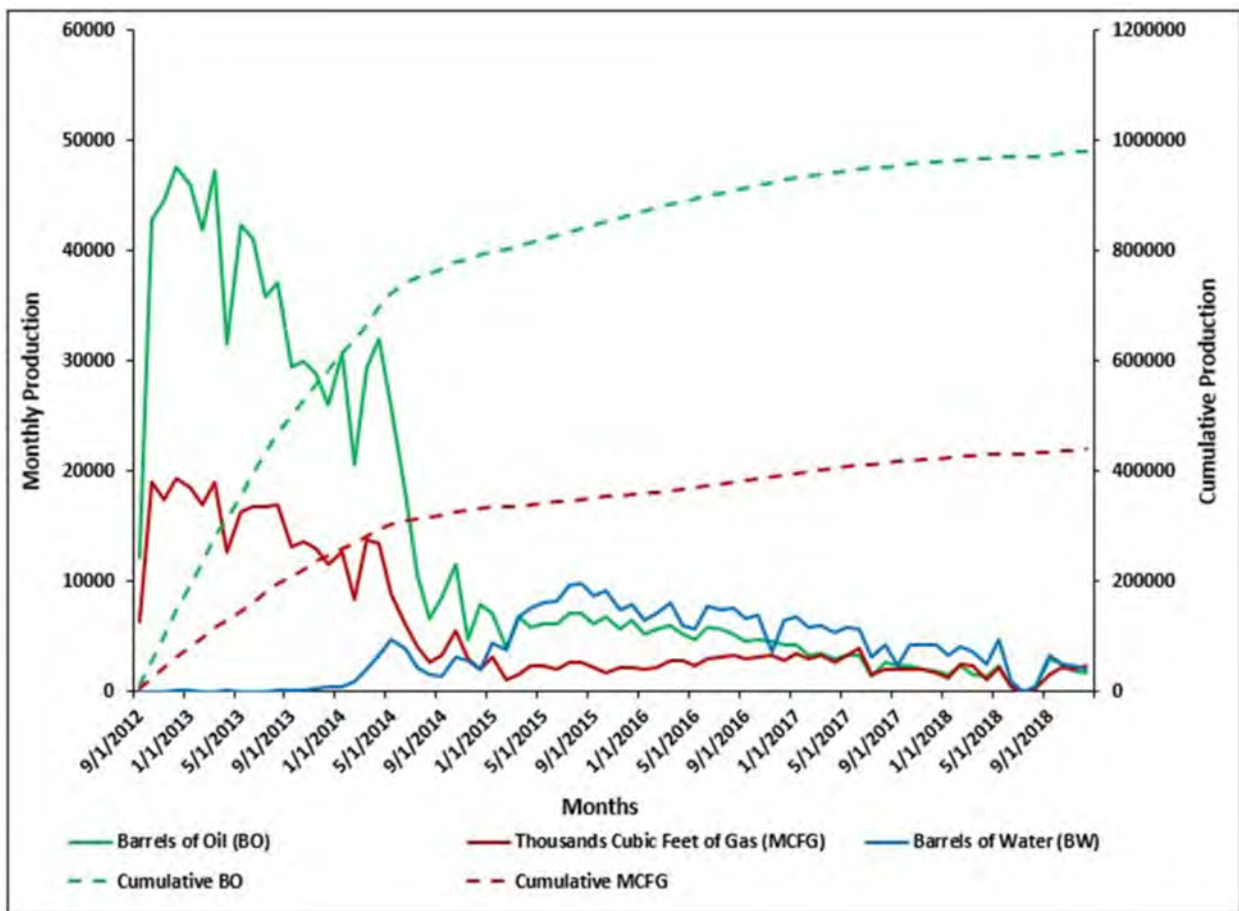


Figure 17. Production curves for Cane Creek 12-1 (section 12, T. 26 S., R. 19 E.), the most productive horizontal well in the Cane Creek unit. In 76 months the well has produced more than 980 MBO and 441 MMCFG. Production data from Utah Division of Oil, Gas and Mining.

Clastic Cycle 19

As seen in newly acquired cores, cycle 19 contains similar depositional rock types as the Cane Creek; however, there have been limited attempts to produce oil from the cycle 19 unit. From one of the new cores, cycle 19 contains a thick (up to 38 ft) package of very fine grained and bioturbated sandstone with porosities between 6 and 8%. Overlying and underlying the sandstone unit are tight anhydritic-dolomitic mudstones that are interbedded with organic-rich mudstones. This succession is similar to the designated A, B, and C zones for Cane Creek.

In the Big Flat area, four wells have produced from cycle 19: Kane Springs 16-1 (section 16, T. 25 S., R. 18 E.), Cane Creek 36-3H (section 36, T. 25 S., R. 19 E.), and the vertical Cane Creek 1-1 (section 1, T. 26 S., R. 19 E.) (figure 18). The Long Canyon 1 was recompleted with perforations in cycle 19 and the production was commingled with the Cane Creek. Production from cycle 19 is estimated to have contributed about 100 MBO to the total production from the Long Canyon 1 well (Morgan and Stimpson, 2017). The 16-1 was drilled horizontally in cycle 19 and completed in 1993 producing 93 BOPD. The well was converted to a water disposal well in 1998 after producing a total of 15,589 BO, 27,465 MCFG, and 2368

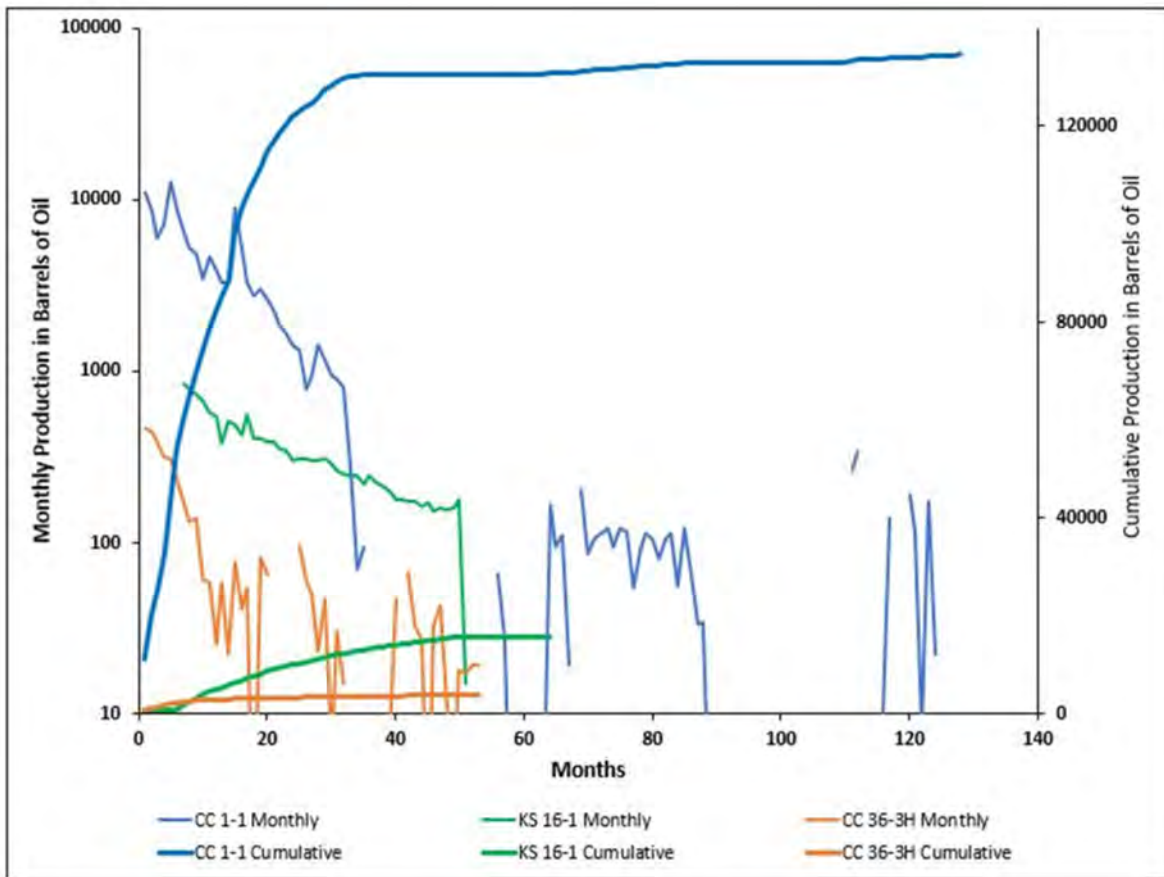


Figure 18. Oil production curves from cycle 19 of the Paradox Formation for Cane Creek 1-1 well (section 1, T. 26 S., R. 19 E.), Kane Springs 16-1 well (section 16, T. 25 S., R. 18 E.), and Cane Creek 36-3H well (section 36, T. 25 S., R. 19 E.). KS 16-1 and CC 36-3H are horizontal wells, CC 1-1 produced from a vertical borehole. Each well was completed at different times but the production for all wells is shown starting at month 1 for easy comparison. Data from Utah Division of Oil, Gas and Mining.

BW. The Cane Creek 1-1 well is a vertical completion and the best cycle 19 producing well. The well was completed in 2008 producing 439 BO per day and 262 MCFG per day. Total production through December 2018 is 135 MBO and 135 MMCFG; the well was shut-in in November 2015 and reopened June 2017. The 36-3H well was completed in 2014 producing 54 BOPD and 50 MCFGPD. Total production through December 2018 is 3821 BO and 1775 MCFG, production for the month of December 2018 was 19 BO.

DRILLING AND COMPLETION METHODS

Drilling Techniques

The Cane Creek shale and other Paradox Formation clastic beds often display good oil shows when drilled but are difficult to establish long term production. Drilling in the Big Flat area during the 1950s and 1960s was focused on the Mississippian Redwall Limestone, but when a well failed to establish production from the Redwall, the operators would often attempt to complete the well in the overlying Cane Creek. Although many wells tested small volumes of oil, only one well, Long Canyon 1, was an economic success.

Drilling is complicated due to the unique challenges presented by the thick accumulations of salt in the Paradox Formation. Best practices involve drilling to the top of the salt and setting casing. The sedimentary sequence above the salt is low pressure due to exposure along the canyons of the Colorado River. The salt has very high fluid pressure requiring weighted mud that would be lost into the lower pressure formations above. Most operators drill with an oil-base mud to prevent dissolving the salt and creating large wash outs in the drill hole. To complete a well, high-strength casing is required in the Paradox salt section, otherwise the casing can collapse by the plastic movement of the ductile salt.

Renewed interest in the Cane Creek shale came from the development of horizontal drilling, which greatly increases the volume of the reservoir exposed in the well bore and increases the potential to encounter fractures. A horizontal well was completed in 1991 by Columbia Gas in the Kane Springs unit, establishing economic production from the Cane Creek in what would become the Big Flat field. In 2007, Fidelity E&P purchased the Columbia Gas assets in the Cane Creek play. Fidelity E&P shot 3D seismic, drilled vertical pilot holes, collected core from the Cane Creek, then moved uphole and began drilling at an angle to intersect the Cane Creek horizontally. The Fidelity wells are typically drilled on seismically imaged local structures and fault closures.

Natural fractures are an important reservoir characteristic for economic completion in the Cane Creek shale and can provide high-volume oil production without artificial stimulation of the reservoir. Drilling horizontally greatly increases the probability of intersecting open fractures. The orientation of the fractures in the area is northwest to southeast with a smaller conjugate set of fractures trending northeast to southwest (appendix C). Most fractures are steeply dipping and those cemented with halite and/or anhydrite are generally the widest. The direction of the horizontal wellbore is based on the dip of the structure being tested, the available surface location, and lease and reservoir drainage models. The orientation and length of each horizontal well is different. Comparison of horizontal lengths and direction to the flush production (first six months) of the wells displays no correlation. For example, some short laterals parallel to the regional fracture trends have out-produced long reach laterals drilled in a similar direction or perpendicular to the fracture trend. Each well location is structurally unique; each location has unique lease and drainage objectives, greatly complicating development of the area.

The objective of horizontal drilling in the Cane Creek shale is to penetrate the Cane Creek with the drill bit parallel to the bedding plane. The Cane Creek is not a flat-lying bed so the trajectory of the wellbore can be very complex. It is generally desirable to drill the bed at low dip (up or down) so the drill string can slide through the section. Secondary folding from salt movement resulted in a wave-like structure of the Cane Creek, with approximate wave heights of 300 feet and distances of 1000 feet (Grove and others, 1993); as a result, an ideal horizontal well in the Cane Creek has a wave-pattern following structural dip.

Completion Techniques

The Cane Creek and other Paradox Formation clastic intervals are overlain and underlain by anhydrite and thick salt (halite) deposits (figure 4). Inducing fractures through artificial stimulation runs the risk that the fractures will extend into the overlying and underlying salt and, along with saturated brine within the formation, mobilize the salt and redeposit it in the main reservoir, perforations, and production tubing.

Several of the wells in the Greentown area were treated with a slick-water and proppant stimulation. Many of the treated wells reported salt plugging during testing. However, the casing collapsed in those wells, unrelated to the stimulation, so without long-term production it is unknown if salt plugging would have persisted or if it was only a temporary problem. The Federal 28-11 well was perforated and treated with a slick-water and proppant stimulation in repeated sections of the Cane Creek and cycle 19 and is the only producing well in the Greentown field. The well records show salt plugging during production testing but it is not publicly known if plugging continues to be a problem.

The Greentown 36-24H well was first drilled as a vertical well. The Cane Creek and lower clastic intervals were perforated and treated with an oil-based proppant stimulation. Oil-base fluid is used to prevent dissolving and mobilizing the formation salt. Some frac-sand fill problems were reported during production testing but there was no report of salt plugging. The well was swabbed recovering minor shows of oil and gas but never fully recovered the treatment volume (load). The Greentown 36-24H was plugged and abandoned after two unsuccessful attempts were made to drill horizontally in the cycle 19 interval.

The Fidelity E&P Cane Creek 32-1-25-19 horizontal well (SWSW section 35, T. 25 S., R. 19 E.) was completed (May 2014) as a low-volume oil well in the Cane Creek shale. The well produced 18 MBO and 10 MMCFG in 7 months and averaged 94 BO per day. The well was then treated with about 200 to 400 barrels of mineral oil with proppant per stage, in 6 stages (November 2014). After treatment, the well produced 26 MBO, 13 MMCFG in 7 months averaging 128 BOPD. The increase in production is minor but this was a poor producing well to begin with; high-volume producing wells may respond better to fracture stimulation.

CRESCENT STATE CORES

The Crescent State 21-22 well (CS 21-22) (NWNE section 22, T. 22 S., R. 19 E.) and Crescent State 22-09 well (CS 22-09) (NENE section 9, T. 22 S., R. 19 E.), as well as five other CS wells (not included in this study), were drilled and cored by Pinnacle Potash Inc. through the Paradox Formation along the northern extent of the Salt Valley anticline as part of a potash exploration program (figures 3 and 6). The Cane Creek shale (cycle 21) and cycle 19 were cored in the CS 21-22 well at 4753–4854 feet and 4457–4520 feet, respectively (figures 19 and 20). Well log interpretations suggest a possible repeated, or partially repeated, cycle 19 section in the CS 22-09 core at depths of 2924–2955 ft and again at 2970–3070 ft (figure 21), but both sections appear condensed in comparison to the complete cycle 19 in the CS 21-22 core.

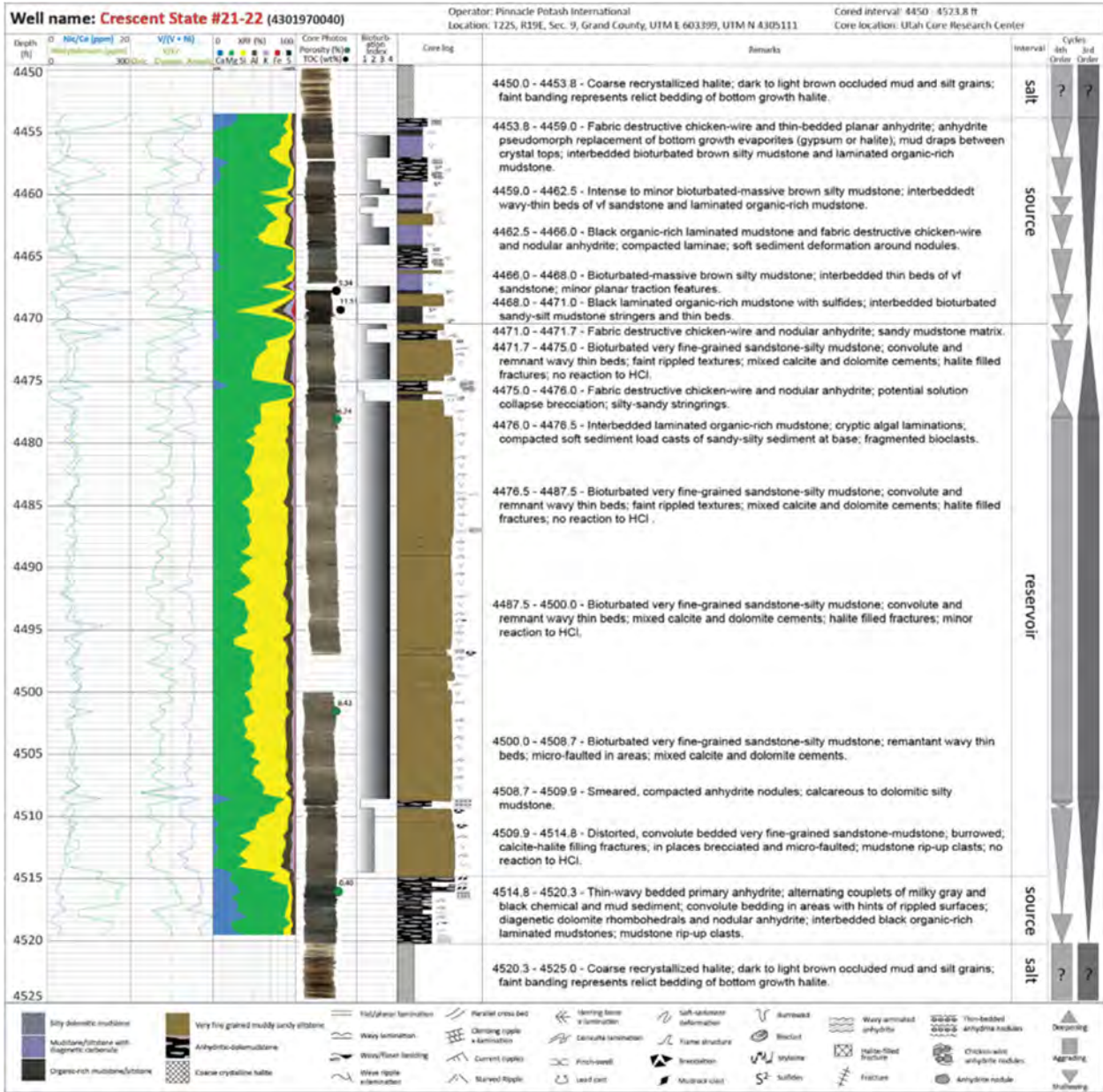


Figure 20. Core description of cycle 19 from Crescent State #21-22.

Considering salt movement and deformation along the Salt Valley anticline, thrusted, repeated, sedimentary sections can be expected where salt has been partially removed and mobilized. The mobilization of salt can also entrain allochthonous sedimentary units into salt welds and recumbent fold structures making the identification of stratigraphic location complex. In this scenario, and based on some sedimentological differences, the cored cycle 19 section in the CS 22-09 well may represent a combination of different entrained clastic cycles and may not be representative of a complete cycle 19 section. High-angle dipping bed sets, halite-filled fractures (up to inches wide), rubble zones, abundant halite-cemented breccias, and entrained intraclasts in overlying and underlying salt beds are key indicators for salt deformation.

Both cored intervals contain overlying and underlying coarse-grained recrystallized salt (halite) beds (appendix E). Portable handheld x-ray fluorescence (pXRF) was conducted on both cores to correlate elemental abundances to relative mineralogy and to utilize elemental paleo-redox proxies for understanding paleoenvironmental conditions and the preservation of organic matter (appendix F).

The cores are housed at the UGS Utah Core Research Center (UCRC) in Salt Lake City. Coring was completed in October 2014 and the wells were slightly deviated due to structural and stratigraphic complexity. Therefore, the cored intervals exhibit steeply dipping bed sets attributed to the southwest and northeast dipping limbs of the anticline. No oil shows were documented from the cores; however, the cores have a petroliferous odor and source rock analyses indicate maturity within the oil window (discussed more below).

Cane Creek - A Zone

The A zone of the Cane Creek was cored from 4752.5 to 4793.0 feet in the CS 21-22 well (figure 19). The zone is highly heterolithic with a numbered frequency of beds (n) consisting of calcareous-dolomitic silty mudstone (n = 6), dolomitic mudstone (n = 6), abundant calcareous organic-rich mudstone (n = 9), nodular and bedded anhydrite (n = 7), and less common thin siltstone (n = 2) (figures 19 and 22). Much of the zone is dolomitic mudstone containing abundant anhydrite (figure 23). Minor attributes include pin-point porosity in dolomite, highly bioturbated calcareous silty mudstones, finely laminated organic-rich mudstones represented by a wavy algal lamina appearance, rippled and burrowed siltstones, and compacted rip-up mudstone intraclasts. Numerous thin fractures are filled with anhydrite (1-3 mm) and wider (5-10 mm) fractures are filled with halite. Open fractures were noted but it is not known if they are natural or coring induced. The zone has a strong petroliferous odor and bitumen is observed in fractures and occluded in halite cements (figure 22).

Anhydrite occurs as nodular aggregates that are fabric destructive (“chicken-wire” anhydrite) (figure 23). Nodular anhydrite deforms primary layering and is indicative of former displacive growth gypsum that precipitated within sulfate saturated pore waters. Some convolute, complex anhydrite textures may resemble solution breccias of bedded anhydrite (see Cycle 19 section below for discussion). This implies the breccias formed by solution collapse when more dilute water infiltrated anhydrite-hosted pores; this can occur on the surface or in the subsurface and distinguishing between these two possibilities is difficult. Regardless, the presence of anhydrite, sulfide minerals, and a lack of burrows implies saline conditions and reducing environments.

Two thin sections of laminated black organic-rich mudstones at 4753.4 and 4790.4 ft were prepared by Wagner Petrographic. Due to the fine-scale laminations, both samples delaminated during preparation (figure 24A and B). Nonetheless, sedimentary grain texture and composition indicate that most of the organic-rich mudstones are heterolithic and calcareous, chiefly composed of calcite and silt-sized quartz with subordinate mica, clays, and dolomite and confirmed by x-ray diffraction (XRD) analysis. Interspersed are recognizable organo-mineralic

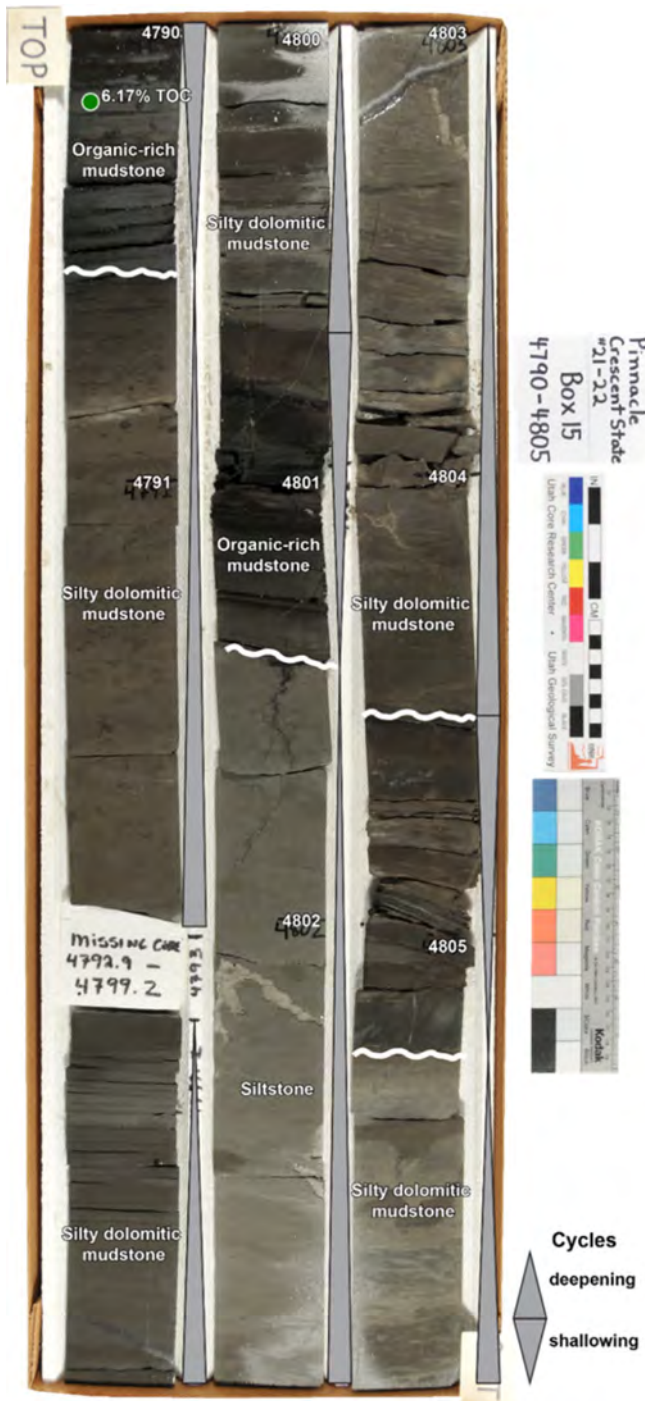


Figure 22. Photograph of core from the Cane Creek shale A zone from the Crescent State #21-22 core (4790--4805 ft) showing representative facies including organic-rich mudstone, bioturbated silty dolomitic mudstone, and siltstone. Gray triangles show interpreted shallowing-upward cycles. White wavy lines are flooding surfaces. Green circle is location for source rock analysis that yielded 6.17 wt% TOC.

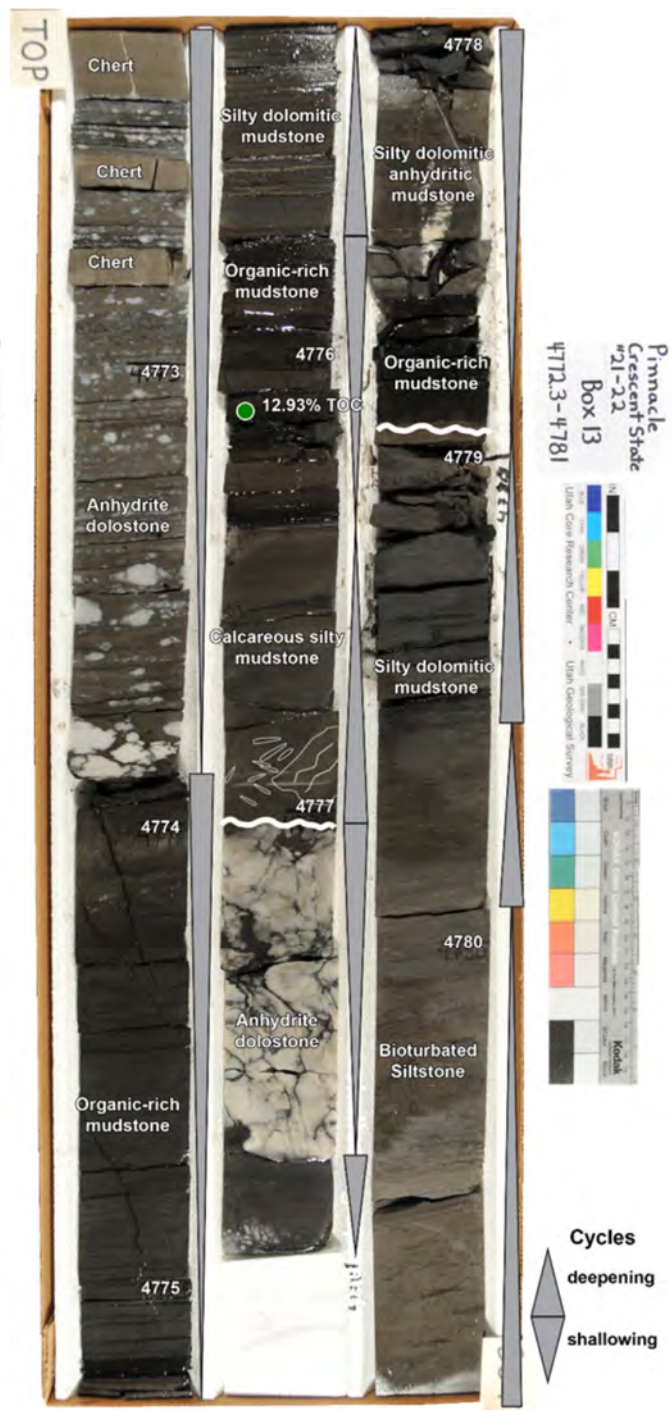


Figure 23. Photograph of core showing representative cyclic facies for the Cane Creek A zone, Crescent State #21-22 (4770-4781 ft). Common facies include laminated black organic-rich mudstones, bioturbated silty dolomitic mudstone, siltstone, and mottled nodular anhydrite. Gray triangles show interpreted shallowing-upward cycles. Outlined in white are mud rip-up clasts above a flooding surface. Green circle is sample location for source rock analysis that has 12.93 wt% TOC.

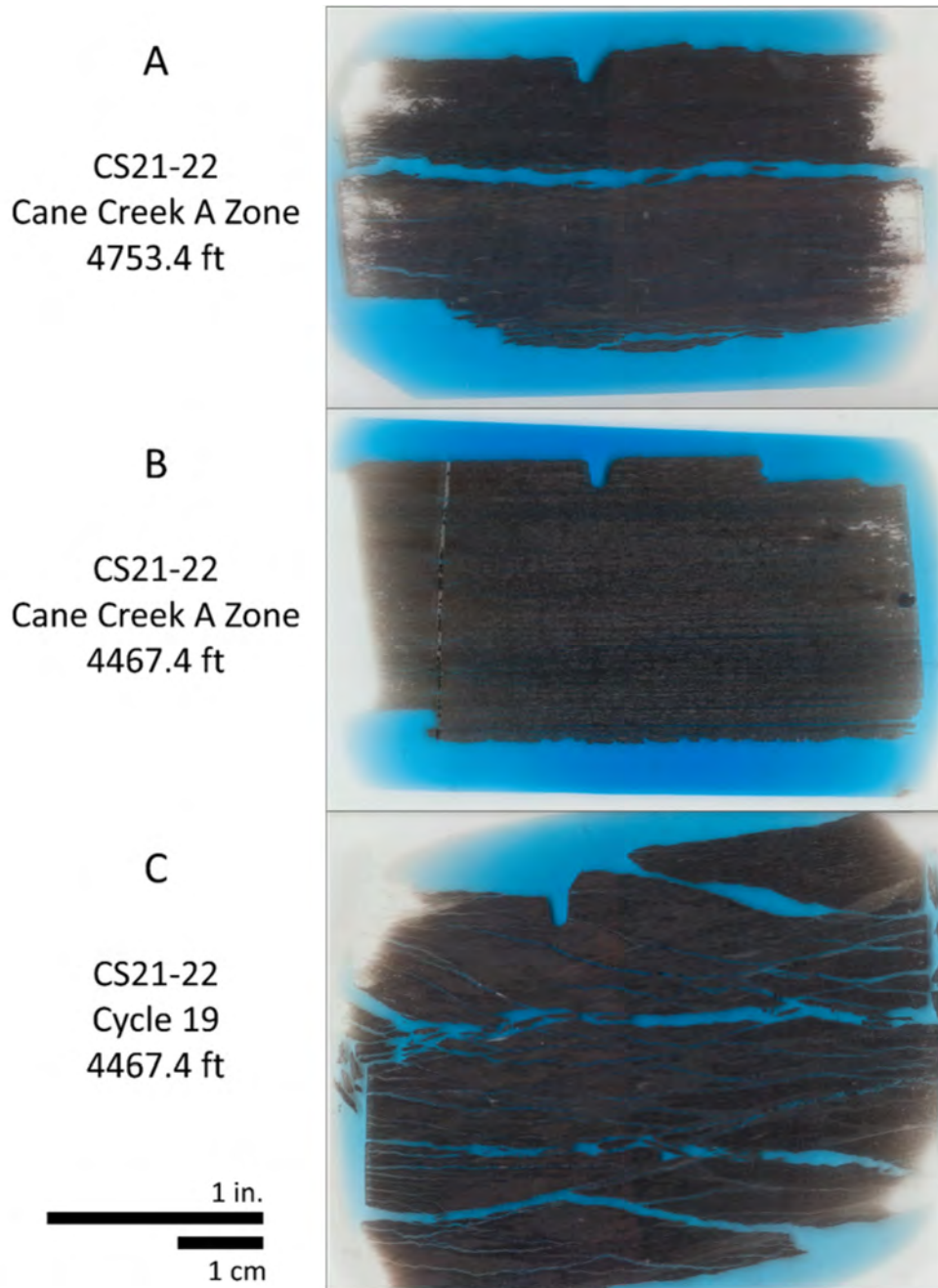


Figure 24. Thin section photomicrograph scans of organic-rich mudstone from Crescent State #21-22 and Crescent State #22-09 cores. Notch cavity on top indicates up direction. Note the large, induced fractures created by sample processing. A, B) Representative source rock samples from Cane Creek (cycle 21). Small-scale (mm) induced fractures cannot be seen for (B) at this scale. C) Representative source rock sample from cycle 19.

aggregates, probable peloidal fecal pellets, and traces of pyrite (figure 25A, B). Under reflected light, algal macerals (bitumen) and liptinite (coaly fragments) are distinguishable and represent both sapropelic and terrestrial organic matter. The paleo-redox proxies V/(V+Ni), V/Cr, Ni/Co, and molybdenum concentrations show some agreement for dysoxic and anoxic conditions during the deposition and preservation of organic matter (figure 19). Speckled sulfides (pyrite) and a lack of burrows and bioclasts also support that deposition occurred in reducing conditions (figures 19 and 25A)

Source rock analyses on three organic-rich samples from the A zone measured relatively high S1 (present hydrocarbons), mature and productive indices, and total organic carbon (TOC) wt% of 10.51 (4753.4 ft), 12.93 (4776.2 ft), and 6.17 (4790.4 ft) (figures 26, 27, 28, 29; table 4). Calculated oil in place from S1 equates to 197, 265, and 74 bbl oil/acre-ft, respectively, using the generalized equation below:

$$\text{Oil in-place (bbls/acre-ft)} = \text{S1 (mgHC/gRock)} \times \text{unit conversion factor} \quad (1)$$

where the unit conversion factor is 21.89 to convert from mg/g to bbls/acre-ft (Javier and other, 2007). This calculation is a rough estimate that does not consider density of oil, rock bulk density, or a reservoir/source rock height; however, it provides an early estimate of oil in place.

Due to the carry-over effect of heavier residual S1 onto S2 kerogen, the samples have suppressed maturity, albeit the estimated maturity of 0.66 to 0.88 %V_{ro} from the Belle Fourche & Second White Specks Model (and other V_{ro} models) suggests the northern extent of the Cane Creek is within the oil window (figure 30). A Pseudo Van Krevelen plot (hydrogen index vs. oxygen index) also indicates a mixed maceral system of both Type I and Type II kerogen, implying a mixture of restricted lagoonal (algal) and marine (planktonic) hydrocarbon sources (figure 31).

Cane Creek - B Zone

The B zone was cored from 4786.0 to 4825.0 feet and is the primary reservoir and productive zone in the Cane Creek. However, no core was retrieved from 4792.8 to 4799.2 ft. The zone consists of calcareous mudstones with dolomite (n = 6), laminated black organic-rich mudstones (n = 5), siltstone to very fine grained sandstone (n = 6), and a thin bed of wavy anhydrite (n = 1) (figures 18, 25C, and 32). The B zone contains much less anhydrite than in the A and C zones. The abundant siltstone to very fine grained sandstone is predominantly bioturbated and is the reservoir facies in the B zone. Interbedded with the reservoir facies is laminated black organic-rich mudstone and massive-bioturbated calcareous mudstone that contains siltstone stringers. The siltstone-sandstone is feldspathic and quartz-rich (subarkose to arkose) with dolomite rhombohedral grains (potentially aeolian) and subordinate micas (muscovite and biotite), and in places, argillaceous material (feldspathic litharenite). Many of the quartz grains are angular, moderately sorted, and have quartz overgrowths at their point contacts. Intergranular pore space is primarily occluded by diagenetic calcite and anhydrite based on one thin section from a lenticular bedded siltstone-sandstone at 4821.4 ft (figure 25C); however, conventional plug analysis by Core Labs yielded a porosity of 17% (figure 33; table 5). Unfortunately, the core plug fractured along bedding surfaces and was compromised for permeability measurements (figures 32 and 33; table 5). XRD measured from this sample shows abundant feldspar (23%) and mica (54%) (table 6). Although not microscopically observed, micro- to nano-scale porosity may be present as intergranular and intercrystalline pores in partially dissolved feldspars or as slit pores in the micas. Core Labs scanning electron microscopy (SEM) studies from Cane Creek 26-3 core showed many of the feldspars and plagioclase grains are partially dissolved and contain pitted pores, as well as abundant micro

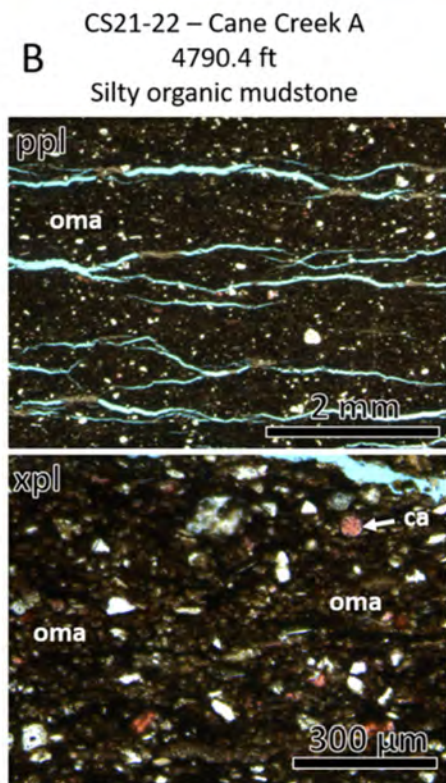
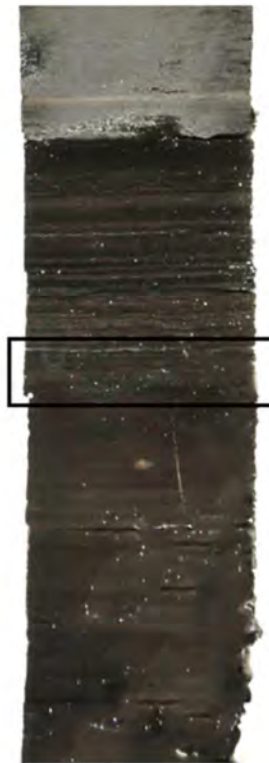
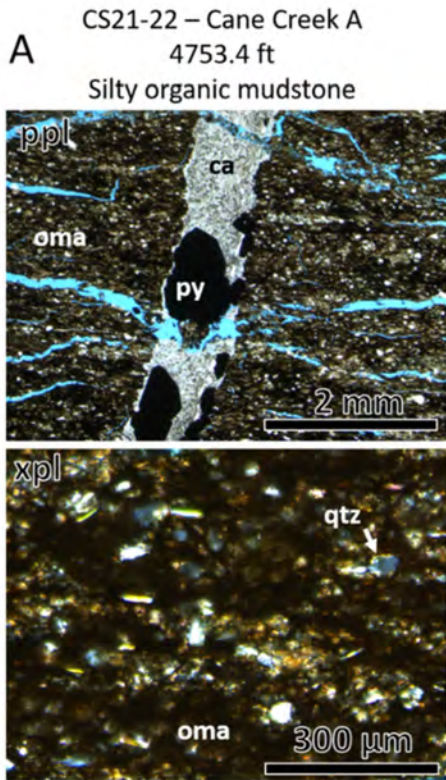


Figure 25. Core slab photos and thin section photomicrographs for zones from the Cane Creek unit, Crescent State #21-22 core. Photomicrographs are under plane polarized light (ppl) or cross polarized light (xpl). A) A zone: Silty organic-rich calcareous mudstone, partially argillaceous, with quartz (qtz) silt, mica, and organo-mineralic aggregates (oma). Calcite (ca) filled fracture contains pyrite (py). B) A zone: Representative silty organic-rich calcareous mudstone with oma.

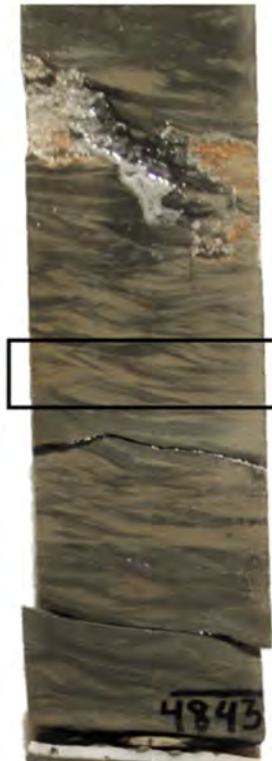
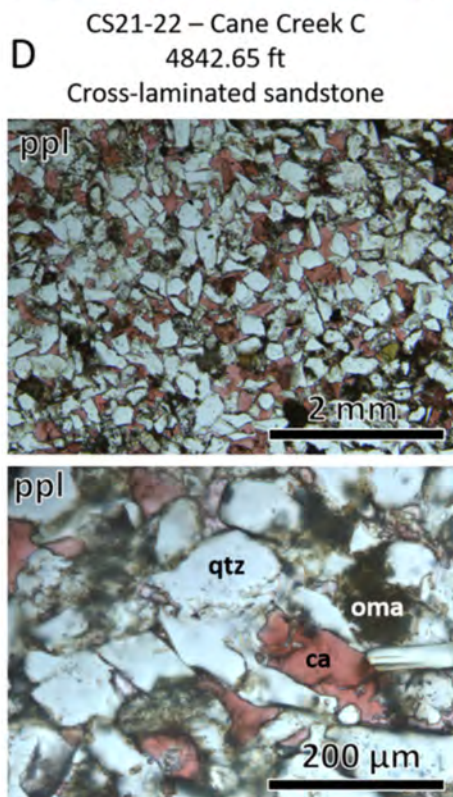
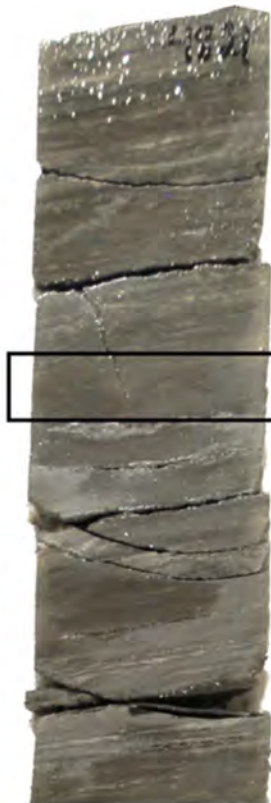
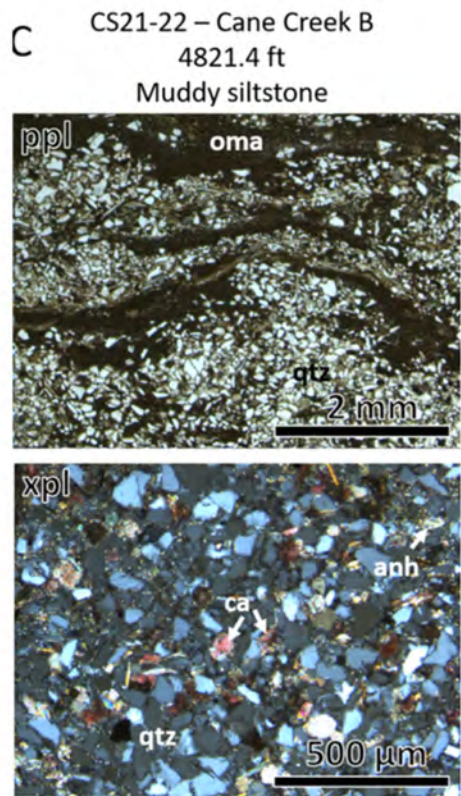


Figure 25 continued. Core slab photos and thin section photomicrographs for zones from the Cane Creek unit, Crescent State #21-22 core.

Photomicrographs are under plane polarized light (ppl) or cross polarized light (xpl). C) B zone: Lenticular bedded muddy siltstone with qtz, mica, and oma. D) C zone: Wavy bedded, wave rippled very fine grained sandstone. Matrix and pore space contains calcite cement (red) and oma.

CS21-22 – Cane Creek C
E 4840.25 ft
Sandstone

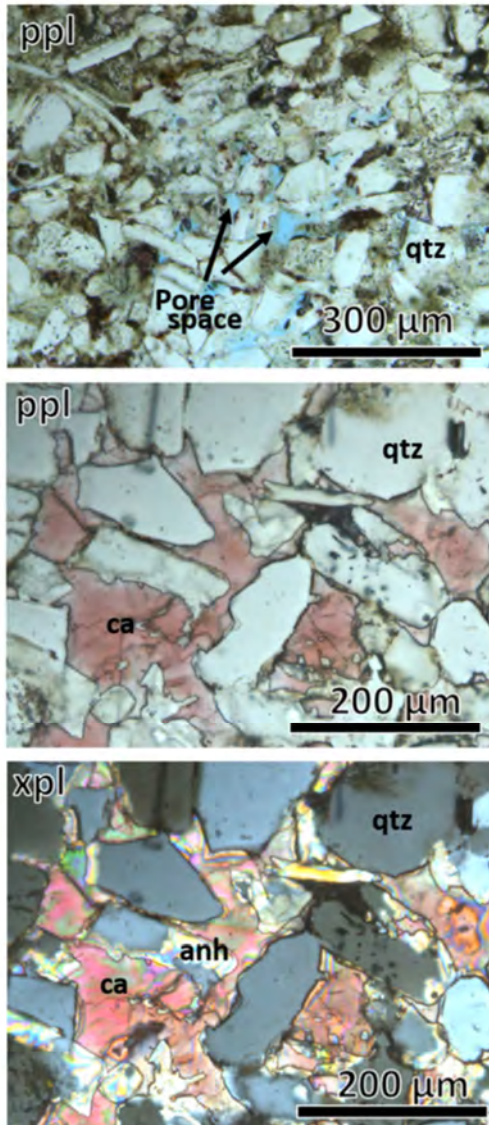


Figure 25 continued. Core slab photos and thin section photomicrographs for zones from the Cane Creek unit, Crescent State #21-22 core. Photomicrographs are under plane polarized light (ppl) or cross polarized light (xpl). E) C zone: Flaser bedded and bioturbated very fine grain sandstone. Mud drapes composed of clay and mica. Angular quartz matrix cemented with calcite (red stain) and some anhydrite (anh).

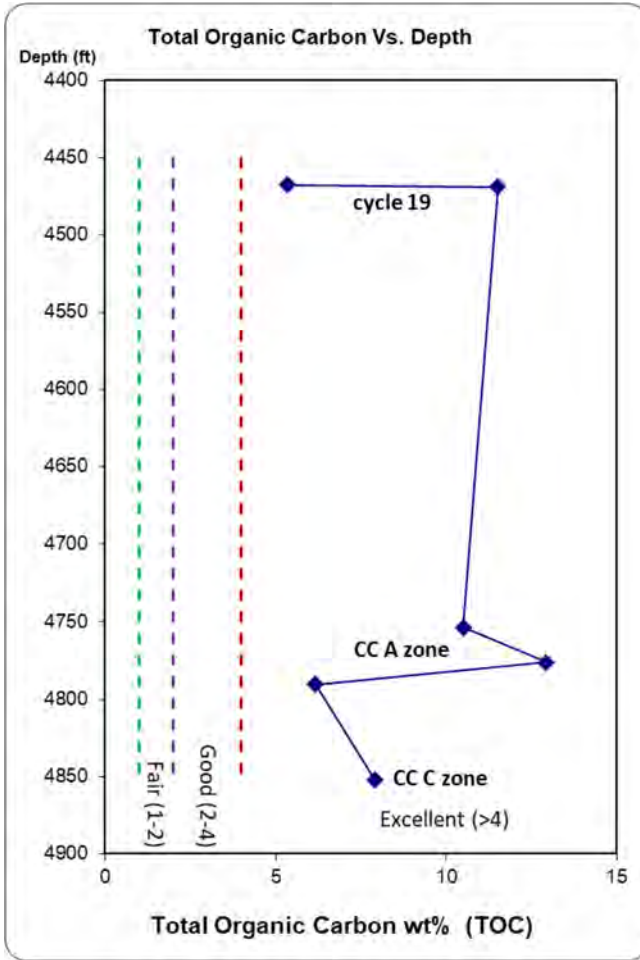


Figure 26. Total organic carbon (TOC) analysis from the cycle 19 and Cane Creek (CC), Crescent State #21-22 core, showing exceptionally high organic content in source rock shales. Analysis by Core Labs, Denver, CO.

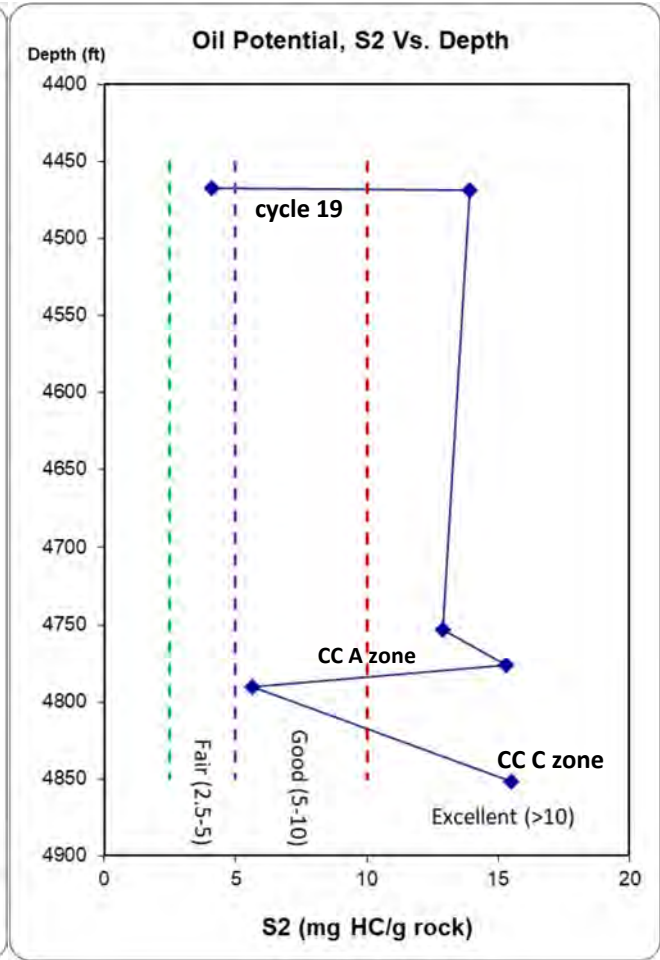


Figure 27. Oil potential (milligrams hydrocarbons per gram) from source rock analysis of organic-rich shales from cycle 19 and Cane Creek (CC), Crescent State #21-22 core. Analysis by Core Labs, Denver, CO.

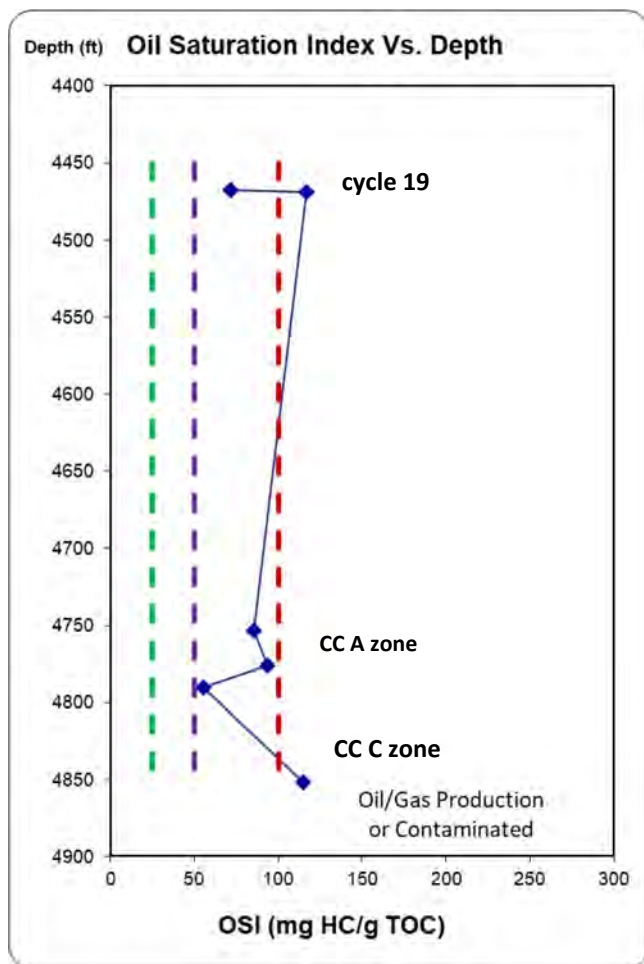


Figure 28. Oil saturation index (mg HC/g TOC) from source rock analysis of organic-rich shales from cycle 19 and Cane Creek (CC), Crescent State #21-22 core. Analysis by Core Labs, Denver, CO.

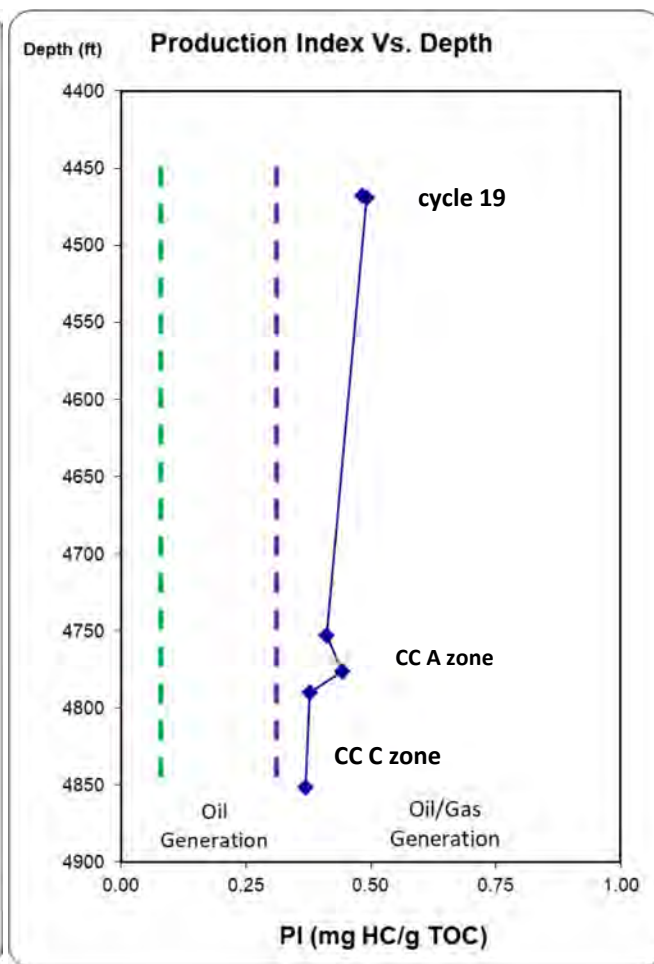


Figure 29. Production index from source rock analysis of organic-rich shales from cycle 19 and Cane Creek (CC), Crescent State #21-22 core. Analysis by Core Labs, Denver, CO.

Table 4. Source rock analysis from Crescent State 21-22. Analysis by Core Labs, Denver, CO.

Well Name	Cycle/Zone	Depth (ft)	TOC (wt%)	S1 (HC mg/g)	S2 (HC mg/g)	S3 (CO ₂ mg/g)	S3 (CO mg/g)	Tmax (°C)	HI	OI	PI	OSI	Oil in Rock (bbl oil/ac-ft)	V _{ro} %
CS 21-22	19	4467.50	5.34	3.82	4.1	0.26	0.04	439	76.78	4.87	0.48	71.54	83.62	0.79
CS 21-22	19	4469.00	11.51	13.43	13.94	0.27	0.08	441	121.11	2.35	0.49	116.68	293.98	0.83
CS 21-22	21/A	4753.40	10.51	9	12.89	1.26	0.05	431	122.65	11.99	0.41	85.63	197.01	0.66
CS 21-22	21/A	4776.20	12.93	12.11	15.29	1.36	0.16	440	118.25	10.52	0.44	93.66	265.09	0.81
CS 21-22	21/A	4790.40	6.17	3.42	5.65	1.12	0.11	444	91.57	18.15	0.38	55.43	74.86	0.88
CS 21-22	21/C	4852.00	7.9	9.06	15.52	0.66	0.02	439	196.46	8.35	0.37	114.68	198.32	0.79

HI: Hydrogen Index

PI: Production Index

OSI: Oil Saturation Index

OI: Oxygen Index

V_{ro}%; calculated from Tmax using Belle Fourche and Second White Speck Model

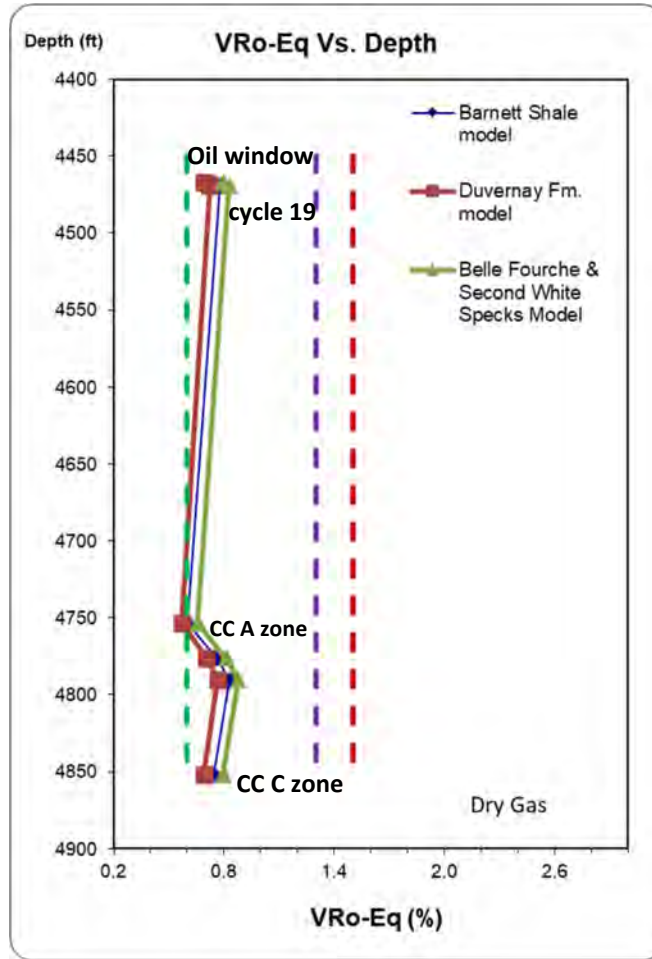


Figure 30. V_{ro} from cycle 19 and Cane Creek, Crescent State #21-22 core, indicating the source rocks are within the oil window in the northern Paradox Basin. Barnett shale, Duvernay Fm., and Belle Fourche & Second White Specks are three primary models to calculate V_{ro} from T_{max} . Analysis by Core Labs, Denver, CO.

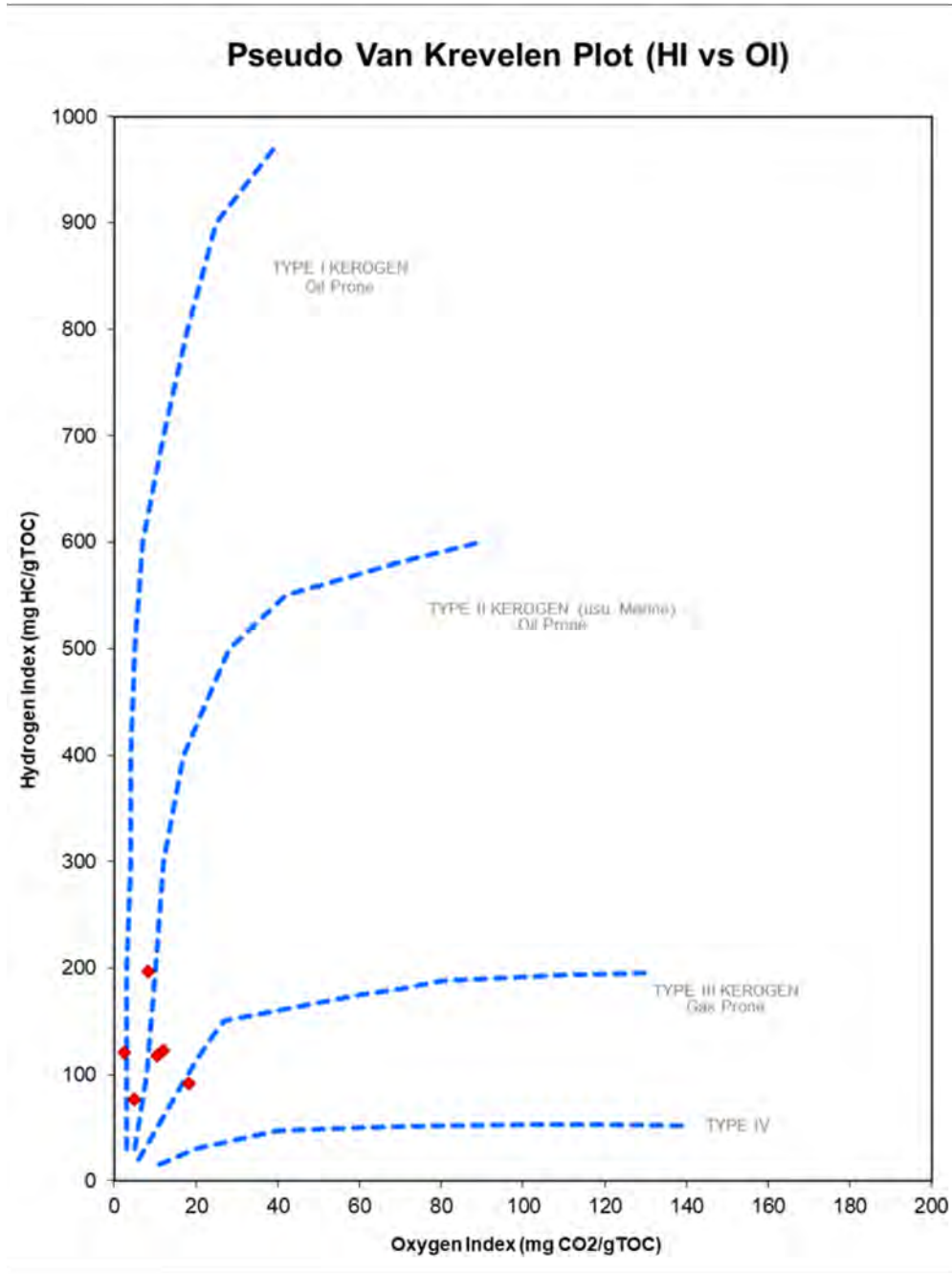


Figure 31. Pseudo Van Krevelen plot from organic-rich shale samples from the cycle 19 and Cane Creek, Crescent State #21-22 core. The analysis indicates a mixture of Type I and Type II kerogen, suggesting a mixture of restricted lagoonal algal and marine planktonic hydrocarbon sources. Analysis by Core Labs, Denver, CO.

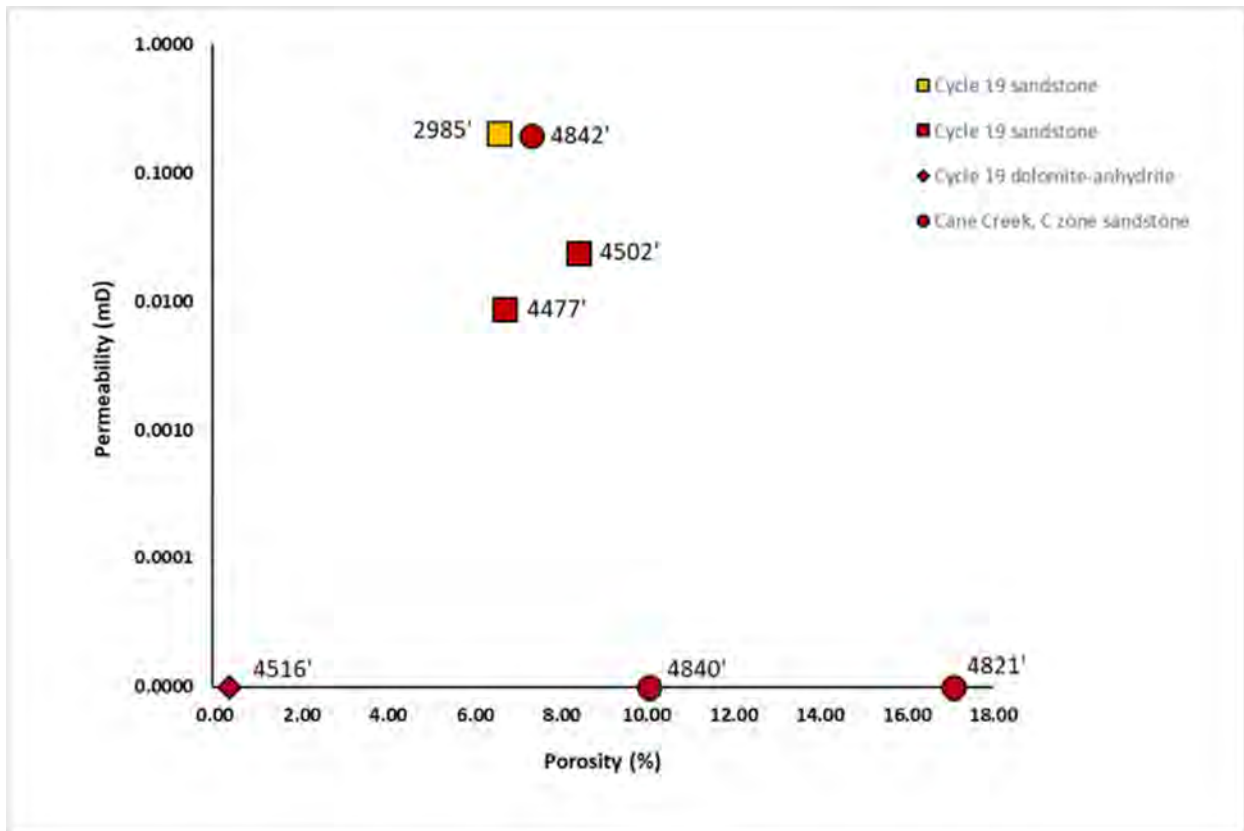


Figure 33. Porosity and permeability cross plot from cycle 19 and Cane Creek core plug analysis from reservoir facies and one dolomite-anhydrite sample. Yellow: Crescent State #22-09; Red: Crescent State #21-22. Samples along the x-axis were unsuitable for permeability measurements due to induced fractures and are plotted to only show porosity. Note the dolomite-anhydrite sample has extremely low porosity (0.4 %). Analysis completed by Core Labs, Denver, CO.

Table 5. Porosity and permeability analysis from Crescent State 22-09 and Crescent State 21-22. Analysis by Core Labs, Denver, CO.

Depth (ft)	Cycle/Zone	Rock Type	Net Confining stress (psi)	Porosity (%)	Permeability (mD)	Grain density (g/cm ³)
Crescent State 22-09						
2985.20	19	sandstone	2270	6.61	0.202	2.613
Crescent State 21-22						
4477.80	19	sandstone	2270	6.74	0.009	2.665
4502.20	19	sandstone	2270	8.43	0.024	2.639
4516.00	19	dolomite-anhydrite	Ambient	0.40	***	2.939
4821.40	21/B	sandstone	Ambient	17.09	***	2.694
4840.25	21/C	sandstone	Ambient	10.06	***	2.653
4842.65	21/C	sandstone	2270	7.36	0.197	2.672

*** Sample unsuitable for permeability measurements due to induced fractures

Table 6. XRD results from Crescent State 21-22.

		Crescent State 21-22 XRD Results																			
Depth	Cycle/ Zone	Rock Type	Quartz (%)	Calcite (%)	Dolomite (%)	Magnetite (%)	Anhydrite (%)	Sylvite (%)	Halite (%)	Gypsum (%)	Mica (%)	Illite (%)	Montmorillonite (%)	Kaolinite (%)	Muscovite (%)	Feldspar (%)	Sandine (%)	Albite (%)	Biotite (%)	Anorthite (%)	Oligoclase (%)
4465.60	19	dolomitic-anhydritic mudstone	4.50	0.04	45.29	14.53	30.60	0.07	0.03	0.02	0.09	1.19	0.68	0.51	0.05	0.18	0.56	0.95	0.10	0.22	0.38
4467.50	19	argillaceous mudstone	7.99	0.03	1.34	16.78	0.46	1.16	0.16	0.12	38.57	9.03	5.39	6.15	3.14	2.99	0.71	0.22	4.50	0.87	0.37
4469.00	19	argillaceous mudstone	10.17	0.09	0.89	12.14	0.39	1.34	0.32	0.02	40.85	9.63	2.85	8.52	1.76	2.22	3.92	0.43	0.02	2.99	1.47
4477.80	19	sandstone	40.56	0.03	0.73	25.63	0.17	0.09	7.60	0.02	17.21	1.03	0.01	0.19	1.08	1.97	1.54	0.12	1.44	0.37	0.18
4486.30	19	sandstone	52.21	0.14	0.97	13.21	0.20	0.01	8.93	0.01	17.40	0.44	0.36	3.58	0.06	1.30	0.16	0.36	0.35	0.15	0.14
4502.20	19	sandstone	54.45	0.04	0.80	17.32	0.20	0.20	8.18	0.02	0.09	3.07	6.16	7.36	0.05	1.20	0.26	0.14	0.02	0.22	0.21
4504.20	19	sandstone	39.38	0.03	1.31	14.78	0.05	1.29	10.50	4.00	23.18	2.76	0.01	0.18	0.47	0.21	0.16	0.26	0.71	0.19	0.52
4516.00	19	dolomitic-anhydritic mudstone	1.94	0.22	0.12	6.86	58.57	0.02	3.04	0.03	1.16	4.48	2.63	0.40	1.83	0.37	0.84	0.23	16.21	0.71	0.33
4517.70	19	dolomitic-anhydritic mudstone	0.91	0.03	0.04	10.26	87.25	0.10	0.30	0.02	0.06	0.10	0.01	0.14	0.09	0.19	0.08	0.10	0.01	0.15	0.14
4753.40	21/A	organic-rich mudstone	6.97	33.75	11.01	2.08	0.28	0.03	5.86	1.17	16.13	7.62	1.88	1.10	2.15	0.62	0.24	2.16	3.07	0.94	2.93
4766.40	21/A	silty dolomitic mudstone	48.40	0.04	27.69	0.97	0.59	0.01	1.03	0.18	0.15	6.61	7.09	1.80	0.05	3.75	0.19	1.00	0.02	0.21	0.23
4776.20	21/A	silty dolomitic mudstone	14.09	0.30	26.08	0.05	0.33	0.33	1.44	1.22	3.31	9.91	0.01	1.06	19.27	1.06	1.70	16.85	0.77	1.14	1.08
4790.40	21/A	silty dolomitic mudstone	5.53	13.33	33.36	2.10	1.01	0.03	0.71	0.21	23.88	9.83	0.28	2.06	1.63	0.58	1.05	0.75	1.56	1.03	1.09
4801.00	21/B	organic-rich mudstone	20.40	8.99	7.60	2.91	0.71	0.60	5.62	0.42	0.14	38.12	0.03	7.50	1.80	0.68	0.51	1.82	0.89	0.61	0.65
4819.35	21/B	sandstone	38.99	0.03	11.16	0.11	0.13	0.11	1.38	0.02	0.44	5.43	5.19	10.85	0.04	23.84	0.50	0.51	0.01	0.79	0.50
4821.20	21/B	sandstone	11.69	5.16	7.66	0.05	1.21	0.64	1.52	0.14	53.67	0.89	0.95	6.42	0.73	0.44	0.20	0.75	5.96	0.92	1.02
4840.10	21/C	sandstone	54.60	0.00	11.00	0.30	0.70	0.20	5.10	0.00	14.30	0.50	1.50	0.90	0.20	5.70	0.60	0.30	2.10	1.00	0.90
4842.95	21/C	sandstone	36.11	1.1	11.58	0.39	0.18	0.22	1.24	.02	25.2	2.49	2.12	11.64	0.16	0.44	1.53	1.23	2.32	.78	1.25
4852.00	21/C	organic-rich mudstone	6.78	0.02	23.99	2.45	1.00	0.05	0.01	0.14	16.47	2.00	2.36	2.52	1.02	22.46	0.24	11.41	3.53	0.57	3.02

intergranular porosity (see appendix C, Plate 19D and 21D). SEM and porosimetry analysis is recommended to determine pore types, size, and distribution in the reservoir facies from the CS 21-22 core. Overall, the petrographic details suggest the siltstone-sandstones have considerable high porosity and likely good permeability.

Vertical to near-vertical millimeter- to centimeter-scale fractures were observed in all facies and are generally filled with anhydrite, halite, or calcite and some contain bitumen (figure 32). The widest fractures are mostly halite filled.

For comparison, the oil-productive B zone of the Cane Creek 26-3 well in the Big Flat field, as studied from core, contains similar reservoir facies including argillaceous sandstone, sandstone, dolomitic argillaceous siltstone, and silty dolomite (Morgan and Stimpson, 2017). The reservoir contains well-sorted coarse siltstone to very fine grained sandstone, is mostly bioturbated, some with distinct burrows. Microfractures were observed in thin sections and are filled with halite, anhydrite, and calcite. Peloids and quartz silt grains are common in the dolomitic mudstones. The siltstone-sandstone is mostly feldspathic litharenite with some samples classified as litharenite, sublitharenite, lithic arkose, and subarkose. The siltstone-sandstone contains moderate amounts of potassium feldspar, minor amounts of limestone and dolomite rock fragments, minor to trace amounts of calcite replacement grains and muscovite. Other minor to rare grains include plagioclase, volcanic rock fragments, heavy minerals, and elongate plant fragments. Cement in the siltstone-sandstone is commonly quartz overgrowth and dolomite.

Cane Creek - C Zone

The C zone was cored from 4825.0 to 4855.0 feet and contains both reservoir and source rock facies. The zone consists of dolomitic mudstone (n = 5) with abundant nodular and bedded anhydrite at the top and base (n = 2), a thick (~10 ft) sandstone package, laminated black organic-rich mudstone (n = 2), and some calcareous mudstone (n = 2) (figures 19, 25D,E, and 34). The sandstone is very fine grained grading to siltstone, locally bioturbated, and predominantly contains current ripples, parallel cross-bedding, and lenticular to flaser bedding. Fine-scale mud drapes occur along the ripple foresets. Calcareous and dolomitic mudstones are interbedded with the sandstones. Near-vertical halite-filled fractures are also common.

The sandstone in the C zone is arkosic, composed of quartz, mica, dolomite, and has minor amounts of feldspar. The sandstone package is thicker and slightly different in composition (feldspar lean and mica rich) than the sandstone in the B zone, as well as less bioturbated. Much of the pore space has also been occluded by diagenetic cements, including calcite and anhydrite, but some intergranular porosity between quartz grains is preserved (figure 25E). Porosity measurements were 7 to 10% from samples at 4840.25 and 4842.65 ft, and a permeability of 0.197 mD (197.0 μ D) was measured at 4842.65 ft (figure 33; table 5).

Laminated black organic-rich mudstone occurs above and below the dominant sandstone package and is associated with nodular and bedded anhydrite. Laminae are crinkled to wavy, which could represent relic laminated algae. The laminae contain rhombohedral dolomite, mica, feldspars, and albite, indicating that the organic-rich mudstone is relatively heterolithic. The presence of sulfides (pyrite) and the paucity of burrows also suggest the black organic-rich mudstone was deposited in reducing and dysoxic to anoxic conditions. Source rock analyses from one sample at 4852.0 ft measured 7.9% TOC with an estimated oil in place of 198 bbl oil/acre-ft and maturity of 0.79 % V_{ro} (figures 26 and 30; table 4).

By comparison, Core Labs analyzed 11 thin sections from the C zone in the Cane Creek 26-3 well that included samples of dolomitic sandstone, dolomitic siltstone, argillaceous siltstone, dolomite, dolomitic anhydrite, and anhydrite. The siltstone-sandstone contains moderate to well-sorted coarse silt to very fine sand. Samples are bioturbated with some



Figure 34. Photograph of core from the Cane Creek C zone, Crescent State #21-22. A) Calcareous sandstone reservoir facies interbedded with dolomitic mudstone and calcareous bioturbated mudstone. B) Contact of C zone with underlying halite (4854.3 ft). Organic-rich mudstone, anhydrite, and dolomitic mudstone are common C zone facies, in addition to prevalent sandstone reservoir facies. Note prominent vertical to near-vertical thin to wide (cm-scale) fractures, which are present in all facies. Fractures are generally filled with anhydrite, halite, or calcite and some contain bitumen. Green and blue circles represent location for core plug and source rock analysis; green: 7.9% TOC; blue: 10% porosity.

microfractures. Quartz overgrowths are moderate in abundance in the siltstone and minor to rare in the sandstone. There are minor occurrences of pore-filling dolomite and pyrite, and trace amounts of feldspar overgrowths, calcite, anhydrite, titanium oxides, and halite cement.

Cycle 19

Cycle 19 was cored from 4453.5 to 4519.5 ft in the CS 21-22 core and is a potential secondary target above the Cane Creek (figures 4 and 20). Along the Salt Valley anticline, cycle 19 consists of thick, very fine grained sandstone (up to ~30 ft), magnesian (MgCO_3) mudstone with subordinate dolomite ($n = 5$), thin bedded laminated black organic-rich mudstone ($n = 7$), and thin bedded nodular dolomitic anhydrite ($n = 8$) (figures 20, 35, and 36; table 7; appendix E). The presence of magnesite is peculiar; it rarely forms as a primary mineral in sedimentary environments and is mostly an alteration product of carbonates from metamorphism or chemical weathering. Magnesite abundance in cycle 19 ranges from 6.0 to 25.6% and occurs in all lithologies suggesting that it is either detrital and sourced from the Uncompahgre uplift or a secondary diagenetic mineral. The elemental XRF profile for cycle 19 also shows trace amounts of Ca^{2+} and high amounts of Mg^{2+} (figure 20). One possible explanation for a diagenetic origin is cation exchange from Mg-rich fluids that converted calcite (CaCO_3) or dolomite (CaMgCO_3) to magnesite.

The composition of the sandstone, except for the presence of magnesite, is similar to the sandstones in the underlying Cane Creek, implying the sediment was sourced from the same provenance (Uncompahgre plateau?). The sandstone is bioturbated and most of the sedimentary textures have been disrupted by burrowing organisms. Porosity and permeability measured from two sandstone samples at 4477.8 and 4502.2 ft range from 6.7% to 8.4% and 0.009 to 0.024 mD, respectively (figures 33 and 35B; table 5). Porosity was not observed in thin section, indicating the presence of micro-to nano-scale pores; whether the porosity is intergranular, intercrystalline, or from micro-fractures is difficult to determine without SEM analysis. Halite-filled fractures and pore-filling cements are also common throughout the sandstones, which adds complexity to understanding matrix permeability and porosity.

Thin beds of laminated black organic-rich mudstone are heterolithic with silty quartz grains, mica, and abundant organic aggregates (figures 35A and 36B). Reflected light shows the occurrence of pyrite/sulfides, laminated algal macerals, and liptonite. Source rock analysis measured from two samples at 4467.5 and 4469.0 ft indicates moderate to high TOC of 5.3% and 11.5% with estimated oil-in-place of 84 and 294 bbl oil/acre-ft, respectively (figures 26 and 35A; table 4). Calculated V_{ro} of 0.79% and 0.83% and Tmax of 439°C and 441°C also indicate that cycle 19 is within the oil window (figure 30; table 4).

Anhydrite occurs above and below the main sandstone sequence and is interbedded with the black organic-rich mudstone. The anhydrite occurs as three main textures: 1) wavy thin-bedded, 2) convolute clast supported, and 3) nodular aggregates that are fabric destructive (“chicken-wire” anhydrite). The wavy thin-bedded anhydrite is interbedded with silty dolomitic mudstone, mud rip-up clasts, and forms alternating couplets of mudstone-anhydrite. The bedded anhydrite occurs as microcrystalline needles and as pseudomorphs after bottom growth gypsum or halite (figure 37). The microcrystalline needles form wavy thin beds that have tepee-like antiformal buckles. This feature can be interpreted in two parts: 1) cumulate crystals (probably gypsum) precipitated at the air-water interface and settled to bottom of a shallow brine body to form a layered crust, and 2) lateral pressure from continued expansive gypsum growth contorted the subaqueous crust into kinked heterolithic folds. The complicated convolute clast-supported textures may resemble solution collapse breccias by fresher water input. A representative sample of this texture at 4516.0 and 4517.7 ft has a measured porosity of 0.40% indicating the anhydrite-dolomite dominated facies are extremely tight (figures 33 and 36D;

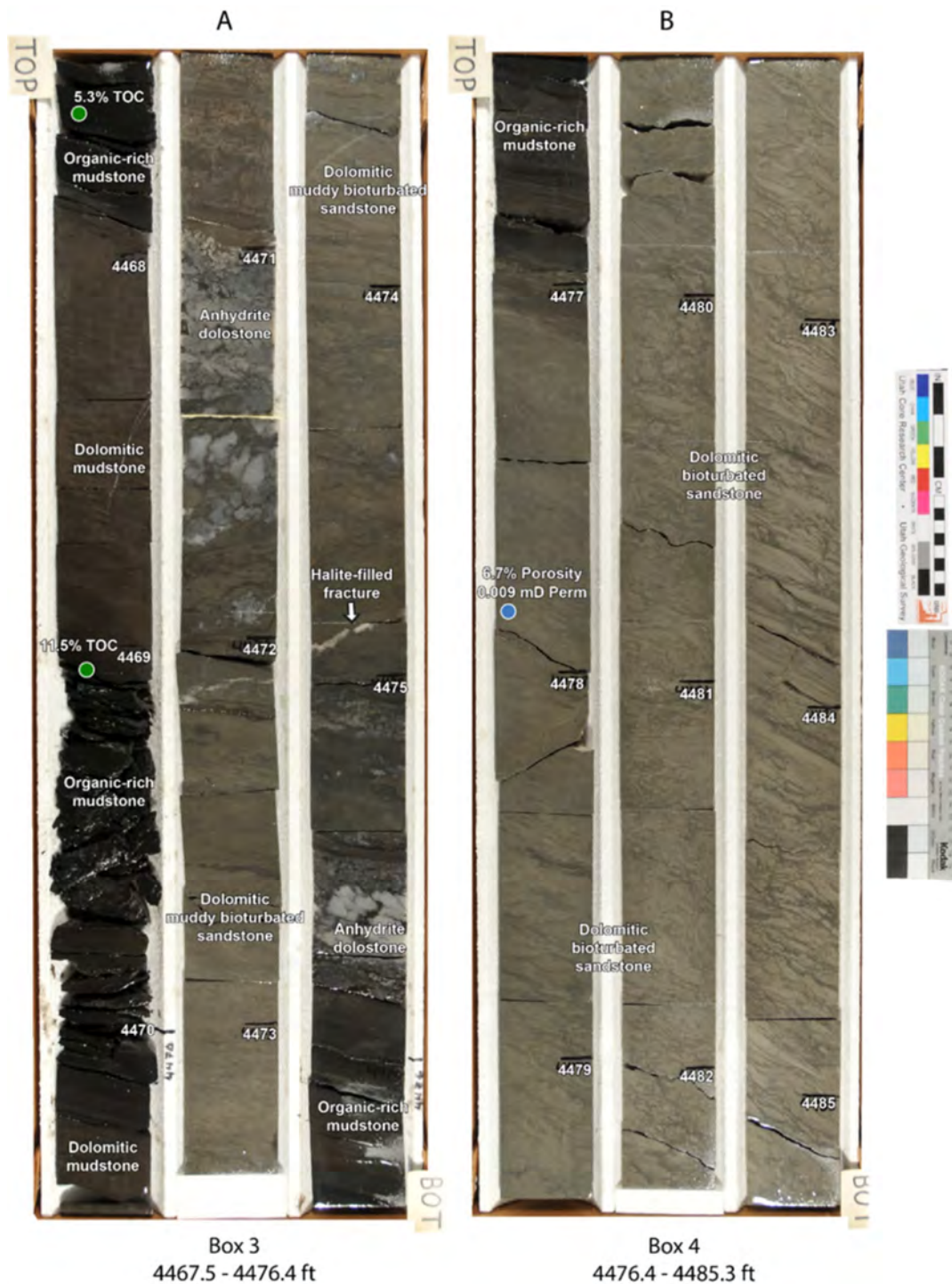


Figure 35. Photograph of core from the cycle 19, Crescent State #21-22. A) Dolomitic and anhydritic source rock interval with organic-rich mudstone and interbedded muddy bioturbated very fine grained sandstone. B) Dolomitic bioturbated very fine grained sandstone representative of the reservoir facies. Green and blue circles represent location for core plug and source rock analysis; green: 5.3 and 11.5% TOC; blue: 6.7% porosity and 0.009 mD permeability.

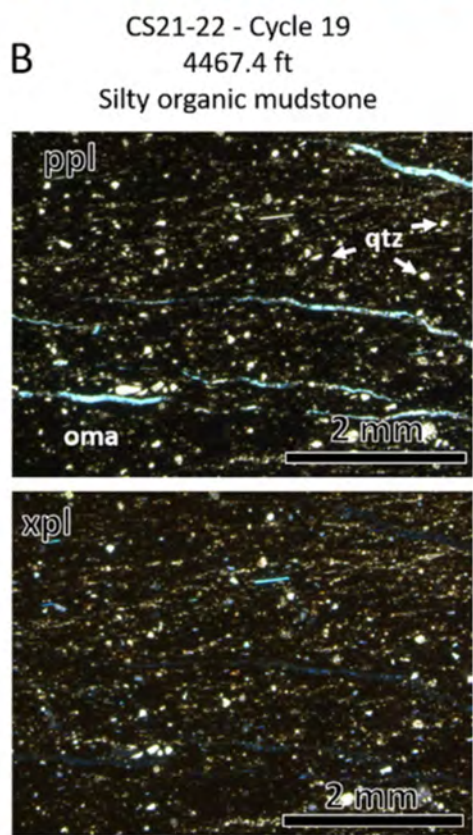
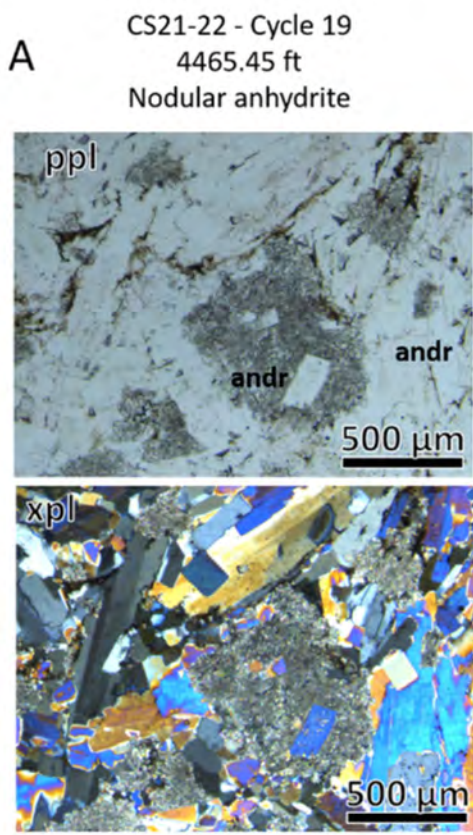


Figure 36. Core slab photos and thin section photomicrographs from cycle 19, Crescent State #21-22 and Crescent State #22-09. Photomicrographs are under plane polar light (ppl) or cross polar light (xpl). A) Nodular to bedded coarse crystalline anhydrite (andr) B) Silty quartz (qtz) organic-rich calcareous mudstone with organo-mineralic aggregates (oma).

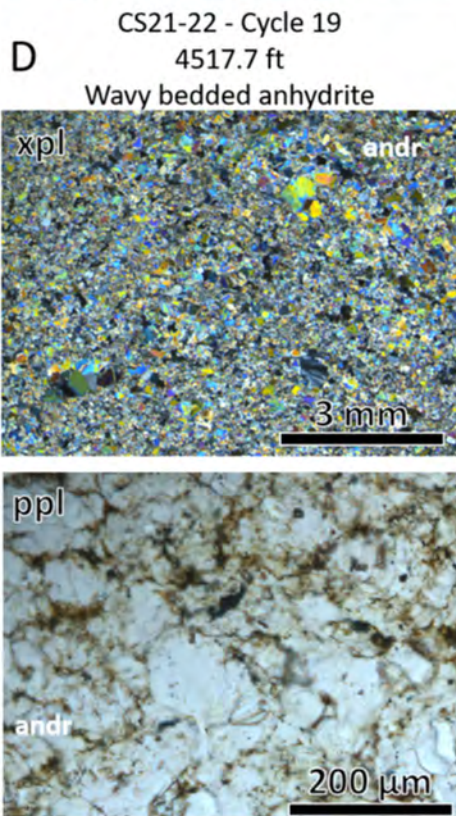
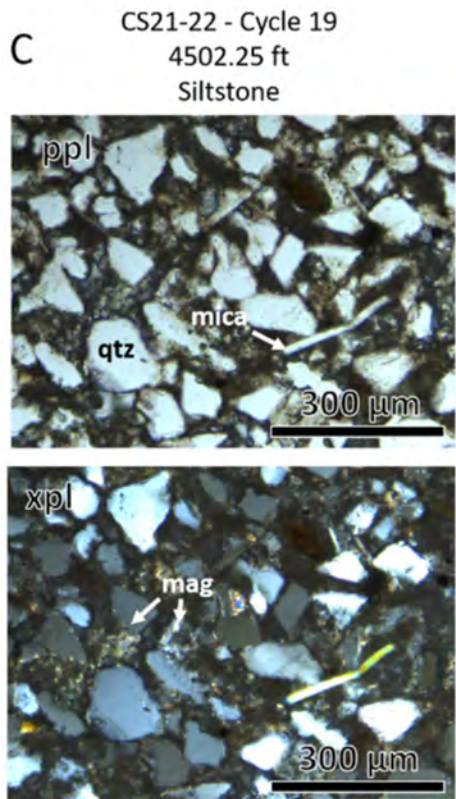


Figure 36 continued. Core slab photos and thin section photomicrographs from cycle 19, Crescent State #21-22 and Crescent State #22-09. Photomicrographs are under plane polar light (ppl) or cross polar light (xpl). C) Bioturbated siltstone with mica and magnesite cement. D) Wavy bedded microcrystalline anhydrite. E) Cross-laminated siltstone with mud drapes along foresets; dolomite and calcite (c) replacement has occluded pore space.

E CS22-09 - Cycle 19
2985.2 ft
Siltstone with dolomite-calcite replacement

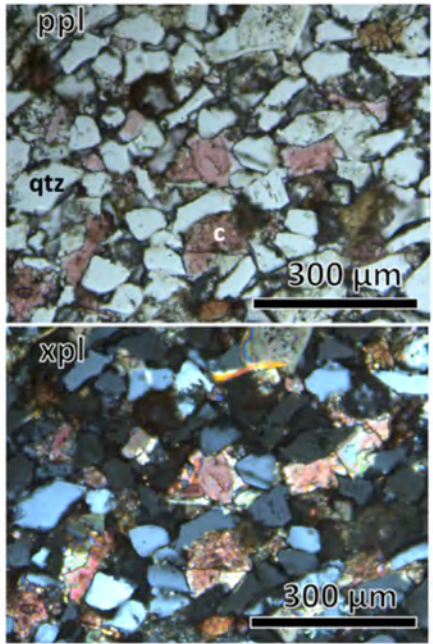


Figure 36. Core slab photos and thin section photomicrographs from cycle 19, Crescent State #21-22 and Crescent State #22-09. Photomicrographs are under plane polar light (ppl) or cross polar light (xpl). E) Cross-laminated siltstone with mud drapes along foresets; dolomite and calcite (c) replacement has occluded pore space.

Table 7. XRD results from Crescent State 22-09.

Crescent State 22-09 XRD Results

Depth	Cycle	Rock Type	Quartz (%)	Calcite (%)	Dolomite (%)	Magnesite (%)	Anhydrite (%)	Sylvite (%)	Halite (%)	Gypsum (%)	Mica (%)	Illite (%)	Montmorillonite (%)	Kaolinite (%)	Muscovite (%)	Feldspar (%)	Sandine (%)	Albite (%)	Biotite (%)	Anorthite (%)	Oligoclase (%)
2936.90	19	silty dolomitic mudstone	1.76	0.04	89.70	0.18	0.17	0.01	0.53	0.13	0.59	0.50	0.35	0.06	0.48	0.45	2.55	0.58	0.42	0.77	0.74
2951.20	19	silty dolomitic mudstone	6.54	0.13	76.35	0.06	0.26	0.01	1.46	0.97	0.51	7.03	0.36	1.41	0.21	2.12	1.14	0.32	0.07	0.39	0.67
2985.40	19	sandstone	48.99	0.05	23.18	0.10	0.78	0.25	11.44	0.02	3.07	1.28	1.88	1.75	2.36	1.05	0.41	1.35	0.02	1.37	0.64
2987.00	19	sandstone	17.17	3.32	36.19	1.18	0.44	0.01	0.36	0.20	25.75	0.28	0.73	2.49	1.51	0.12	0.20	8.88	0.81	0.19	0.18
3010.00	19	sandstone	33.67	0.03	34.14	0.05	0.25	0.02	9.36	0.02	0.08	0.79	0.76	2.22	0.79	2.53	0.10	13.68	1.03	0.28	0.18
3033.00	19	silty dolomitic mudstone	13.62	0.04	61.70	1.25	0.71	0.02	0.02	0.21	9.28	7.84	0.42	1.52	0.44	0.22	0.29	0.38	0.88	0.77	0.40
3033.00 CHK	19	silty dolomitic mudstone	13.46	0.05	61.21	1.04	0.60	0.02	0.38	0.21	10.58	3.70	1.15	1.60	1.92	0.50	0.28	0.33	1.94	0.72	0.32
3064.70	19	silty dolomitic mudstone	3.73	0.02	85.86	0.54	0.04	0.07	1.92	0.03	0.07	2.41	2.41	0.93	0.13	0.23	0.29	0.14	0.13	0.47	0.55
3065.00	19	silty dolomitic mudstone	22.30	3.75	60.34	0.32	0.94	0.06	0.08	0.08	0.37	0.43	1.43	2.74	0.59	0.84	0.43	1.64	0.88	1.23	1.54

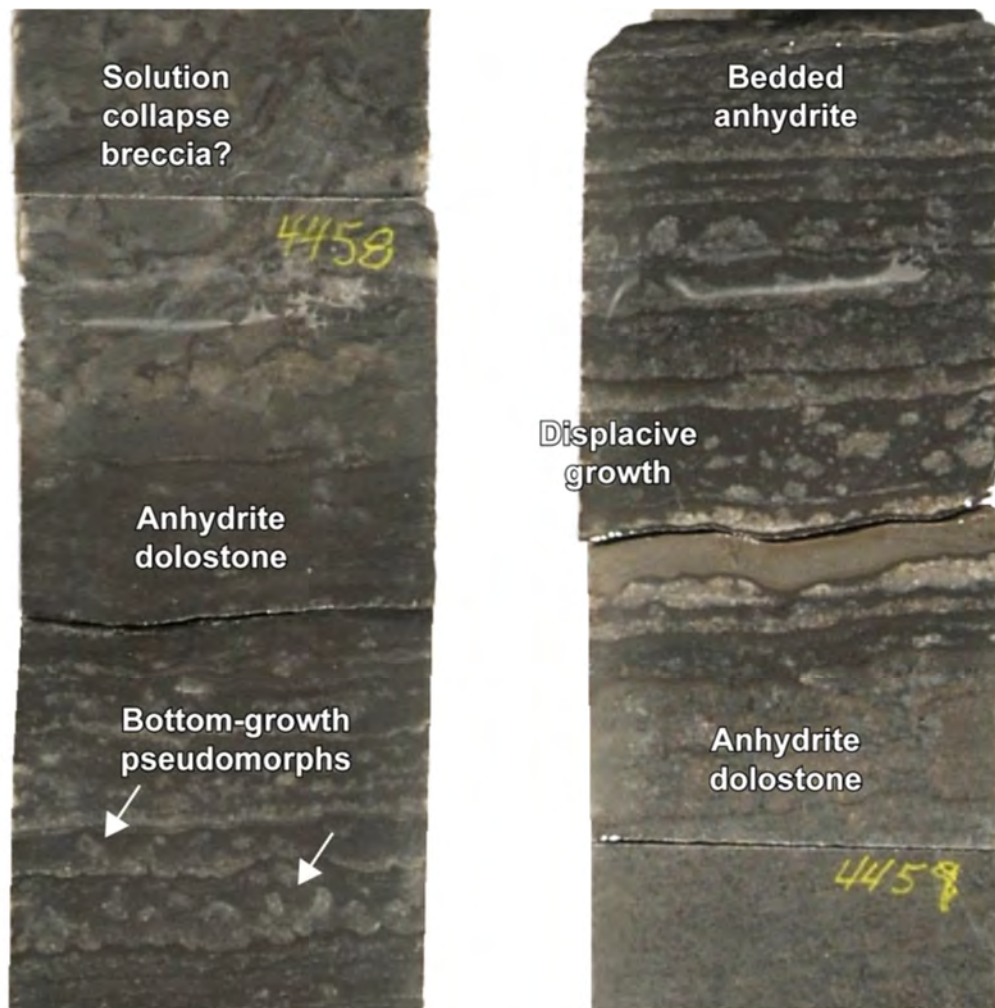


Figure 37. Core photos from cycle 19, Crescent State #21-22 core, highlighting anhydrite morphologies including bottom-growth pseudomorphs, displacive growth, thin bedded anhydrite mudstone couplets, and anhydritic dolostone-mudstone. Bottom-growth pseudomorphs have syntaxial, upward directed crystal shapes (competitive growth) with laminated mud drapes between crystal tops. Chaotic texture at 4458 ft is suggestive of a solution collapse breccia. Thin bedded anhydrite represents cumulate crystals that precipitated at the air-water interface and sank to the bottom of a brine body and formed layered deposits. Displacive growth anhydrite represents gypsum that precipitated in sulfate

table 5). The pseudomorphs exhibit upward-directed crystal shapes that have laminated draping mud between crystal tops. This implies saline, gypsum-halite supersaturated brine conditions. Nodular anhydrite deforms primary layering and is indicative of former displacive growth gypsum or anhydrite that precipitated within sulfate-saturated pore waters.

The source and reservoir facies in “cycle 19” from the CS 22-09 core are slightly different than cycle 19 facies in the CS 21-22 core, including a low percent of magnesite (figures 21 and 38; table 5). The sandstone packages are not as thick and are less bioturbated and coarser grained, ranging from silt to fine-grained quartz. The sandstone exhibits well-preserved sedimentary textures indicative of unidirectional and possibly bidirectional current ripples. Climbing ripples, parallel cross-beds, planar beds, and wave ripples indicate rapid sedimentation and, at times, deposition under upper flow regime conditions (appendix E). Herringbone structures identify bidirectional currents. Mud drapes along the foresets of the current ripples are common and indicate fine-grained sediments (mud, clay) were suspended and subsequently settled after deposition of coarser grained material. Together, these sedimentary features indicate regularly changing flow conditions that can be interpreted as tidal deposits.

The composition of the sandstone is similar to cycle 19 from the CS 21-22 core, with arkosic grains of quartz, micas, and subordinate feldspars. Petrographic observations from the CS 22-09 sandstone showed no obvious porosity, and that intergranular pore space is mostly occluded with diagenetic cements of calcite, dolomite, and halite. XRD identified substantial proportions of dolomite, ranging from 23 to 36 wt%. One sandstone plug at 2985.2 ft yielded 6.6% porosity and 0.202 mD permeability (figure 33; table 5). The moderate porosity but high permeability suggests micro-fractures may contribute to the overall system permeability of the reservoir sandstones.

Silty dolomitic mudstone is the most abundant rock type and is commonly intercalated with wavy thin-bedded siltstone. The mudstone is thin bedded to massive due to extensive bioturbation and in places has diagenetic anhydrite nodules. Laminated black organic-rich mudstone is calcareous and associated with fabric-destructive dolomitic anhydrite facies. Source rock analysis measured on one organic-rich mudstone indicates excellent TOC of 9.68% and estimate oil in place of 205 bbl/acre-ft (table 4). Speckled sulfides and crinkled algal laminations are common at the base of black mudstone that has blebs of small anhydrite nodules. Traces of disarticulated shell fragments occur near the top of one organic-rich mudstone bed that contains anhydrite at its base and implies the water chemistry changed from gypsum saturated (now anhydrite) waters to fresher waters. Typically, the top contact of the organic-rich shales is abrupt with mud rip-up clasts and rippled siltstones.

GEOGRAPHIC THICKNESS

The Cane Creek is regionally extensive throughout the Paradox Basin and its thickness geographically ranges from almost 0 to 200 ft. Within the Cane Creek fairway play area, the thickness ranges from approximately 60 to 90 ft. The thickness changes are due to the asymmetrical shape of the basin and structural highs that influenced the distribution of sediment shed off the Uncompahgre uplift (figures 1, 5, 7, and 8). Post-deposition shortening from salt deformation and faulting has also created variable thicknesses. The deepest part of the basin is near the Uncompahgre uplift where subsidence created accommodation for the infill of alluvial siliciclastic sediment at times of low sea level. The basin shallows to the southwest as shown by the structure of the Mississippian Redwall Limestone. Regional structures affecting the basin are the north-plunging Monument upwarp and the east- to southeast-plunging structure off the San Rafael Swell, converging at the Big Flat area. Structure mapping of the Cane Creek shows

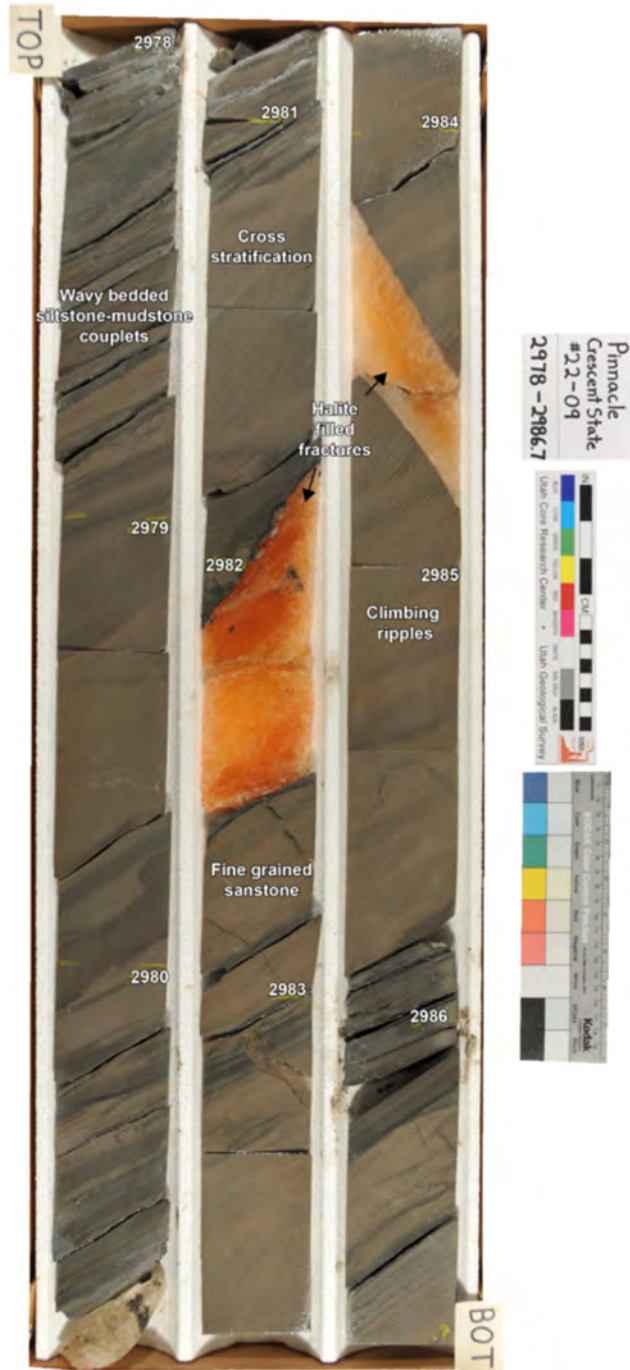


Figure 38. Core slab of cycle 19, Crescent State #22-09 core. Fine to very fine grained sandstones contain climbing ripples and cross-stratification sedimentary textures. Ripple and cross-bedded forests are draped with mud that settled out from suspension. Note red-orange color in large halite-filled fractures is likely a result of subordinate amounts of carnallite or sylvite.

a northwest to southeast strike aligned with the plunging Monument upwarp in the Big Flat area. The Cane Creek plunges steeply to the north in the Greentown area, and new core data supports an increase in siliciclastic infill in this trending direction (figures 7 and 39).

Fluctuations in sea level rise and fall are recorded by the 3-ft-scale cycles (5th to 6th order[?]) described from cores at the center and peripheral parts of the basin, which reflects a combination of tectonics, eustasy, tidal forces, climate, and rate of sediment supply. Correlations of the top and base of the Cane Creek can be carried many miles trending northwest to southeast based on well logs and some cores; its northern lateral extent near Crescent Junction has not been determined until now. Down dip to the northeast is where the thickest salt was deposited resulting in large northwest- to southeast-trending diapiric anticlines (figure 6). The massive movement of the salt and associated clastic cycles combined with few well penetrations, make correlation of individual cycles within the deep basin very difficult. To the southwest, the Cane Creek and other clastic deposits onlap and thin onto the carbonate shelf without the bounding salt beds, making determinations for thickness and lateral extent also difficult.

The thickness of the Cane Creek is approximately 100 ft near Crescent Junction in the CS 21-22 core, where the A, B, and C zones are 35.5, 39, and 30 ft thick, respectively (figures 8 and 39). The B zone may be thicker and extend down into what we have identified as the C zone. The base of the B was chosen because of the occurrence of a thick (~4 ft) anhydrite bed; however, considering the impressive amount of siliciclastics (>10 ft thick) below this bed, the thickness of the C zone may be much thinner and represented as a condensed section of ~7 ft thickness. Regardless, the total thickness for reservoir rock in the B (14 ft thick) and C (13 ft thick) zones is approximately 27 ft. This thickness is of great significance for increasing possible undiscovered resource in the northern Paradox Basin and raises the potential for two stacked landing zones. Cycle 19 in the CS 21-22 exhibits another substantial thickness of reservoir facies, totaling about 38 ft as a secondary upside drilling target. By comparison, at the Big Flat area, the Cane Creek 26-3 core (NESW section 26, T. 25 S., R. 19 E.) shows that the interval is about 86 ft thick and the A, B, and C zones are about 21, 37, and 25 ft in thickness, respectively. The productive B zone apparently has reservoir facies that sum up to ~20 ft in thickness; however, the sandstones are much muddier, bioturbated, and dolomitized which may impact reservoir quality. The reservoir sandstones near Crescent Junction appear much cleaner, in places are less bioturbated, and contain less mud (figures 39 and 40). In the mostly unproductive play area to the southeast (Lisbon area), the Cane Creek is much thinner (~60 ft) and the thinner B zone (~30 ft) is mostly composed of anhydrite and dolomite (figure 39). The siltstone-sandstone reservoir facies is not as abundant and where present the reservoir quality is poor due to volumetrically abundant anhydrite.

In summary, our observations from the CS 21-22 core shows that the Cane Creek thickens to the north and northwest and contains a thicker reservoir B zone and source rock A and C zones. The siliciclastic reservoir facies is also equally or even more abundant than the siltstone-sandstone reservoir facies from the productive Big Flat play area. With the advancements in horizontal drilling, completions, and with a resurgence in oil prices, the northern Paradox Basin showcases the possibility for an emerging source rock play.

CONCEPTUAL DEPOSITIONAL MODEL

The Cane Creek and clastic cycle 19 express vertical stacking of 3-ft-scale, shallowing upward marine successions, particularly near the Salt Valley anticline area. The successions can be considered 5th to 6th order cycles that are typical for the progradation of modern tidal flats, which can be predicted using Walther's Law (figure 41) (Demicco and Hardie, 1994).

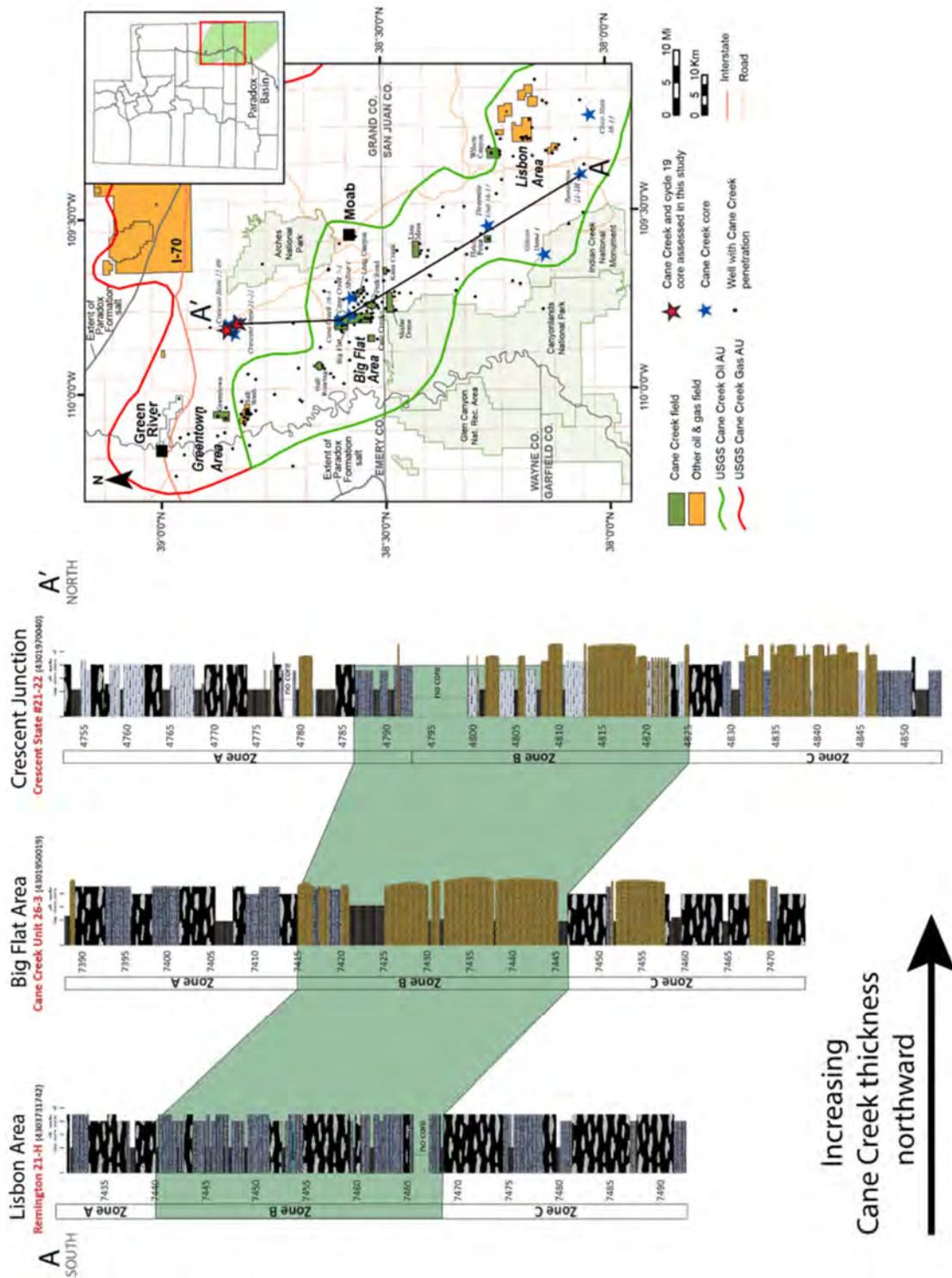
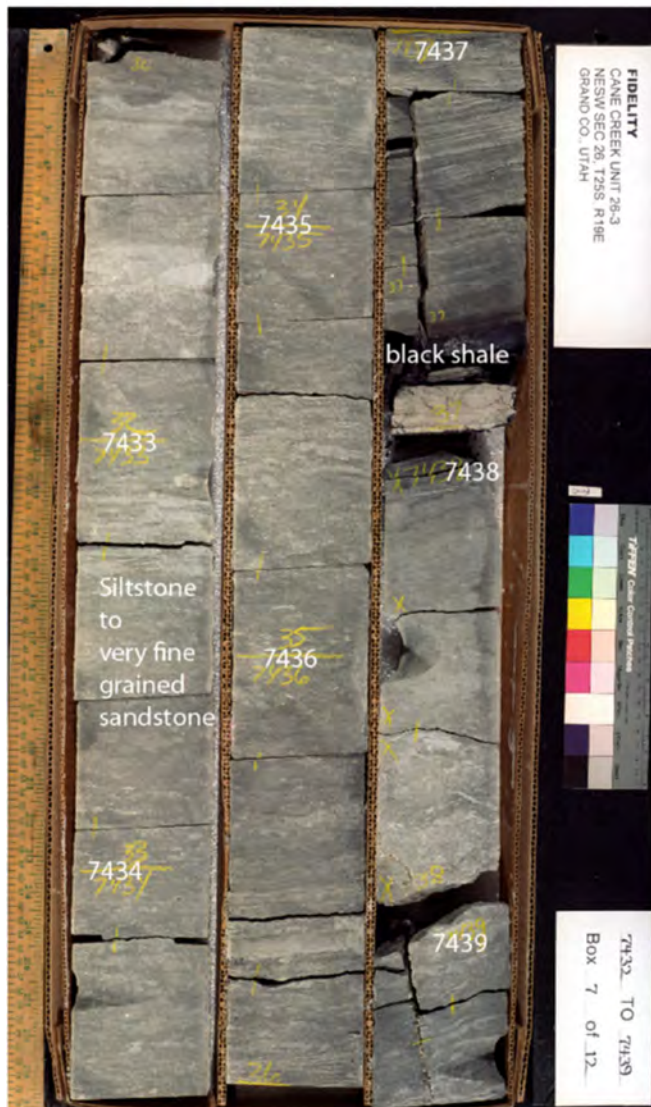


Figure 39. Cane Creek thickness comparison from cores across the Paradox Basin. Transect A-A' is of the Remington 21-H core from the southern Lisbon area, the Cane Creek Unit 26-3 core of the Big Flat area, and the Crescent State #21-22 near Crescent Junction. Note Cane Creek thickness increases to the north.

Cane Creek Unit 26-3 (4301950019)



Crescent State #21-22 (4301970040)

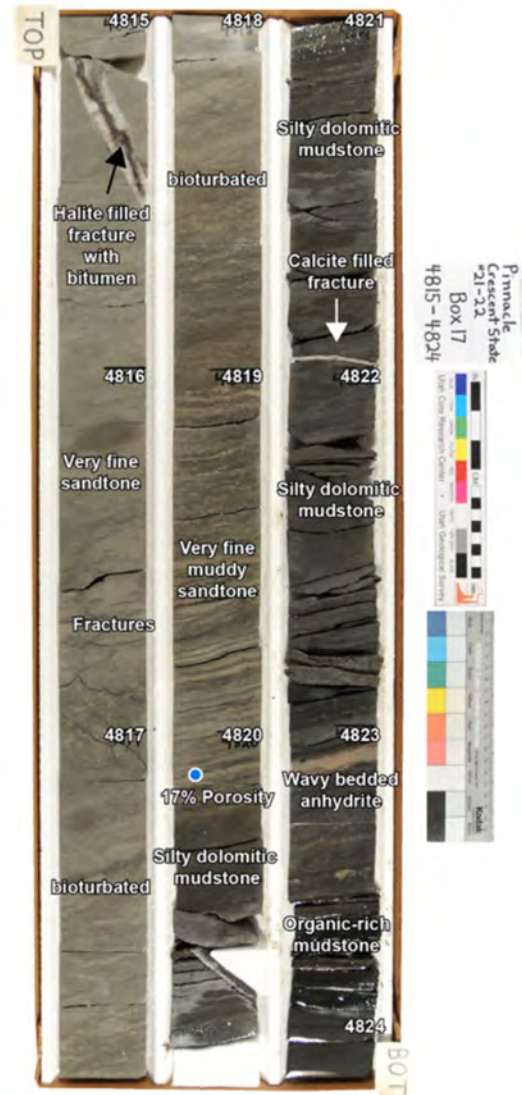


Figure 40. Core slab photographs representative of the B zone reservoir siltstone-sandstone facies from the Cane Creek Unit 26-3 and Crescent State #21-22 cores. Note sandstone from the Cane Creek Unit 26-3 is more bioturbated and muddy in appearance than sandstones in the Crescent State #21-22 core.

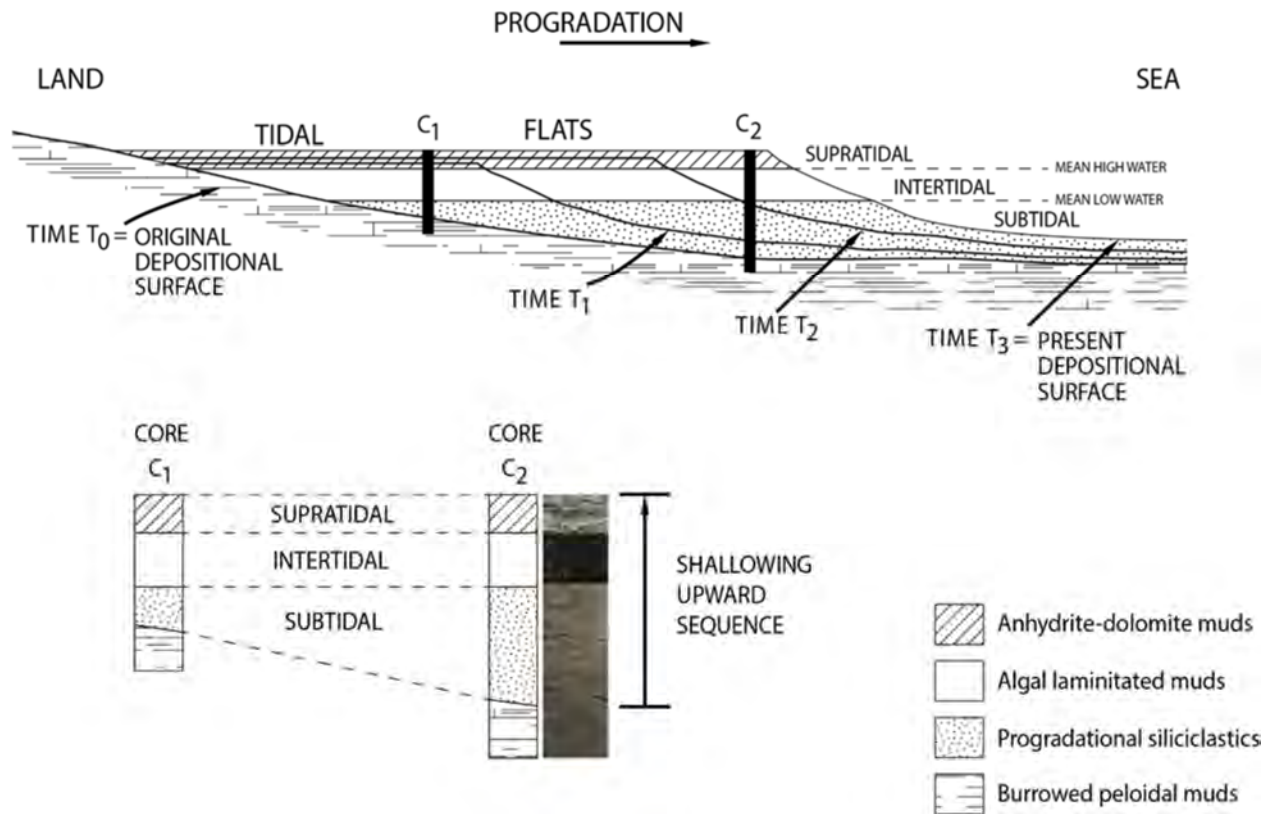


Figure 41. Diagrammatic cross section of a tidal flat depositional environment highlighting a progradational series from time 0 (T_0) to time 3 (T_3). Hypothetical core shows facies interpretation of a shallowing-upward sequence in a nearshore tidal flat environment. Representative core photographs are shown. Modified from Demicco and Hardie (1994).

Depositional environments associated with shallow-marine tidal deposits are characterized from deep to shallow transitional subfacies within subtidal, intertidal, and supratidal zones. The shallowing-upward cycles are recorded by episodes of seaward progradation when sediment supply easily exceeds any relative sea-level changes (combined effects of tidal forces, eustasy, subsidence, tectonic movement). Applying this model and comparative sedimentology for the Crescent State cores can explain the observed sedimentary features and meter-scale successions. Well-suited modern examples are the relatively continuous, laterally accreting sabkha Holocene tidal flat deposits of Abu Dhabi (Persian Gulf) and the siliciclastic sabkha of the Gulf of California (figure 42) (Castens-Seidell and Hardie, 1983; Demicco and Hardie, 1994). There, the subtidal zone is represented by burrowed lagoonal peloidal muds, and the lower and upper intertidal zones are characterized by tidal sands (eolian and fluvial sourced) and algal laminites. The supratidal zone contains evaporites (gypsum-anhydrite) and silty-sandy shoals. Transgressive and regressive changes in sea level, as well as changes in sediment supply, control the rhythmic progradation of the tidal flat subfacies.

During Cane Creek time, the Middle to Late Pennsylvanian climate was subtropical and arid which is analogous to the modern climate for these sabkha regions (Demicco and Hardie, 1994). The tidal deposits are primarily characterized by the sedimentary textures in the sandstone packages that contain climbing ripples, bidirectional cross-stratification, and mud drapes along ripple foresets, all common features for tidal bundle deposits. Bioturbated sandstone-siltstone implies progradation in the subtidal zone, along with interbedded massive-

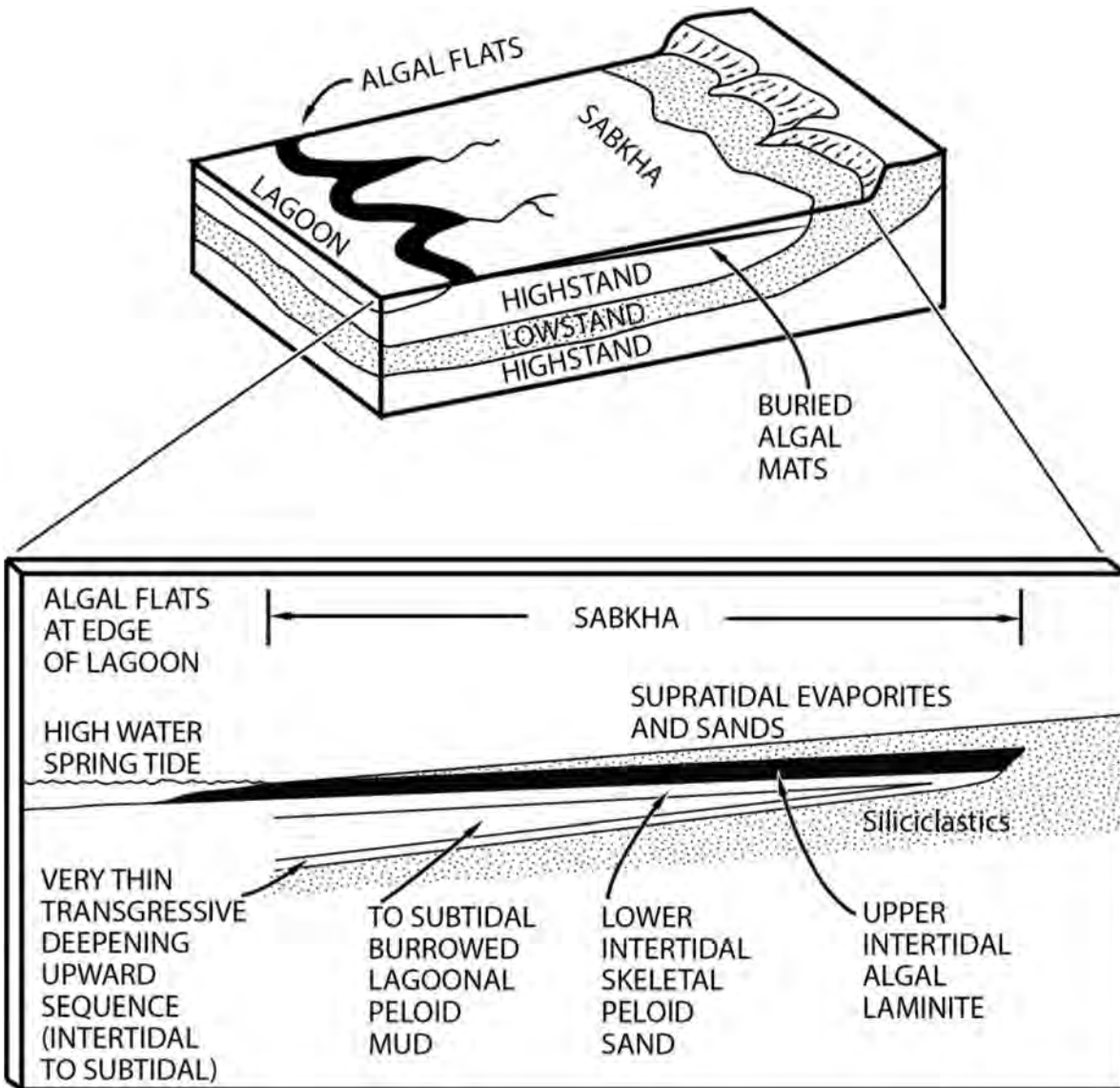


Figure 42. Diagrammatic box model of a sabkha depositional environment highlighting nearshore stacking patterns observable through sea-level rise and fall. Modified from Demicco and Hardie (1994).

bioturbated dolomitic-calcareous mudstone. The combination of sea-level rise, episodic flooding by inland storms, and flooding by seawater from onshore storms likely promoted stepwise transgression of intertidal deposits, such as algal laminite or black laminated organic-rich mudstone (figures 41 and 42). In core, this flooding surface is generally marked by mud rip-up clasts and flat pebble conglomerates followed by the intertidal algal laminated deposits (figures 23 and 43). Following this transgression, the receding seawater likely formed ponded ephemeral lakes in the supratidal zone. This depositional setting is analogous to the sabkha tidal flat of the Gulf of California where flooding produces large (50 mi²) supratidal ephemeral lakes in linear depressions that border alluvial fans at the landward edge of the sabkha (Castens-Seidell and Hardie, 1983). In this modern setting, the bottom of the ephemeral lake is initially covered by a muddy storm layer that soon becomes covered by cyanobacterial and algal mats. Soon after, evaporation progressively raises the salinity of the lake to a concentrated sulfate-

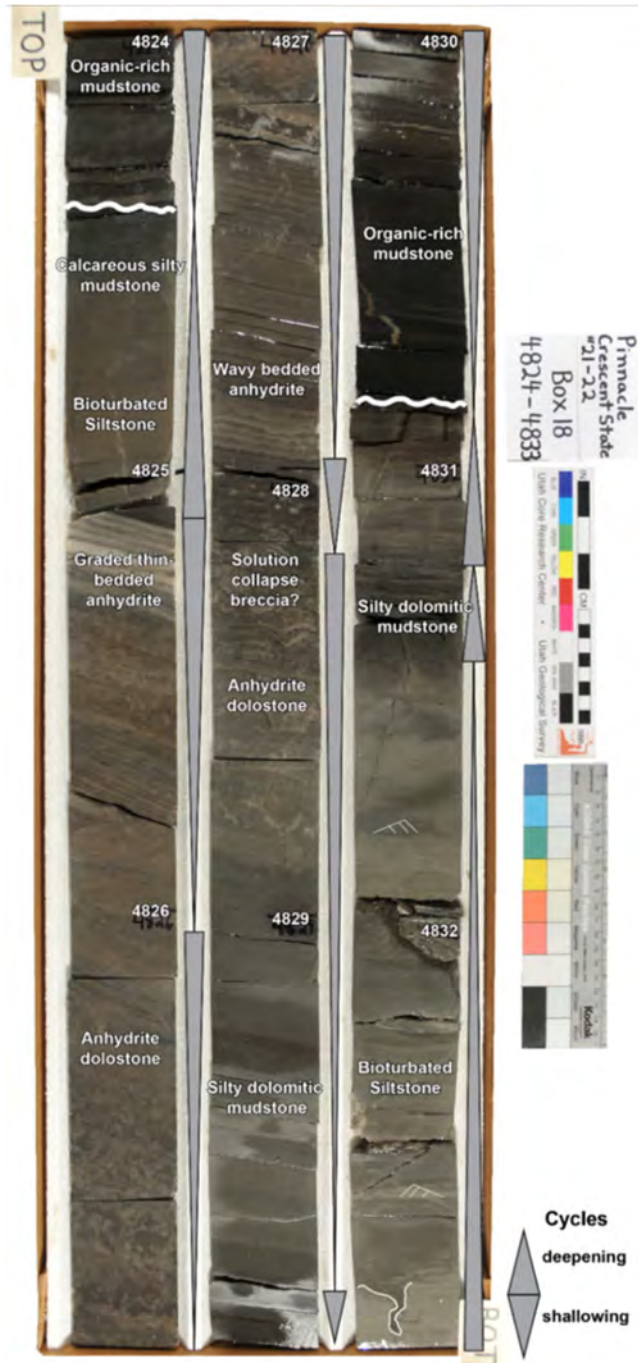


Figure 43. Core slab photographs representative of the C zone, Crescent State #21-22 core, showing examples of shallowing upward cycles. Each cycle begins with siltstone-sandstone deposited during a deepening phase that is followed by an abrupt flooding surface and organic-rich mudstone deposit; anhydrite dolostone caps the sequence and is representative of shallower evaporative waters. Note ripples, an outlined burrow, and wavy flooding surfaces in white.

rich brine and gypsum precipitates. Gypsum needles precipitate at the air-water interface of the shallow brine pool (< 8 ft deep) and sink to the bottom and form layered crusts. The needles also act as nucleation sites for syntaxial growth of vertically-oriented gypsum crystals. The gypsum crust grows on wrinkled cyanobacterial mats and promotes a rumpled morphology and eventually the subaqueous crust begins to buckle due to lateral pressure from expansive crystal growth. Meanwhile, interstitial pore waters are at supersaturation with respect to gypsum and precipitate displacive crystals in the bottom muds. By comparison, the Cane Creek dolomitic-anhydritic beds express similar supratidal sedimentary features, such as the anhydrite pseudomorphs after bottom-growth gypsum, the wavy bedded to kinked microcrystalline anhydrite, and invasive displacive nodular anhydrite. The presence of dolomite throughout much of the Cane Creek and cycle 19 can be interpreted as diagenetic in origin or as a primary precipitate that formed in the evaporative mudflats of the supratidal environment. Dolomite mixed with siliciclastic grains suggests the latter and that the dolomite was transported by fluvial/tidal or aeolian processes. In summary, the combination of laminated organic-rich mudstone with Type I and II kerogen and traces of coaly fragments, as well as the paucity of burrows, indicate the Cane Creek and cycle 19 experienced periods of restricted-evaporative sea waters in an arid sabkha setting.

CONCLUSIONS AND RECOMENDATIONS

The new cores taken along the Salt Valley anticline provide insightful and promising information on source rock quality, thermal maturity, and reservoir potential for the Cane Creek and cycle 19 in the northern Paradox Basin. The acquired core data has allowed for updated mapping of structure and maturity for the northern extent of the Cane Creek play area (figure 7, 8, and 44.). Source rocks from both the Cane Creek and cycle 19 intervals in the northern Paradox Basin are organic-rich shales (6–13 wt% TOC) that are within the oil window (~0.8% calculated V_{ro}). Notably, detailed study of these cores indicates the area contains thick sandstone-siltstone reservoir facies similar to those found in the successfully producing Big Flat field in the central play area. Akin to the Big Flat field, the northern Cane Creek reservoir rocks are tight, having 7–17% porosity and ~0.2 mD permeability, with evidence of natural fractures that could aid stimulated production. The data will serve useful for prospecting reservoir and source rock potential for acreage west of Crescent Junction, as well as provide detailed sedimentological and stratigraphic information for refining the depositional environment and paleogeography of the main reservoir and source rock units. In particular, the reservoir quality characterization and facies descriptions will help guide stratigraphic correlation and input parameters for reservoir modeling near the Gunnison Valley unit.

Significant recoverable reserves may still exist in the northern Greentown and Gunnison Valley areas, but economic deposits have yet to be successfully produced. However, source rock quality, thermal history, and abundant oil shows make these areas great territory for prospecting. Additional studies on the oil generation and migration may help define a more detailed play fairway for exploration. Cycle 19 appears to have significant potential in the northern Paradox Basin, but previous attempts to exploit the reservoir have encountered numerous mechanical problems during drilling, completion, or early production stages. Cycle 19 is much less prospective south of Greentown in the Big Flat and Lisbon areas where it thins dramatically. The Cane Creek appears to thicken to the north (figures 8 and 39) and the reservoir facies have great porosity and decent micro-permeability but understanding the extent of diagenetic overprinting on reservoir quality remains speculative. To fully achieve a comprehensive understanding of the lateral extent of the reservoir facies and quality, more core is needed from the northern Paradox Basin.

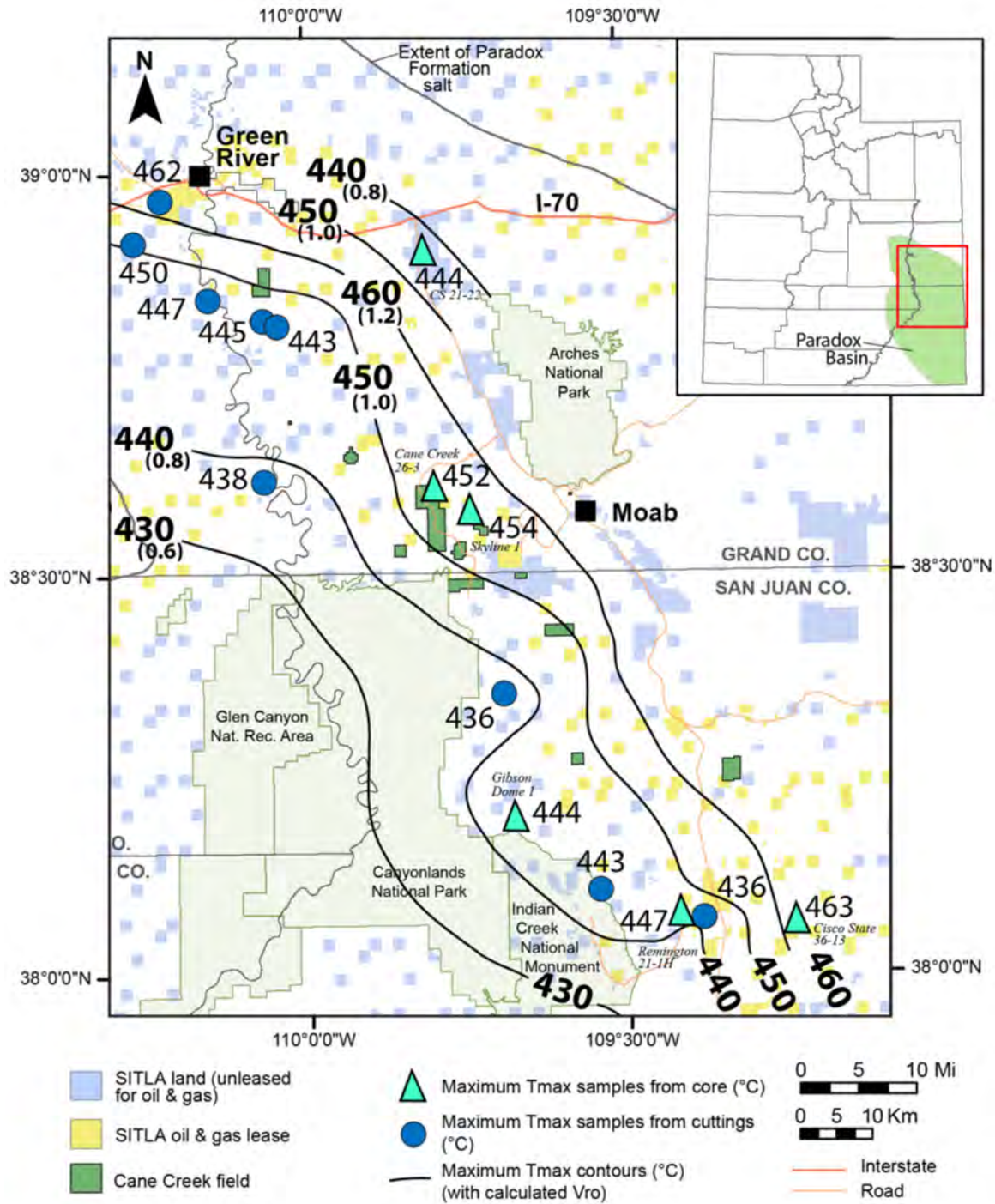


Figure 44. Maximum T_{max} (°C) map of the Paradox Basin, including updated contours in the northern part of the basin using new data collected from source rock analyses from the Crescent State #21-22 core. Contours and sample analyses in C. Calculated V_{ro} is in parentheses.

The following recommendations are considered for enhancing our understanding of the reservoir and source potential in the northern Paradox Basin:

- Document and describe the other cores from the Salt Valley anticline, including other clastic intervals.
- Perform a robust core analysis program to fill data gaps that include additional source rock and conventional plug analyses, geomechanics and preferred fracture orientation, micro-CT and SEM imaging for understanding porosity and permeability.
- Collect gamma response for all cores.
- Correlate geophysical logs with core data and build petrophysical models.
- Build facies maps from historical log data.
- Collaborate with industry partners on improving geologic and reservoir models by utilizing 3D seismic attributes to understand mechanical and stratigraphic properties.

REFERENCES

- Anna, L.O., Whidden, K.J., and Pearson, K.M., 2014, Assessment of continuous oil and gas reservoirs, Paradox Basin, Utah, Colorado, New Mexico, and Arizona: Rocky Mountain Association of Geologists *The Mountain Geologist*, v. 51, no. 2, p. 139–160.
- Baars, D.L., 1966, Pre-Pennsylvanian paleotectonics—Key to basin evolution and petroleum occurrences in paradox Basin, Utah and Colorado: *American Association of Petroleum Geologists Bulletin*, v. 50, p. 2082–2111.
- Baars, D.L., and Stevenson, G.M., 1981, Tectonic evolution of the Paradox Basin—Utah and Colorado, *in* Wiegand, D.L., editor, *Geology of the Paradox Basin: Rocky Mountain Association of Geologists Field Conference Guidebook*, p. 23–31.
- Baker, A.A., Dane, C.H., and Reeside, J.B., Jr., 1933, Paradox Formation of eastern Utah and western Colorado: *American Association of Petroleum Geologists Bulletin*, v. 17, p. 963–980.
- Barbeau, D. L., 2003, A flexural model for the Paradox Basin—Implications for the tectonics of the Ancestral Rocky Mountains: *Basin Research* v. 15, p. 97–115.
- Blakey, R.C., 2009, Paleogeography and geologic history of the western Ancestral Rocky Mountains, Pennsylvanian-Permian, southern Rocky Mountains and Colorado Plateau, *in* Houston, W.S., Wray, L.,L., and Moreland, P.G., editors, *The Paradox Basin revisited—new developments in petroleum systems and basin analysis: Rocky Mountain Association special Publication*, p. 222–264.
- Blakey, R., and Ranney, W., 2008, Ancient landscapes of the Colorado Plateau: Grand Canyon Association Special Publication, p. 222–264.
- Cater, F.W., 1970, *Geology of the Salt Anticline region in southwestern Colorado: U.S. Geological Survey Professional Paper 637*, 80 p.
- Castens-Seidell, B., and Hardie, L.A., 1983, Gypsum-anhydrite deposition in sabkhas—new observations the Holocene tidal flats of the northwest Gulf of California: *Geological Society of America Abstracts with Programs*, v. 15, 540 p.
- Chidsey Jr., T.C. and Eby, D.E., 2017, Potential oil-prone areas in the Cane Creek Shale play, Paradox Basin, Utah, identified by epifluorescence microscope techniques Utah: *Geological Survey Special Study, Vol 160*, 170 pp.

- Condon, S.M., 1997, Geology of the Pennsylvanian and Permian Cutler Group and Permian Kaibab Limestone in the Paradox Basin, southeastern Utah and southwestern Colorado: U.S. Geological Survey Bulletin 2000-P, 46 p.
- Demico, R.V. and Hardie, L.A., 1994, Sedimentary structures and early diagenetic features of shallow marine carbonate deposits: SEPM Atlas Series 1, Society of Sedimentary Geology, 265 p.
- Doelling, H.H., 1988, Geology of Salt Valley anticline and Arches National Park, Grand County, Utah: Utah Geological and Mineralogical Survey Bulletin 122, 58 p.
- Doelling, H.H., Oviatt, C.G., and Huntoon, P.W., 1988, Salt deformation in the Paradox region: Utah Geological and Mineral Survey Bulletin 122, 93 p.
- Goldhammer, R.K., Oswalk, E.J., and Dunn, P.A., 1991, Hierarchy of stratigraphic forcing—example from Middle Pennsylvanian shelf carbonates of the Paradox Basin, *in* Franseen, E.K., Watney, W.L., Kendall, C.G., and Ross, W., editors, Sedimentary modeling—computer simulations and methods for improved parameter definition: Kansas Geological Survey Bulletin, v. 233, p. 361–413.
- Grove, K.W., Horgan, C.C., Flores, F.E., and Bayne, R.C., 1993, Bartlett Flat, Big Flat (Kane Springs Unit), *in* Hill, B.G., and Bereskin, S.R., editors, Oil and Gas fields of Utah: Utah Geological Association Publication 22, unpaginated.
- Grove, K.W., and Rawlins, D.M., 1997, Horizontal exploration of oil and gas-bearing natural fracture systems in the Cane Creek clastic interval of the Pennsylvanian Paradox Formation, Grand and San Juan Counties, Utah, *in* Close, J., and Casey, T., editors, Natural fracture systems in the southern Rockies: Four Corners Geological Society, p. 133–134.
- Grummon, M.L., 1993, Cane Creek shale member of the Paradox Formation, exploiting a self-sourced reservoir with horizontal well bores: American Association of Petroleum Geologists Bulletin, p. 1449–1450.
- Guthrie, J.M., and Bohacs, K.M., 2009, Spatial variability of source rocks—a critical element for defining the petroleum system of the Pennsylvanian carbonate reservoirs of the paradox Basin, SE Utah, *in* Houston, W.S., Wray, L.L., and Moreland, P.G., editors, The Paradox Basin revisited—new developments in petroleum systems and basin analysis: Rocky Mountain Association of Geologists, Special Publication, p. 95–130.
- Herman, G., and Sharp, S.L., 1956, Pennsylvanian and Permian stratigraphy of the Paradox salt embayment, *in* Peterson, J.A., editor, Geology and economic deposits of east central Utah: Intermountain Association of Petroleum Geologists Seventh Annual Field Conference, p. 77–86.
- Hintze, L.F., and Kowallis, B.J., 2009, Geologic history of Utah: Brigham Young University Geology Studies Special Publication 9, 225 p.
- Hite, R.J., 1960, Stratigraphy of the saline facies of the Paradox Member of the Hermosa Formation of southeastern Utah and southwestern Colorado, *in* Smith, K.G., editor, Geology of the Paradox Basin fold and fault belt: Four Corners Geological Society Guidebook, Third Annual Conference, p. 86–89.
- Hite, R.J., Anders, D.E., and Ging, T.G., 1984, Organic-rich source rocks of Pennsylvanian age in the Paradox Basin of Utah and Colorado, *in* Woodward, J., Meissner, F.F., and Clayton, J.L., eds., Hydrocarbon source rocks of the greater Rocky Mountain region: Rocky Mountain Association of Geologist, p. 255–274.
- Hite, R.J., and Cater, F.W., 1972, Pennsylvanian rocks and salt anticlines, Paradox Basin, Utah and Colorado, *in* Mallory, W.W., editor, Geologic atlas of the Rocky Mountain region: Rocky Mountain Association of Geologist, p. 133–138.

- Hite, R.J., and Buckner, D.H., 1981, Stratigraphic correlations, facies concepts and cyclicity in Pennsylvanian rocks of the Paradox Basin, *in* Wiegand, D.L., editor, *Geology of the Paradox Basin: Rocky Mountain Association of Geologists Field Conference*, p. 147–159.
- Houston, W.S., Wray, L.L., and Moreland, P.G., editors, 2009, *The Paradox Basin revisited—new developments in petroleum systems and basin analysis: Rocky Mountain Association of Geologists Special Publication*, 852 p.
- Huffman Jr., A.C., Lund, W.R., and Godwin, L.H., editors, 1996, *Geology and Resources of the Paradox Basin, Utah Geological Association Publication 25*, 460 p.
- Jarvie, D.M., Hill, R.J., Ruble, T.E., and Pollastro, R.M., 2007, Unconventional shale-gas systems—The Mississippian Barnett Shale of north-central Texas as on model for thermogenic shal gas assessment: *American Association of Petroloeuem Geologist*, p. 475-499.
- Kelly, V.C., 1958, Tectonics of the region of the Paradox Basin, *in* Sanborn, A.F., editor, *Guidebook to the geology of the Paradox Basin: Intermountain Association of Petroleum Geologists, Ninth Annual Field Conference*, p. 31–38.
- Kluth, C.F., and Coney, P.J., 1981, Plate tectonics of the Ancestral Rocky Mountains: *Geology*, v. 9, p. 10–15.
- Kluth, C.F., and DuChene, H.R., 2009, Late Pennsylvanian and Early Permian structural geology and tectonic history of the Paradox Basin and Uncompahgre Uplift, Colorado and Utah, *in* Houston, W.S., and Wray, L.L., and Mooreland, P.G., editors, *The Paradox Basin revisited—New developments in petroleum systems and basin analysis: Rocky Mountain Association of Geologists Special Publication—The Paradox Basin*, p. 178–197.
- Mallory, W.W., 1972, Pennsylvanian System—regional synthesis, *in* Mallory, W.W., editor, *Geologic atlas of the Rocky Mountain region: Rocky Mountain Association of Geologists*, p. 111–128.
- Massoth, T.W., 2012, Well database and maps of salt cycles and potash zones of the paradox Basin, Utah: *Utah Geological Survey Open-File Report 600*, 13 p.
- Mitchum, R.M., Jr., and Van Wagoner, J.C., 1990, High-frequency sequences and eustatic cycles in the Gulf of Mexico basin: *Proceedings Gulf Coast Section SEPM 11th Annual Research Conference*, p. 257–267.
- Montgomery, S., 1992, Paradox Basin—Cane Creek play, *in* Cheney, T., Cain, D., editors, *Petroleum Frontiers: Petroleum Information Corporation*, 66 p.
- Morgan, C.D., 1992a, Horizontal drilling potential of the Cane Creek shale, Paradox Formation, Utah, *in* Schmoker, J.W., Coalson, E.B., and Brown, C.A., editors, *Geological studies relevant to horizontal drilling in western North America: Rocky Mountain Association of Geologists Guidebook*, p. 257-265.
- Morgan, C.D., 1992b, Cane Creek exploration play area Emery, Grand, and San Juan Counties, Utah: *Utah Geological Survey Open-File Report 232*, 5 p., 9 plates, scale 1:500,000.
- Morgan, C. D. and Stimpson, R., 2017, Geologic characterization of the Pennsylvanian Paradox Formation Cane Creek shale and other Paradox shales, Paradox Basin, Utah—*in* Vanden Berg, M.D., principal investigator, *Liquid-rich shale potential of Utah’s Uinta and Paradox Basins: Reservoir Characterization and Development Optimization*, Contract Deliverable to U.S. Department of Energy, variously paginated, <https://www.osti.gov/biblio/1417047-liquid-rich-shale-potential-utahs-uinta-paradox-basins-reservoir-characterization-development-optimization>

- Morgan, C.D., Yonkee, W.A., and Tripp, B.T., 1991, Geological considerations for oil and gas drilling on state potash leases at Cane Creek anticline, Grand and San Juan Counties, Utah: Utah Geological Survey Circular 84, 24 p.
- Nuccio, V.F., and Condon, S.M., 1996, Burial and thermal history of the Paradox Basin, Utah and Colorado, and petroleum potential of the Middle Pennsylvanian Paradox Formation: U. S. Geological Survey Bulletin 2000-O, 41 p.
- Peterson, J.A., and Hite, R.J., 1969, Pennsylvanian evaporite-carbonate cycles and their relation to petroleum occurrence, southern Rocky Mountains: American Association of Petroleum Geologists Bulletin, v. 53, p. 884–908.
- Rasmussen, D.L., 2014, Namakiers in Triassic and Permian formations in the Paradox Basin (USA) with comparisons to modern examples in the Zagros Fold Belt, Iran, *in* MacLean, J.S., Biek, R.F., and Huntoon, J.E., editors, Geology of Utah's far south: Utah Geological Association Publication 43, p. 689-756.
- Rasmussen, L., and Rasmussen, D.L., 2009, Burial history analysis of the Pennsylvanian petroleum system in the deep Paradox fold and fault belt, Colorado and Utah, *in* Houston, W.S., Wray, L.L., and Moreland, P.G., editors, The Paradox Basin revisited—new developments in petroleum systems and basin analysis: Rocky Mountain Association of Geologists Special Publication, p. 24–94.
- Rasmussen, D.L., Rasmussen, L., Rasmussen, G.J., and Longman, M.W., 2009, Selected bibliography—Paradox Basin and Four Corners region, *in* Houston, W.S., Wray, L.L., and Moreland, P.G., editors, The Paradox Basin revisited—new developments in petroleum systems and basin analysis: Rocky Mountain Association of Geologists Special Publication, p. 780–852.
- Reid, F.S., and Berghorn, C.E., 1981, Facies recognition and hydrocarbon potential of the Pennsylvanian Paradox Formation, *in* Wiegand, D.L., editor, Geology of the Paradox Basin: Rocky Mountain Association of Geologists, p. 111–117.
- Smith, K.T., 1978a, Bartlett Flat, *in* Fassett, J.E., editor, Oil and gas fields of the Four Corners area: Four Corners Geological Society, v. 2, p. 1061–1063.
- Smith, K.T., 1978b, Big Flat, *in* Fassett, J.E., editor, Oil and gas fields of the Four Corners area: Four Corners Geological Society, v. 2, p. 596–598.
- Smith, K.T., 1978c, Cane Creek, *in* Fassett, J.E., editor, Oil and gas fields of the Four Corners area: Four Corners Geological Society, v. 2, p. 624–626.
- Smith, K.T., 1978d, Long Canyon, *in* Fassett, J.E., editor, Oil and gas fields of the Four Corners area: Four Corners Geological Society, v. 2, p. 676–678.
- Smith, K.T., 1978e, Shafer Canyon, *in* Fassett, J.E., editor, Oil and gas fields of the Four Corners area: Four Corners Geological Society, v. 2, p. 700–702.
- Stevenson, G.M., and Wray, L.L., 2014, History of petroleum exploration of Paleozoic targets in the Paradox Basin, *in* Houston, W.S., Wray, L.L., and Moreland, P.G., editors, The Paradox Basin revisited—new developments in petroleum systems and basin analysis: Rocky Mountain Association of Geologists, Special Publication, p. 1-23.
- Stokes, W.L., 1986, Geology of Utah: Utah Museum of Natural History, Occasional Paper Number 6, 280 p.
- Szabo, E., and Wengerd, S.A., 1975, Stratigraphy and tectogenesis of the Paradox Basin, *in* Fassett, J.E., editor, Canyonlands country: Four Corners Geological Society Guidebook 8th field conference, p. 193–210.
- Trudgill, B.D., 2011, Evolution of salt structures in the northern Paradox Basin—controls on evaporate deposition, salt wall growth and supra-salt stratigraphic architecture basin research: Basin Research, v. 23, p. 208–238.

- Trudgill, B.D., and Arbuckle, W.C., 2009, Reservoir characterization of clastic cycle sequences in the Paradox Formation of the Hermosa Group, Paradox Basin, Utah: Utah Geological Survey Open-File Report 543, 106 p.
- Wengerd, S.A., and Matheny, M.L., 1958, Pennsylvanian system of the Four Corners region: American Association of Petroleum Geologists Bulletin, v. 42, p. 2048–2106.
- Whidden, K.J., Anna, L.O., Pearson, K.M., and Lillis, P.G., 2012, Assessment of undiscovered oil and gas resources in the Paradox Basin province, Utah, Colorado, New Mexico, and Arizona: U. S. Geological Survey Fact Sheet 2012-3031, 4 p.
- Whidden, K.J., Lillis, P.G., Anna, L.O., Pearson, K.M., and Dubiel, R.F., 2014, Geology and total petroleum systems of the Paradox Basin, Utah, Colorado, New Mexico, and Arizona: Rocky Mountain Association of Geologists The Mountain Geologist, v. 51, no. 2, p. 119–138.